B88 951025 800

PROJECT Sequoyah DISCIPLINE M
CONTRACT 95N2H-154714   UNIT 1
DESC. RV Head Penetration Seal Weld Overlay Design Report
DWG/DOC NO. SIR-95-105
SHEET - OF - REV 00 ECN/FCR - FILE -
DATE 10/23/95

RV Head Penetration Seal Weld Overlay Design Report

DESIGN AND ANALYSIS OF A WELD OVERLAY REPAIR FOR THE SEQUOYAH UNIT 1 CRDM LOWER CANOPY SEAL WELDS

Prepared by:

Structural Integrity Associates, Inc.

Prepared for:

Tennessee Valley Authority

Prepared by: _H. L. Gustin_   Date: 10/5/95
H. L. Gustin, P.E.

Reviewed by: _____   Date: 10/5/95
N.G. Cofie

Approved by: _H. L. Gustin_   Date: 10/5/95
H. L. Gustin, P.E.

RIMS, WT 3B-K

Structural Integrity Associates, Inc.

Table of Contents

List of Tables

List of Figures

List of Figures (continued)

1.0 INTRODUCTION AND SUMMARY

A weld overlay repair design was developed for application to potentially leaking control rod drive mechanism (CRDM) lower canopy seal welds (CSWs) at the Sequoyah Nuclear Power Plant Unit 1. An evaluation of the predicted weld residual stress distributions resulting from this repair was performed. The weld residual stress and the applied stresses on the CSWs were used to determine the design life of the overlay repaired CSWs, assuming the mechanism for repair degradation to be stress corrosion cracking (SCC). This repair uses Alloy 625 filler metal, applied by the GTAW process.

Previous work performed by Structural Integrity Associates (CSW weld overlay repairs at other plants) was used as part of the basis for the overlay design for Sequoyah.

1.1 Background

Potential leakage has been detected in three Sequoyah CRDM lower CSWs. The overlay design in this report was prepared to repair these potentially leaking canopy seals.

In the past, through-wall defects were detected in the CRDM CSWs, between the head adapter and head adapter plug, on spare CRDMs at Zion, Unit 1, and weld overlay repairs using Alloy 625 were designed and implemented. The geometry and dimensions of the CRDM lower canopy seal at Sequoyah [1] are essentially identical to those at the Zion Nuclear Power Plant [2], for the purpose of this analysis, and are shown in Figures 1-1 and 1-2.

Failure analysis results on the Zion-1 CSWs, concluded that transgranular stress corrosion cracking (TGSCC) was the mode of failure, resulting in local through-wall cracks and leakage, similar to that at Diablo Canyon [2,3]. TGSCC can be caused by local contamination with impurities such as chloride ions or caustic [2,3,4], although such impurities were not conclusively identified at the time of this report.

Structural Integrity Associates, Inc.

In spare CRDMs at Zion, a major factor in promoting the cracking and leakage appeared to have been the lack of weld penetration and poor quality of these CSWs. Such crevices can exacerbate off-chemistry conditions and lead to local concentrations of impurity ions which result in SCC initiation. It is believed that SCC led to local through-wall cracking and leakage, with the time of SCC initiation not being certain. At least one of the Sequoyah CRDM lower CSWs in question was on an active CRDM. It is expected that SCC has been present in the active CRDMs as in the spare CRDMs at Zion.

The weld overlay repair method for the lower CSWs at Sequoyah is discussed in this report. In particular, these repairs were designed for leaking CSWs observed at Sequoyah during the Fall 1995 outage. The weld overlay repair concept [5] has been employed many times for the repair of intergranular stress corrosion cracks (IGSCC) in boiling water reactor (BWR) stainless steel piping welds. It was also used for CRDM canopy seal repairs at the Zion, Diablo Canyon, Callaway, and Prairie Island pressurized water reactor (PWR) plants among others. Weld overlay repair concepts similar to those used at these plants are used to design CRDM canopy seal repairs for Sequoyah. Details of the overlay design are in accordance with ASME Section XI IWB-3642 [6] and References 5 and 7. ASME Code Case N-504-1 provides additional guidance. The overlay design is based upon assumed stresses equal to ASME Code allowable stress limits. Details of the design considerations are presented in the following section of this report.

The service life of the Sequoyah repairs is predicted to be in excess of 40 effective full power years.

The failure analysis of the CSWs from Zion-1 concluded that SCC was the mode of cracking and this mode of cracking is expected to be operative at Sequoyah. Therefore, the SCC resistance of the repair was evaluated to predict the remaining life. In order to perform this evaluation, including a fracture mechanics crack growth analysis, the weld residual stress distributions from the repair were estimated by using the WELD3 computer program [8], an elastic-plastic, thermo-mechanical finite element program. This residual stress distribution is much more significant than the sustained loads [2,3] in providing the driving force for SCC. The residual stress is used as a principal input to the fracture mechanics SCC crack growth law to predict the remaining life of the repair.

1.2   Summary

A weld overlay repair was designed for the Sequoyah CRDM lower CSWs. This design is based on meeting the requirements of ASME Section XI, IWB-3640 [6] and the NRC requirements outlined in NUREG-0313, Rev. 2 [5] for the repair of SCC flaws. Based on an assumed maximum stress of $1.0 S_m$ (16.2 ksi), for Type 304 at 650°F for primary membrane stresses in accordance with ASME Section III, NB-3227-7 [6], the minimum required overlay thickness is 0.0511 in. The width of the overlay is such that it should be blended into the thicker sections of the head adapter and CRDM, pressure housing, as shown in this report. In order to provide SCC resistance, the repair weld material was selected as Alloy 625 filler, using the GTAW weld process [9].

Weld residual stresses were computed with the **WELD3** computer program [8] for the repair model. The model consisted of depositing three layers of Alloy 625 weld metal, each layer being 0.12 inch thick and welded starting from the top. This model was confirmed on a weld mock-up performed for the Zion spare CRDM CSW overlay [2].

A fracture mechanics SCC crack growth law, a factor of ten slower than the upper bound NRC curve for IGSCC of 304 [5] was used for the remaining life predictions. This law is based on the superior SCC resistance of Alloy 625 (similar to I-82 filler, which is judged to be SCC resistant [5]), and a literature survey (discussed in this report). This crack growth law, combined with the 3-layer overlay residual stress distribution, and a bounding 2 ksi applied membrane stress, gave a predicted remaining SCC life in excess of 50 years.
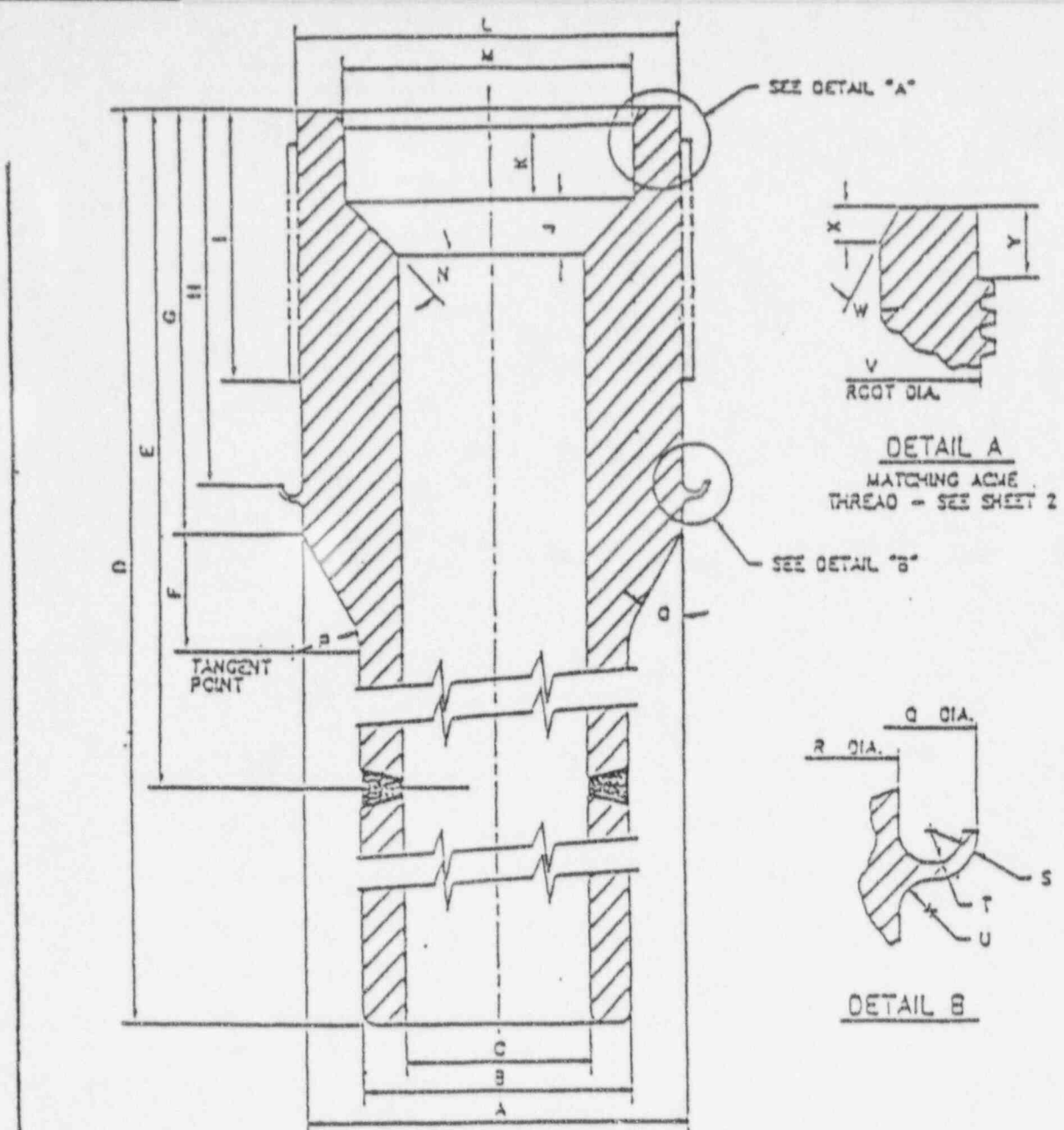
SECTION OF HEAD ADAPTER

DETAIL A
MATCHING ACME
THREAD — SEE SHEET 2

DETAIL B

DIMENSIONAL DATA

A = 5.66"	F = 2.604"	K = 1.370"	P = 1.0"	U = 0.160"
B = 4.0"	G = 6.0"	L = 5.701"	Q = 6.45"	V = 5.738/5.74"
C = 2.75"	H = 5.177"	M = 4.300"	R = 5.66"	W = 30°
D = 27.75 to 59.281	I = 3.875"	N = 45°	S = 0.075"	X = 0.25"
E = 11.0"	J = 0.78"	O = 30°	T = 0.160"	Y = 0.50"

Figure 1-1. Geometry of Spare CRDM Head Adapter Used for Zion Canopy Seal Weld Overlay Model Development
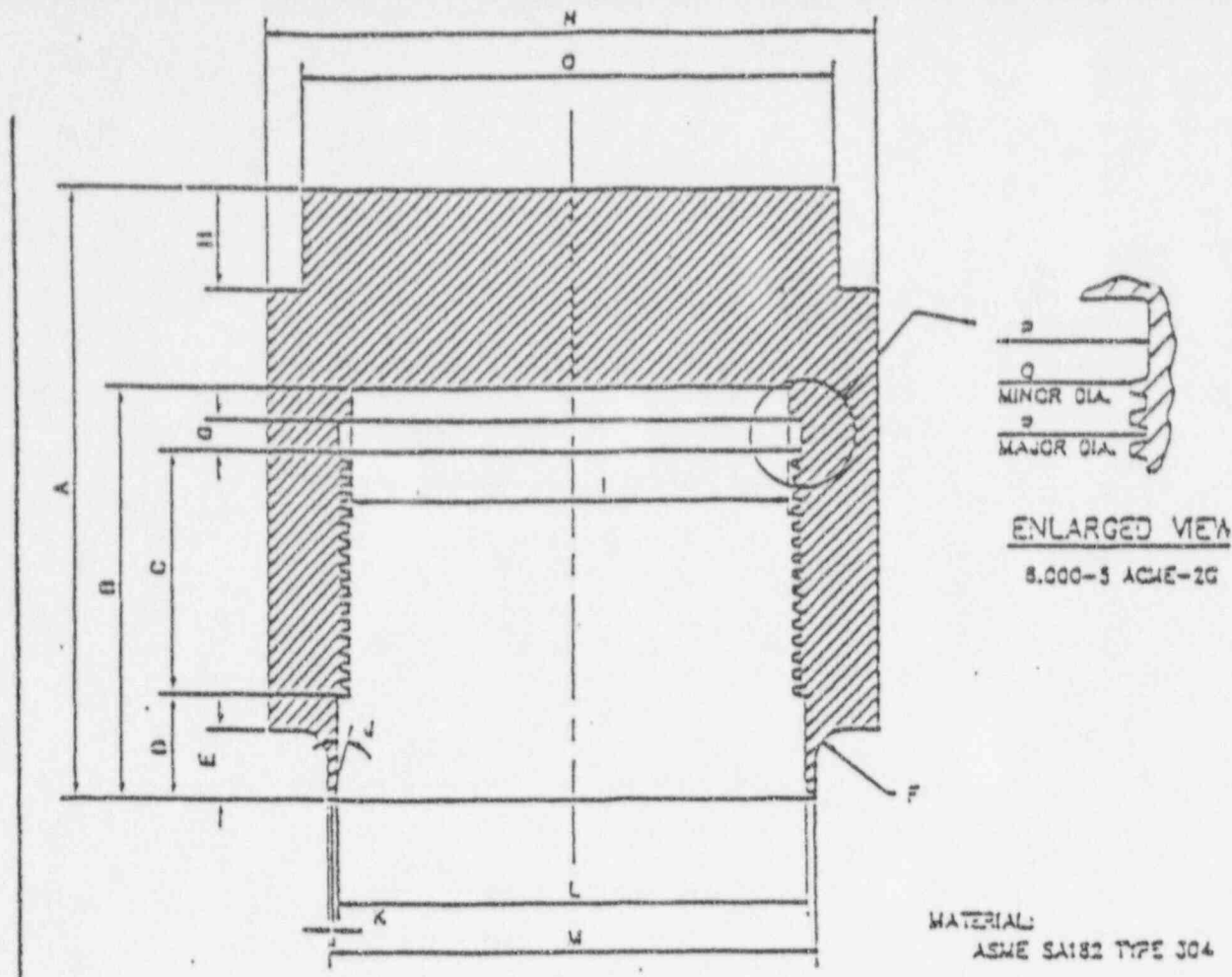
Structural Integrity Associates, Inc.

SECTION OF
HEAD ADAPTER PLUG

ENLARGED VIEW
8.000-5 ACME-2G

MATERIAL:
ASME SA182 TYPE 304

DIMENSIONAL DATA

A = 7.59"	H = 1.25"	O = 6.995"
B = 5.125"	I = 5.71"	P = 6.06"
C = 3.00"	J = 15°	Q = 5.80"
D = 1.30"	K = 0.075"	R = 6.02"
E = 0.485"	L = 6.122"	
F = 0.40"	M = 6.440"	
G = 0.40"	N = 8.00"	

Figure 1-2. Geometry of Spare CRDM Head Adapter Plug Used for Zion Canopy Seal Weld Overlay Model Development

Structural Integrity Associates, Inc.

2.0 WELD OVERLAY DESIGN

Details of the CSW overlay design are in accordance with ASME Section XI IWB-3640 [6] and References 5 and 7. Since the overlay weld process is GTAW, a relatively tough and ductile repair results, and secondary stresses (such as thermal and residual stresses) are not required [6] to be considered in the design of overlay thickness. Thus, the design is conservatively based upon assumed primary stresses equal to the ASME Section III Code allowable values.

The overlay thickness required for structural reinforcement to satisfy the preceding rules of ASME Section XI [6] and the NRC requirements [5] is significantly less than that needed for a practical remaining life, based on residual stress and SCC crack growth predictions.

Because the failure analysis of the Zion-1 CSWs resulted in the conclusion that stress corrosion cracking was the mode of failure [2], the methods outlined in NUREG-0313, Revision 2 [5] were considered in designing and evaluating the remaining life of the CSW repairs in this report, in order to appropriately consider resistance to stress corrosion cracking. The present analysis conservatively assumes that a crack is already present in the original CSW, and considers crack growth by the stress corrosion mechanism per NUREG-0313, Revision 2 [5]. Dimensional and weld material requirements are described below.

2.1 Dimensions

The weld overlay repair thickness was derived in accordance with References 5 and 7, in order to reduce both the nominal stresses and the ratio of flaw through-wall dimension to wall thickness (a/t) to meet the requirements of ASME Section XI, IWB-3640 [6]. This repair is sufficient for the maximum possible postulated defect (360° by through-wall) in the original canopy seal weld, thus meeting the requirements of a standard weld overlay [5]. Although the guidelines of Reference 5 are, strictly speaking, applicable to BWR stainless steel pipe welds, the subject CRDM repair is close enough in material and design basis, such that the weld overlay guidelines are considered to be directly applicable.

Structural Integrity Associates, Inc.

The methodology of Reference 7, the net section collapse criterion (NSCC), serves as a basis for flaw acceptance and repair in austenitic stainless steels, to satisfy ASME Section XI IWB-3640 [6] and NRC requirements in NUREG-0313, Rev. 2 [5]. A brief description of the NSCC methodology follows.

The NSCC, as illustrated in Figure 2-1, assumes that the pipe with a crack of depth "a" and a length of "2θ" (included angle) will fail by plastic collapse when the net section reaches the flow stress σ_f. This criterion considers the fact that when a circumferentially cracked pipe is placed under an axial load, due to the primary membrane and bending stresses P_m and P_b, a shift in the neutral axis of the pipe will occur by the angle β.

The equations to predict the acceptable flaw size as a function of the applied stresses P_m and P_b are given in Reference 7 as:

Case 1: $\theta + \beta \leq \pi$

$$P_b = 2\sigma_f \left[2Sin\beta - (a/t)*(Sin\theta)\right] / \pi$$

$$\beta = \left[(\pi - \theta a/t) - (P_m/\sigma_f)\pi\right] / 2$$

Case 2: $\theta + \beta > \pi$, then

$$P_b = 2\sigma_f\left[(2-a/t)Sin\beta\right] / \pi$$

$$\beta = \pi\left[1 - a/t - P_m/\sigma_f\right] / \left[2 - a/t\right]$$

The flow stress, σ_f, for use in the above equations is estimated as three times the S_m value (16.2 ksi at 650°F) from Section III of the ASME Code for Type 304, the material to be repaired.

Structural Integrity Associates, Inc.

The weld overlay repair thickness as shown on the attached design sketch (Figures 2-2 and 2-3) was computed with the Structural Integrity Associates computer program pc-CRACK [11] (based on the above NSCC methodology) for an applied stress equal to the ASME Code allowable stress level.

This allowable stress level is provided in ASME Section III, NB-3227.7 [6] wherein the CSW shall be designed to meet the pressure induced general primary stress intensity limit of $P_m = S_m$, as given in Figure NB-3221-1 of ASME Section III. The value of S_m is taken as 16.2 ksi at 650°F, from Appendix I of ASME Section III Appendices [6].

A safety factor of 3 is placed on the above stress ratio, for design of the overlay, in accordance with IWB-3640 [6] and Reference 5. The overlay design thickness resulting from the above stress ratio is 0.0511 in., as shown in the attached pc-CRACK output (Table 2-1). The number of weld passes to meet these dimensions should be determined by the procedure qualification and the dimensions should be verified on the actual welds. A final overlay thickness of 0.36 inch is specified to account for stress corrosion cracking mechanisms.

The minimum width of the 360° circumferential weld overlay repair is also illustrated in the attached design sketch (Figure 2-2). When overlay thickness requirements are computed, as above, an iterative computation is performed to both decrease the ratio of flaw depth to wall thickness (a/t) and decrease the nominal stress in the wall as the overlay thickness is increased. The assumed decrease in nominal stress in proportion to the increased wall thickness is valid only if the overlay width is sufficient to effectively transfer stresses across the discontinuity (flawed region).

2.2   Weld Procedure and Material

The combination of the Alloy 625 weld metal and the selected welding process (GTAW) assures adequate weld toughness. Therefore, per [5], secondary (thermal expansion) stresses do not need to be considered in the weld overlay design. Alloy 625 also provides a sound weld with resistance to pitting corrosion, crevice corrosion and stress corrosion cracking (SCC), as these are potential

failure mechanisms for the postulated defect. It is assumed that this overlay repair is performed subsequent to drying, to avoid the possibility of blow-outs during welding.

The following measurements and controls for the repair are recommended, when practical.

1.   Perform preweld "bake", or drying to avoid blow-outs during welding.

2.   Measurement of final weld overlay repair thickness and width.

3.   Measurement of axial (vertical), diametral (at the canopy seal region), and angular (from vertical) distortions produced by the weld repair.

Although all the above measurements may not be practical in the field application, it is recommended that at least a mock-up of the repair be performed to verify acceptable results in this respect, before the repair is implemented.

2.3   Code Reconciliation

The CSW repair design and remaining life analyses of this report were performed in accordance with the 1989 Edition of ASME Sections III and XI [6], in addition to NUREG-0313, Revision 2 [5]. Additional guidance was taken from ASME Code Case N-504-1. Paragraph 4.1 of the NUREG [5] states that the 1986 Edition of Section XI now provides appropriate criteria for the flaw evaluation and repair of all types of welds, in contrast to earlier editions for some cases. This comment specifically applies to Section XI paragraphs IWB-3641 and IWB-3642, which were used for the CSW analysis. There is no difference between the 1986 and 1989 Editions of Section XI which is pertinent to the present analysis. The 1989 Edition of Section XI is approved in 10CFR50.55.

The residual stress analysis documented in Appendix A was performed using material properties from the 1968 Edition of ASME Section III with the Winter 1968 Addenum. The Code of record for the Sequoyah reactor vessel is the 1968 Edition of ASME Section III [12]. The CRDM lower CSW

overlay repair work is specified to be done to the 1989 Edition of ASME Section XI. The 1980 Edition of Section XI, with Addenda through Winter 1981, is the Edition/Addenda to which the Sequoyah Unit 1 FSAR is committed.

A Code search was performed to determine any significant technical changes which could affect reconciliation of the 1989 Edition analyses with the above Codes of record. It was noted that paragraph IWA-4120 of Section XI was revised in the Winter 1983 Addenda to permit an Owner to use later Editions of Section XI when performing repairs, subject to approval by the regulatory authority (the 1986 Edition has been approved by the NRC). Section XI previously had permitted use of later editions of Section III for repairs, in this paragraph.

In addition to the above guidance by NUREG-0313, Revision 2 [5] to use the 1986 Edition of Section XI, and paragraph IWA-4120 of Section XI permitting later editions of Sections III and XI to be used when performing repairs (as discussed above), specific Code paragraphs used in relation to this current study were searched for significant technical changes. Specifically, it was found that NB-3227.7, and NB-4360, added provisions for specially designed welded seals, such as omega and canopy seals, in the Winter 1971 Addenda of Section III. Thus, later Code editions give more specific, improved rules for CSW design. In earlier Editions [eg. 1968] of Section III it was found that S_m at 650°F was 15.3 ksi, rather than the value of 16.2 ksi in the 1989 Edition, for SA-182, Grade F304, the head adapter and plug material. Since the present analysis for designing the CSW repair thickness assumes general membrane stresses in the CSW to be at the Code limit, use of the higher value of 16.2 ksi is conservative.

In view of the above discussions, as well as considering other less significant Code changes, it is concluded that the 1989 Editions of Sections III and XI would be permitted by current rules for Section XI repairs, and also provide more specific and complete rules for the repairs of CSWs, as designed in this report. Thus, the current analysis is enhanced by use of the 1989 Edition of the Code. The integrity of the repair design is improved relative to that which would result from the Section III Code of record for Sequoyah. The 1989 Editions of both Section III and Section XI are approved by the NRC in 10CFR50.55. More recently, Code Case N-504 [13] was published. This

Code Case specifically deals with weld overlay repairs of austenitic stainless steel pipes. This Code Case offers additional guidance for the overlay repair design for CSWs at Sequoyah.

Table 2-1

Structural Reinforcement Sizing Evaluation

tm
pc-CRACK
(C) COPYRIGHT 1984, 1990
STRUCTURAL INTEGRITY ASSOCIATES, INC.
SAN JOSE, CA (408)978-8200
VERSION 2.1

Date: 23-Sep-1995
Time: 15: 2:55.15

STRUCTURAL REINFORCEMENT SIZING EVALUATION

STRUCTURAL REINFORCEMENT SIZING USING SOURCE EQUATIONS FOR CIRCUMFERENTIAL CRACK

WSI-20Q: SEQUOYAH CRDM CANOPY SEAL WELD OVERLAY REPAIR

WALL THICKNESS=	0.0750		
MEMBRANE STRESS=	16.2000	SAFETY FACTOR=	3.0000
BENDING STRESS=	0.0000	SAFETY FACTOR=	1.0000
STRESS RATIO=	3.0000		
ALLOWABLE STRESS=	16.2000		
FLOW STRESS=	48.6000		

	L/CIRCUM					
	0.50	0.60	0.70	0.80	0.90	1.00
FINAL A/T	0.6475	0.6182	0.6025	0.5967	0.5947	0.5947
REINFORCEMENT THICK.	0.0408	0.0463	0.0495	0.0507	0.0511	0.0511

Nominal stress in the uncracked section of pipe

$P_m + P_b$

σ_f - Flow stress

P_m

Neutral axis

93247r1
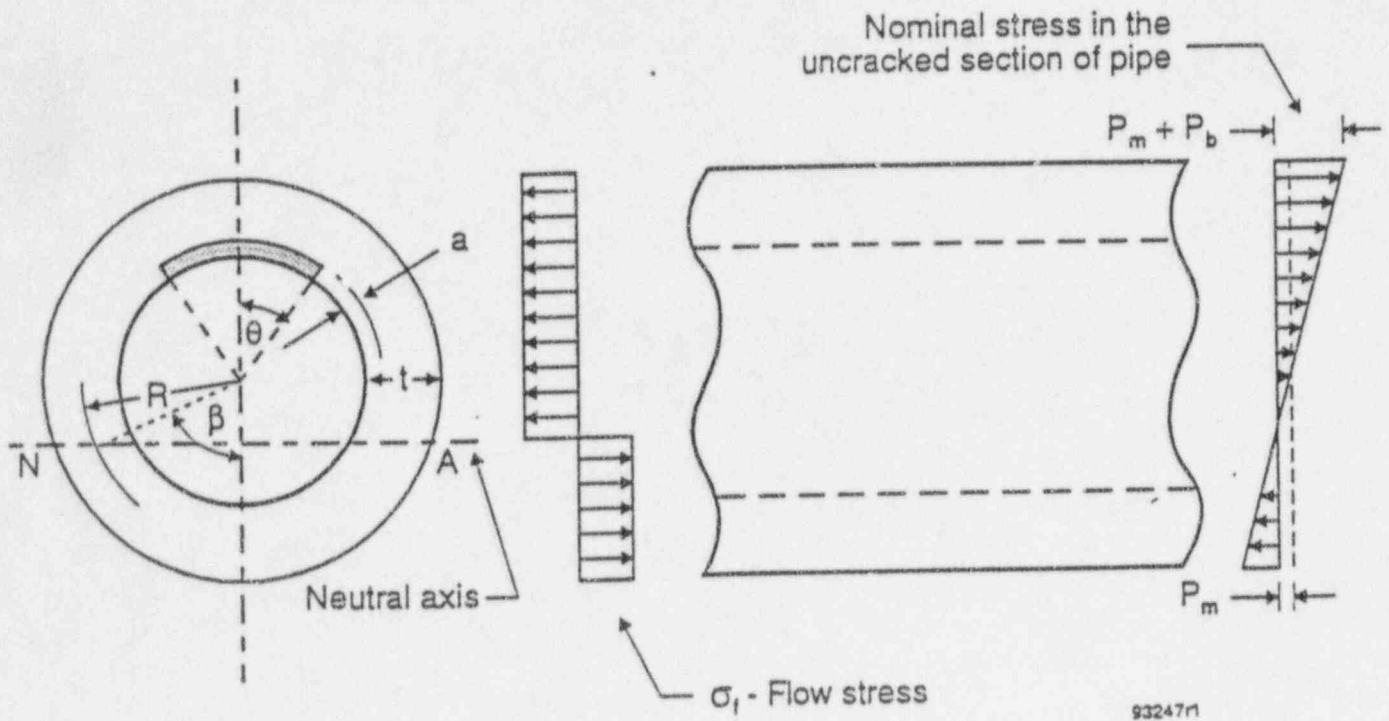
Figure 2-1.   Illustration of Net Section Collapse Criterion (NSCC) for Circumferential Crack of Depth a and Length 2θ in a Pipe [7]

0.07" to 0.08" (ref)

15° (ref)

Blend Into Thicker Section As Shown

0.38"R (ref)

C̶L̶ of Original Weld

0.155 to 0.160"R (ref)

Weld Overlay Thickness .36"

5.660 O.D. (ref)

0.155" to 0.160"R (ref)

Blend Into Thicker Section As Shown
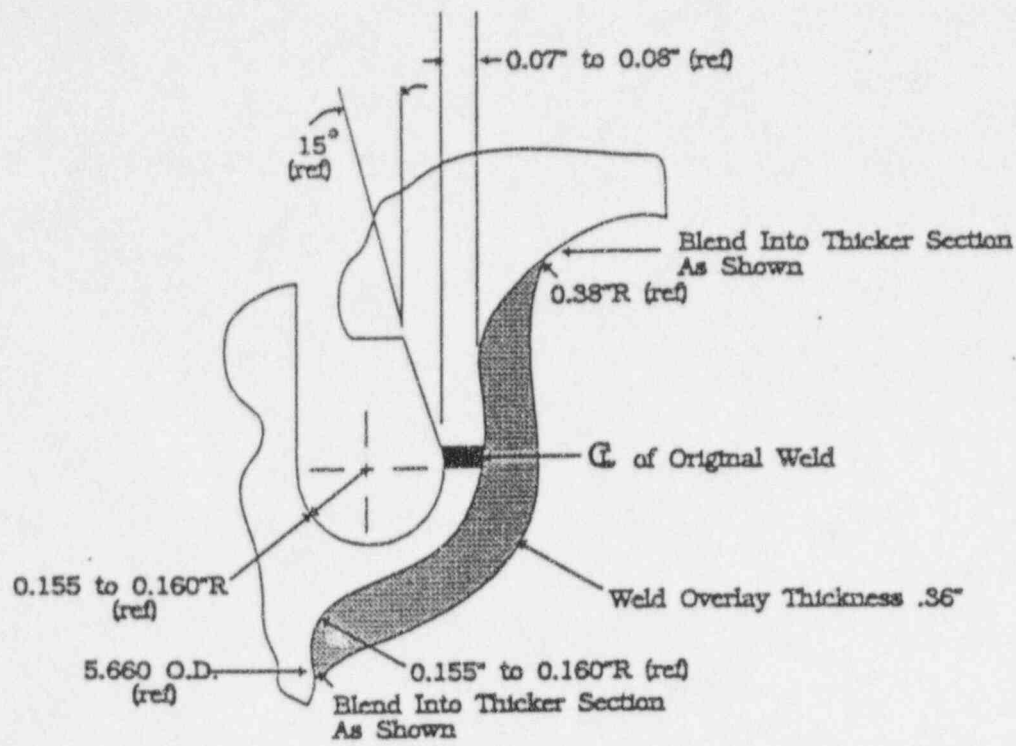
NOT TO SCALE

Figure 2-2. Canopy Seal Weld Overlay Design and Dimensions Used in Analysis

Structural Integrity Associates, Inc.

0.075" →

21
11
22
1
12
23
2
13
3
14
24
4
15
5
25
16
6
26
7
17
27
10
18
28
9
19
20
29
8
30

Each weld layer = 0.120" thick

NOT TO SCALE
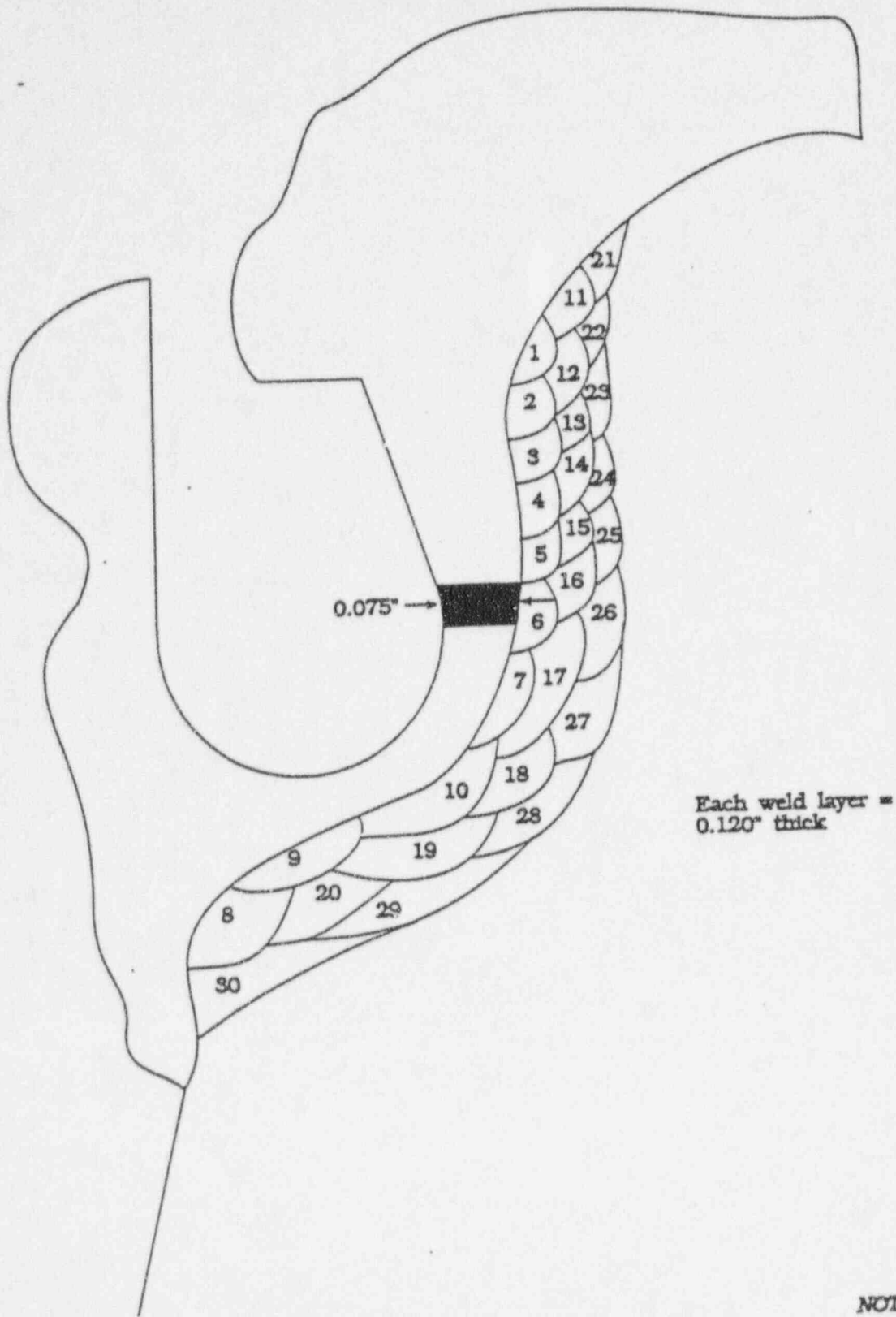
Figure 2-3. Canopy Seal Weld Overlay Design Bead Sequence

Structural Integrity Associates, Inc.

3.0 WELD RESIDUAL STRESS AND STRESS INTENSITY FACTOR ANALYSIS

Weld overlay repair residual stress and stress intensity factor analyses for the Sequoyah CRDM lower canopy seal were performed, for use in fracture mechanics crack growth evaluations of the repair.

3.1 Methodology

These stress predictions are made through the use of a thermal-elastic-plastic finite element program **WELD3** [8]. Details of the methodology, including assumptions, are given in Appendix A to this report. Dimensions of the component (Figures 1-1 and 1-2) are similar to those at Zion and Diablo Canyon [2,3], and welding parameters are given in Appendix A, as used in this analysis. It can be seen in Appendix A that this analysis consists of essentially two parts; a thermal analysis and a stress analysis, to model the welding process in both thermal and mechanical respects.

Fracture mechanics stress intensity factors (K) were also computed for the design repair, using a finite element model and the concept of elastic energy release rate [14], as detailed in Appendix A. This result was used to check the more general fracture mechanics crack model [11] results used in crack growth remaining life predictions. Such verification of K is considered important for the CRDM lower CSW geometry, because of the boundary conditions and constraints imposed by the adjacent thicker sections of the component.

3.2 Residual Stress Analysis and Results

Detailed residual stress results are given in Appendix A. The results of this analysis are to be used to develop fracture mechanics stress intensity factor (K) solutions for use in a fracture mechanics crack growth law.

3.2.1 Model

The overall finite element model used for the **WELD3** analysis is shown in Figure 3-1.

Figure 3-2 shows the sequence of welding the repair overlay. This model was developed to provide the capability to analyze up to three 0.12 inch thick layers of Alloy 625 weld overlay, with each layer bead sequence starting at the top as shown in Figure 3-2. Note that the bead sequences run from top to bottom in all cases, except for segments 4 and 5 in the first layer. This model is in accordance with the Zion repair mock-up results [9].

The meridional stresses at Section C are of primary interest for the crack growth analysis. However, a study of stress contours resulting from the **WELD3** analysis (Appendix A) revealed that the highest meridional stresses occur at Section D, which is immediately adjacent to the original lower CSW location. The meridional stress results for Sections A, B, C and D are shown after each of the three layers are deposited for the final design in Figures 3-3 through 3-5. These residual stresses are those resulting from welding, and after the component is cooled to 100°F. Note that the stresses after the third layer are significantly lower in the region at the inner surface of the CSW. Figure 3-3 shows the resultant residual stresses after the 3-layer repair, for Sections A, B, C and D, when heated to a service temperature of 550°F. It can be seen in Figure 3-3 that the stresses at the inner surface, where a crack could exist, are lower at 550°F than at 100°F in Figure 3-4. This is further illustrated in Figure 3-5. Thus, the results at 100°F will be used as the bounding case for the crack growth remaining life predictions. Additional verification of this conclusion was found in stress intensity factor calculations which showed that the crack growth rates for cracks with initial depths of up to 0.075 inches are smaller for the 550°F stress distribution than for the 100°F distribution.

3.3   Stress Intensity Factor

The pc-**CRACK** Model A is shown in Figure 3-7. This model represents a continuous surface crack in half space [11]. This crack model realistically models the decrease in stress field due to the secondary nature (and thick-section constraints) of this stress, as the crack extends.
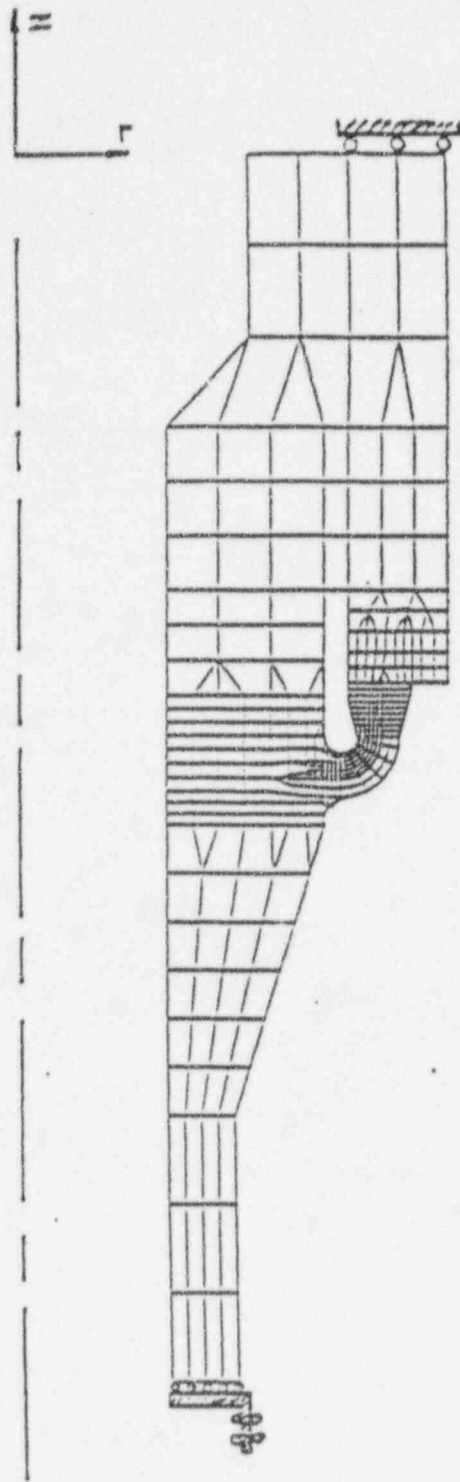
(illustrated mesh is for a 0.32 inch overlay thickness)

Figure 3-1.   WELD3 Axisymmetric Finite Element Grid Used for Overlay Weld Modeling with Illustration of Boundary Conditions
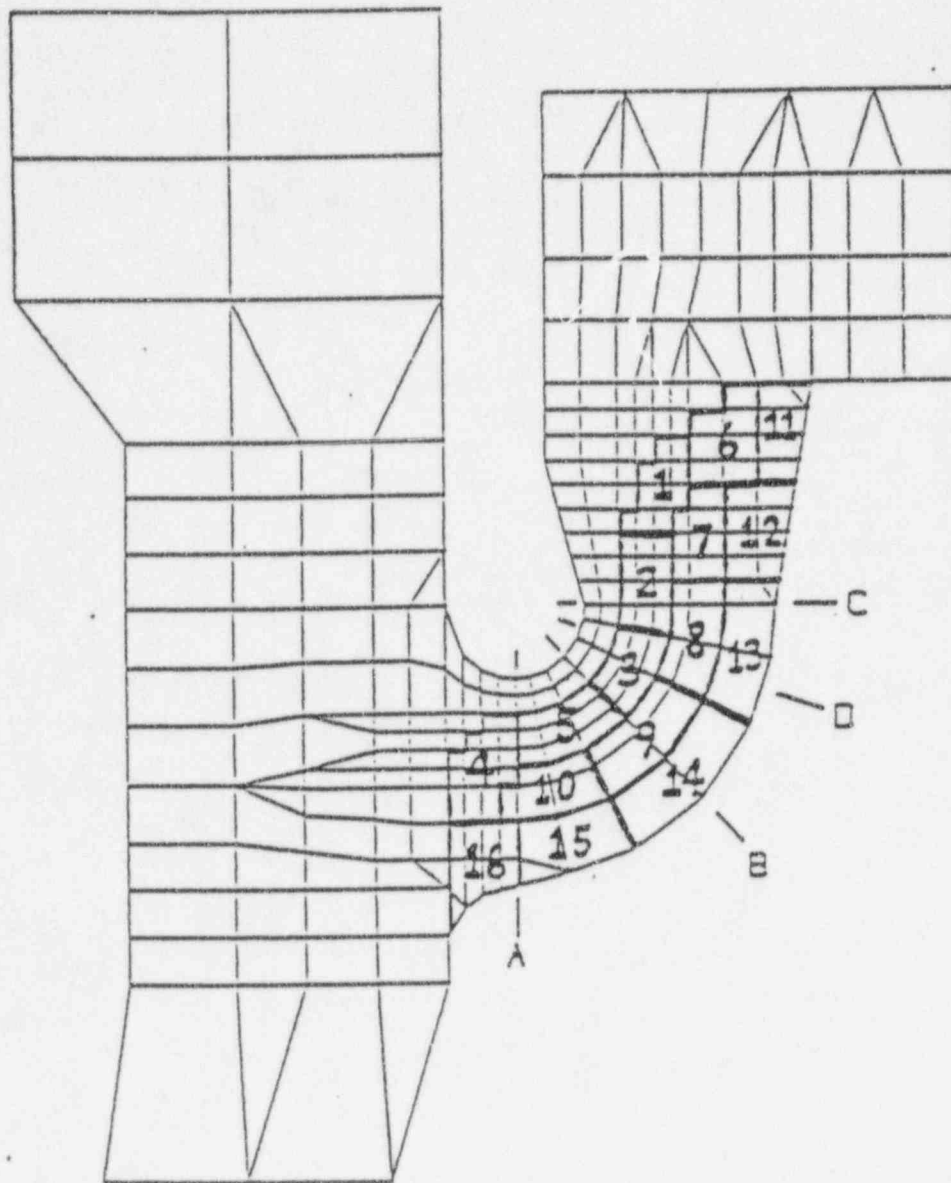
Figure 3-2. Definition of Overlay Weld Model Segments for the Overlay Design Analysis

Structural Integrity Associates, Inc.
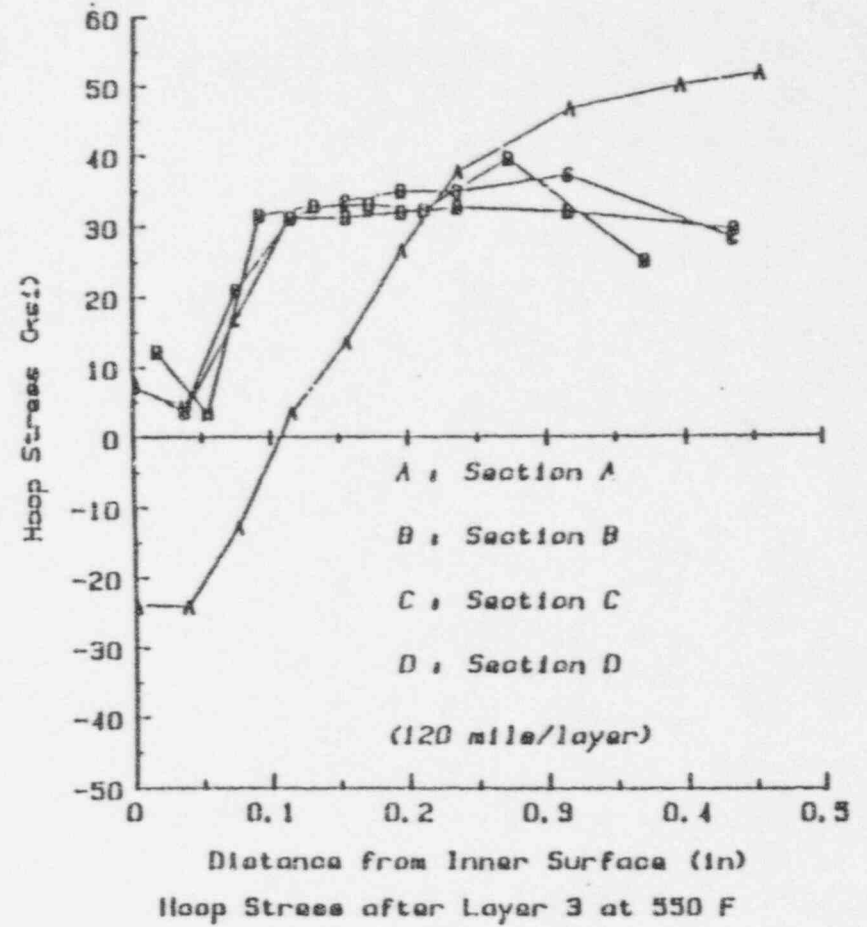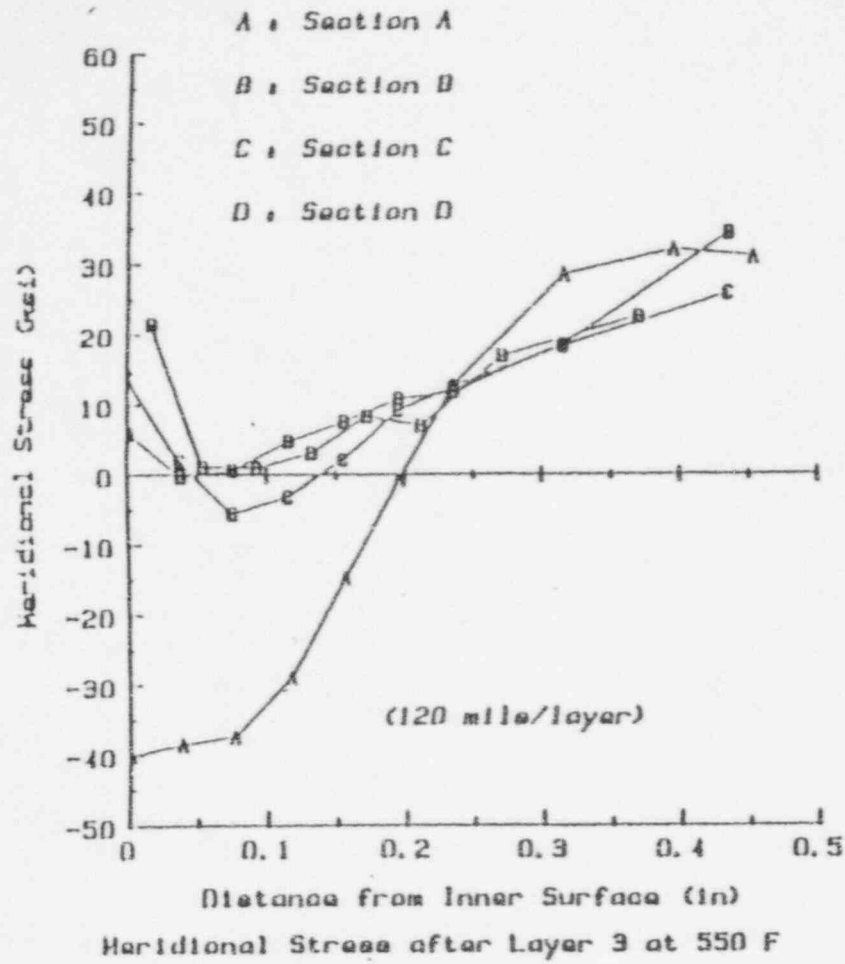
Figure 3-3.   Stresses at Sections A, B, C, and D After the Last Layer of the 3-Layer Overlay Design and After Being Heated to 550°F
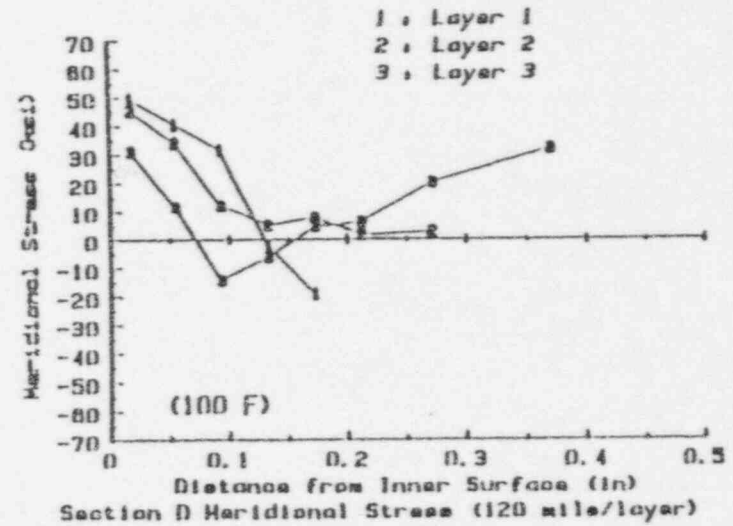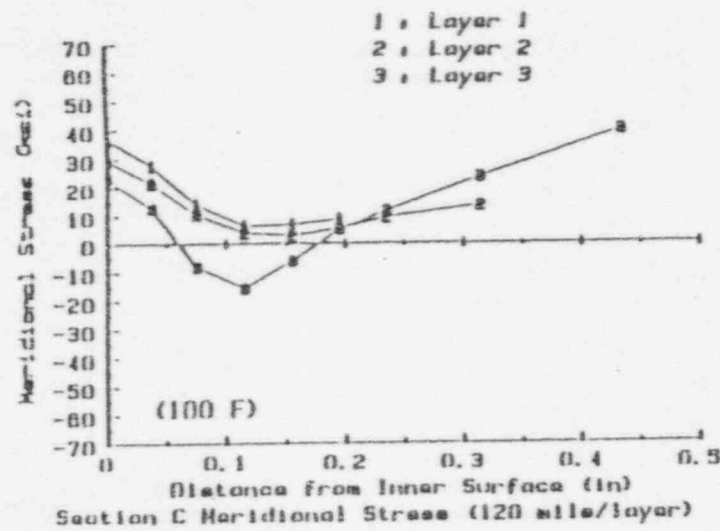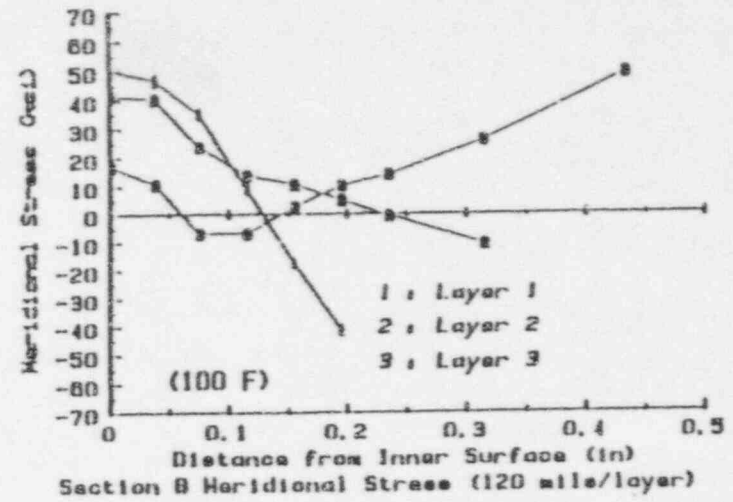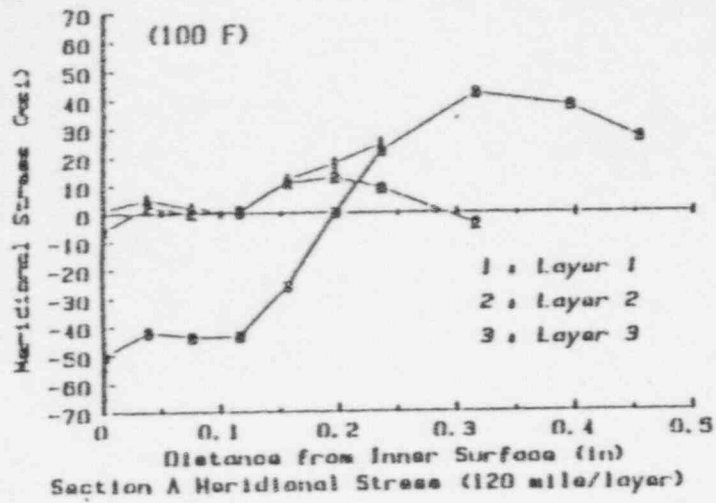
Figure 3-4. Meridional Stresses at Sections A, B, C, and D After Each Layer of the 3-Layer Overlay Design at 100°F
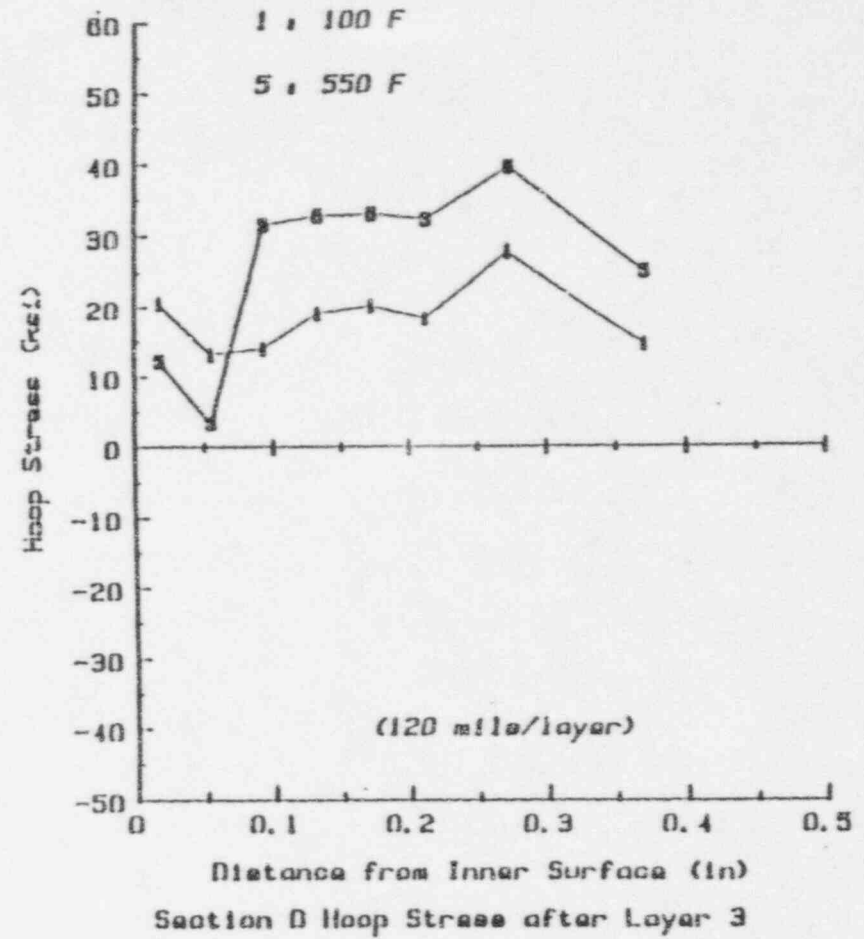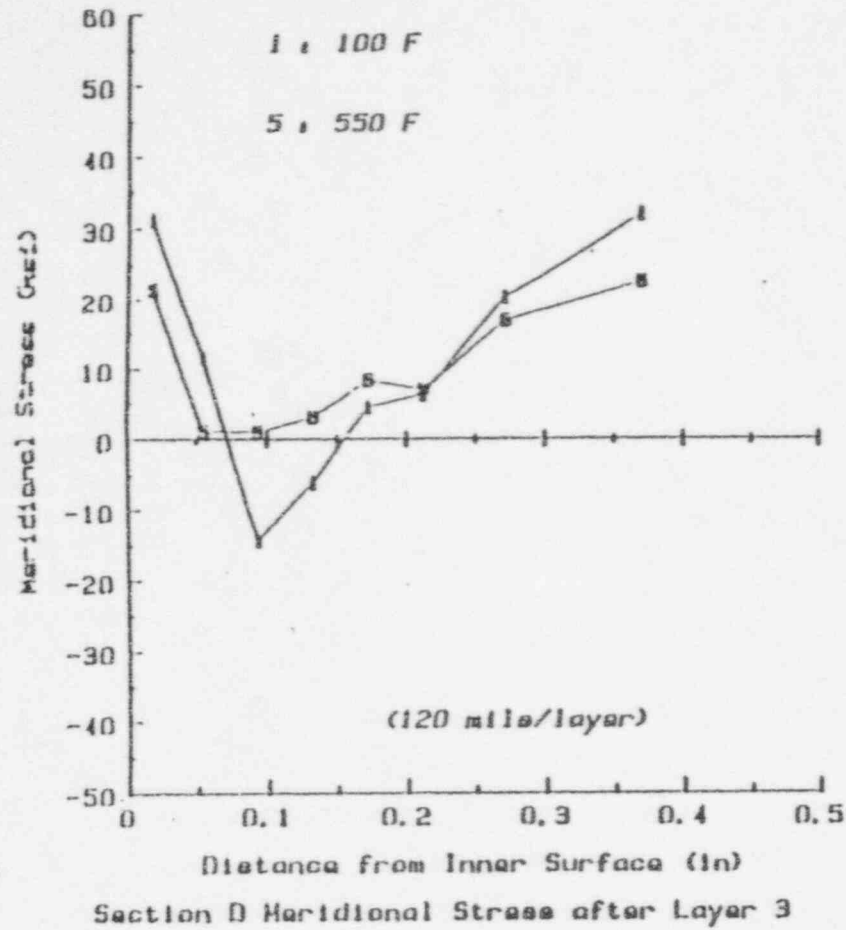
Figure 3-5.   Comparison of Stresses at Section D for the As-Welded Condition at 100°F and After Heating to 550°F

The figure shows a continuous surface crack in half space with the stress distribution:

$$\sigma = C_0 + C_1 x + C_2 x^2 + C_3 x^3$$

with axes z and r (x), and crack depth a.
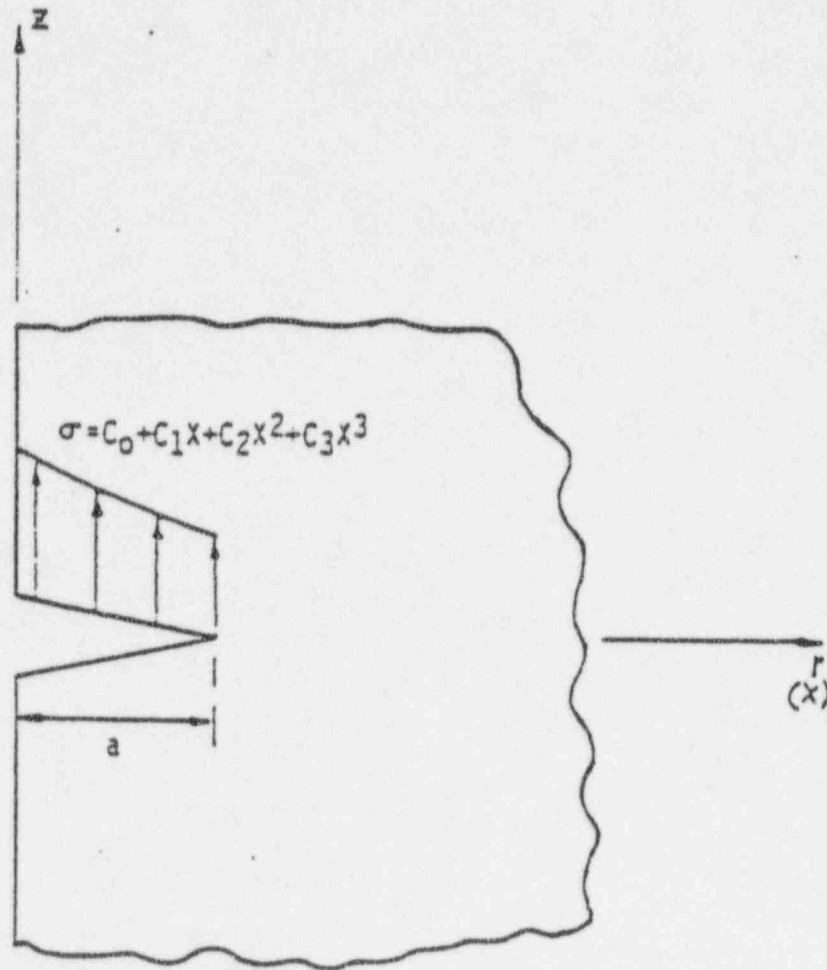
Figure 3-6. Fracture Mechanics Crack Model A - Continuous Surface Crack in Half Space [11]

Structural Integrity Associates, Inc.
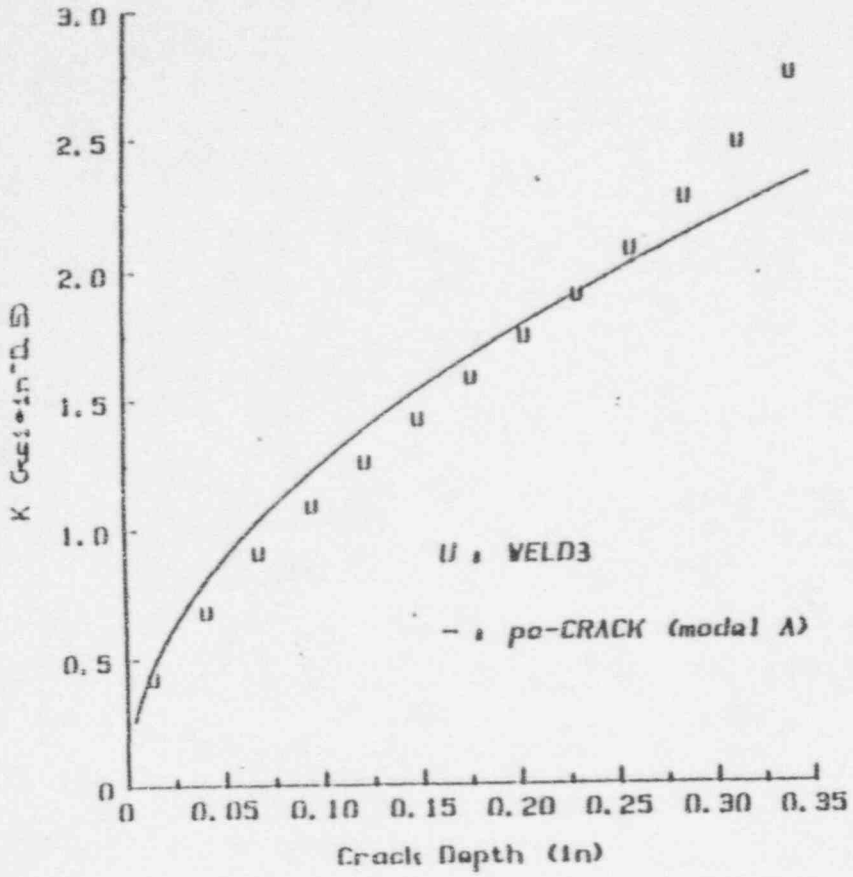
a. Uniform 2 ksi applied stress
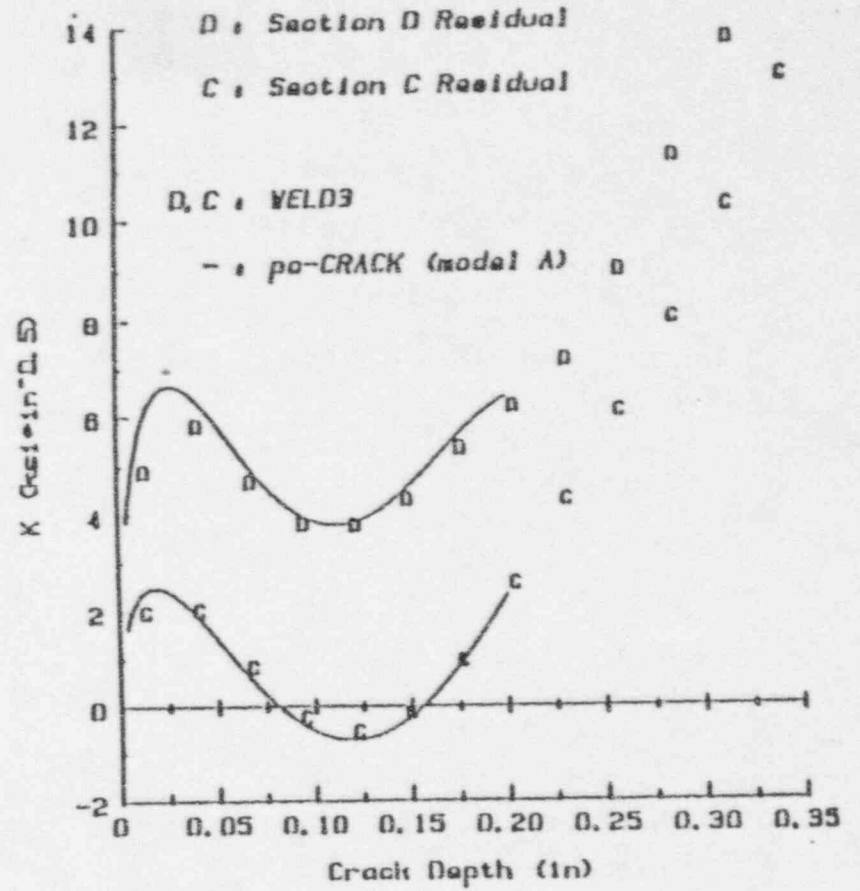
b. Section D and C residual stresses

Figure 3-7.   Comparison of WELD3 Stress Intensity Factor Calculations with those of pc-CRACK

4.0 CRACK GROWTH RATE EVALUATIONS

The fracture mechanics program pc-CRACK [11] was employed with the preceding calculated residual stress distributions and the following crack growth law to estimate SCC crack growth rates in the repairs. The initial flaw for such an evaluation is conservatively assumed to be completely through the wall of the original CSW (0.075 inch thick wall).

4.1 Crack Growth Law

The crack growth law for SCC has the following form:

$$\frac{da}{dt} = CK^n$$

where da/dt is the crack growth rate in in/hr, K is the stress intensity factor in ksi $\sqrt{in}$, and C and n are constants which depend on the material and environment. The stress intensity factor K is computed as a function of stress and crack size for a given geometry [11].

The objective here is to estimate an SCC growth law for the fracture mechanics analysis of remaining life of the Alloy 625 weld repair to the Sequoyah lower canopy seal weld on the CRDM. Several references [4,5, 15-20] have disclosed relevant data, for both high oxygen coolant (as in a crevice) and off-chemistry conditions, including sulfates, caustic and chlorides.

Fracture mechanics test crack growth rates from [15], in water with 7 ppm. O_2 and 1 ppm. H_2SO_4 at 550°F, are shown plotted in Figure 4-1 for various Inconel alloys. This figure also shows data on Type 304 stainless steel which was used by the NRC in NUREG-0313, Rev. 2 to derive an SCC law for stainless steel:

$$\frac{da}{dt} = 3.59 \times 10^{-8} K^{2.161}$$

where da/dt is in in/hr and K is in ksi $\sqrt{in}$.

It is assumed that the exponent of the power law remains the same for stainless steel base metal/weldments and Inconel alloys. Thus the exponent of 2.161 is also used for Inconel alloys. Based on this assumption, curves are drawn on Figure 4-1 through the data points for Alloys 600 and 690. The curve for crack growth a factor of 10 lower than the NRC curve, which was derived based on canopy seal weld cracking of Type 308 at Diablo Canyon [3], is also shown. The values of C for these curves are derived as follows:

$$NRC/10: \quad C = 3.59 \times 10^{-9}$$
$$\text{Alloy 600:} \quad C = 1.61 \times 10^{-8}$$
$$\text{Alloy 690:} \quad C = 4.95 \times 10^{-10}$$

References 15 and 17 state that SCC resistance in Fe-Cr-Ni alloys is a strong function of Cr content. Furthermore, the Mo and Nb contents in Alloy 625 are judged [18,19] to further mitigate SCC even though their effect is not as strong as that of Cr content. Thus, C is computed as 1.11×10^{-9} for Alloy 625, based on a Cr content of 21% Cr and linearly interpolating the factor of improvement of 32.5 for C in going from Alloy 600 (15% Cr) to Alloy 690 (29% Cr). This curve for Alloy 625 is plotted as the dashed curve in Figure 4-1. The law for crack growth a factor of 20 slower than the NRC curve for Type 304, and a factor of 2 slower than the NRC/10 curve used for Types 308L and 316L weld metal at Diablo Canyon [3], is shown in Figure 4-1 to be just above the estimated Alloy 625 curve. The Diablo Canyon curve is based upon actual CSW estimated crack growth rates. Thus, the NRC/10 curve is used to bound the Alloy 625 estimated growth rates, and the following law is employed for Sequoyah remaining life predictions for the Alloy 625 weld repair:

$$\frac{da}{dt} = \frac{3.59 \times 10^{-8}}{10} K^{2.161}$$

The following non-quantitative test specimen (U-bend) results generally support the use of the above law for other postulated off-chemistry environments. Results [4] in 50% caustic show Alloy 625 to crack about 90 times slower than Type 304, justifying the NRC/20 curve for this environment. Results [16] in $MgCl_2$ and with 500 ppm Cl show no cracking for Alloy 625, whereas Type 304 cracked. Results [17] in high oxygen (6, 20-100 ppm) with varying pH (some induced by H_2SO_4), show general agreement with the da/dt results in Figure 4-1. The da/dt results are 7 times to 50 times lower than for Type 304 when estimated from U-bend tests for Type 304 and Alloy 625. It should be noted, however, that the above data is generally from tests of Alloy 625 wrought material. Alloy 625 weld material may be slightly more susceptible to SCC propagation [20]. Because of the potential increase of susceptibility of Alloy 625 weld metal as compared to wrought 625 metal, the NRC/10 law will be employed for remaining life predictions in this study.

4.2   Remaining Life Estimate

The fracture mechanics program pc-CRACK [11] was employed to compute crack growth rates and remaining lives (to penetration of the crack to 75% of the repaired wall thickness) for the overlay repair design. The postulated initial defect for these analyses is an infinitely long crack completely through the original 0.075 inch wall of the CSW. A bounding 2 ksi applied stress [2,3] and the residual stress distributions shown in Section 3.0 of this report were used to compute K as input to the NRC/10 crack growth law. This law is as follows:

$$\frac{da}{dt} = 3.59 \times 10^{-9} \ K^{2.161}$$

where da/dt is in in/hr and K is in ksi $\sqrt{in}$.

The meridional residual stress distributions for Sections C and D at 100°F, presented in Section 3.0 for the 3-layer (each layer is 0.12 inch thick) design, were employed as discussed above (with a 2 ksi applied stress) to compute crack growth rates. The remaining life for the repair is predicted to exceed 57 years (the longest the analysis was run).

4.3　Fatigue Crack Growth

The increased section thickness in the canopy seal region reduces the stress significantly as compared to the stresses in the original CSW as reported in [12]. The cyclic stresses in the as-overlay-repaired condition are predicted to be well below the endurance limit for the Alloy 625 material, so fatigue usage for the unflawed material is not a concern. Fatigue crack growth of existing defects is also not a concern, since the as-repaired cyclic stresses are small and the predicted number of cycles [12] is also small.

Figure 4-1. NRC Crack Growth Rate Data and Curve for Type 304 Stainless Steel [5], with Data [15] and Estimated Curves for Fe-Cr-Ni Alloys

5.0   CONCLUSIONS

The following conclusions resulted from this study.

1.   The minimum required design thickness of the CSW overlay repair, in accordance with ASME Sections III and XI, and NRC requirements for structural reinforcement is 0.0511 inch. This thickness accounts only for structural reinforcement, with no crack growth considered. Further considerations of SCC growth rates follow below. This overlay should be blended into the thicker sections of the head adapter and CRDM pressure housing, as shown in this report. In order to provide SCC resistance, the selected repair material is Alloy 625 weld filler metal, using the GTAW (TIG) process.

2.   A fracture mechanics, SCC growth law for Alloy 625 a factor of ten slower than the upper bound NRC curve for IGSCC in Type 304 is justified for the remaining life predictions of the repair. This law is based upon experience with CSW cracking rates with Type 308 welds, upon crack growth rate data for Alloys 600 and 690, and upon a comparison with the SCC resistance of Alloys 600 and 625 versus Type 304 in various off-normal chemistry environments.

3.   A Code reconciliation was performed establishing the acceptability of using the 1989 Edition of ASME Sections III and XI for the overlay repair.

4.   The overlay weld repair design employs three layers, each 0.12 inch thick, of alloy 625 overlay, with the bead sequence starting at the top of the component for each layer. The predicted remaining lives for critical cross-sections of this repair, based on a residual stress analysis and a 2 ksi applied stress, are in excess of 57 years for the NRC/10 law.

5.   The effects of service temperature and repair bead sequence completion were also examined in this analysis. Results suggest that residual stresses are improved for this design when welding heat inputs are kept low; thus, avoid high heat inputs. Furthermore, the significant addition of an SCC-resistant material during this repair serves to substantially mitigate further leakage.

6.0 REFERENCES

1. Westinghouse Electric Corporation Drawing Number 541F469, Revision 2, Control Rod Mechanism Head Adapter Details, March 31, 1977, SI File No. WSI-20Q-213.

2. Copeland, J. F., et al, "Design and Analysis of a Weld Overlay Repair for the Zion CRDM Canopy Seal Welds", SI Report No. SIR-88-040, Revision 1, SI File No. WSI-11Q-200.

3. Copeland, J. F., et al, "Design and Analysis of a Weld Overlay Repair for the Diablo Canyon CRDM Canopy Seal Welds", Structural Integrity Report No. SIR-88-029, September 1988, SI File No. WSI-11Q-201.

4. McIlree, A. R., and Michels, H. T., "Stress Corrosion Behavior of Fe-Cr-Ni and Other Alloys in High Temperature Caustic Solutions", Corrosion-NACE, Vol. 33, No. 2, February, 1977, pp. 60-67, SI File No. WSI-11Q-203-1.

5. NUREG-0313, Revision 2, "Technical Report on Material Selection and Processing Guidelines for BWR Coolant Pressure Boundary Piping", U.S. NRC, January, 1988.

6. ASME Boiler and Pressure Vessel Code, 1989 Edition, Sections III and XI with no Addenda.

7. Section XI Task Group for Piping Flaw Evaluation, ASME Code, "Evaluation of Flaws in Austenitic Steel Piping", Journal of Pressure Vessel Technology, Vol. 108, August, 1986, pp. 352-366, SI File No. WSI-11Q-203-2.

8. Stonesifer, R., et al, "**WELD3** Computer program Verification Manual", April, 1988.

9. Telecopy, Reed, L. (Welding Services, Inc.) to Gerber, D. A., (Structural Integrity), Welding Parameters, SI File No. WSI-11Q-205.

10. Structural Integrity Associates Calculation No. WSI-11Q-302, Revision 0, dated April 13, 1992, "Crack Growth Analysis of CRDM Lower CSW Overlays."

11. Structural Integrity Associates pc-**CRACK**, Version 2.1, 1992.

12. Westinghouse Electric Corporation, "High Speed Control Rod Drive Mechanism Stress Analysis", E3980, Addendum 4.

13. ASME Code Case N-504-1, August 1993.

14. Rybicki, E. F., Stonesifer, R. B., and Olson, R. J., "Stress Intensity Factors Due to Residual Stresses in Thin-Walled Girth Welded Pipes", Journal of Pressure Vessel Technology, Vol. 103, 1981, pp. 66-75.

15. Page, R. H. and McMinn, A., "Stress Corrosion Cracking Resistance of Alloys 600 and 690 and Compatible Weld Metals in BWRs", EPRI Report No. NP-5882M, July, 1988, SI File No. WSI-11Q-203-3.

16. Telecopy, Nelson, J. L. to Giannuzzi, A.J., Alloy 625 SCC Results, October 25, 1988, SI File No. WSI-11Q-203-4.

17. Nelson, J. L. and Floreen, S., "An Evaluation of the SCC Behavior of Inconel Alloy 690 Weldments in a Simulated BWR Environment", SI File No. WSI-11Q-203-5.

18. Yamauchi, K., et al, "Effect of Niobium Addition on Intergranular Stress Corrosion Cracking Resistance of Ni-Cr-Fe Alloy 600", Proceedings of the Corrosion Cracking Program, ASTM, ASME, NACE, etc., Salt Lake City, Utah, December 2-6, 1985, pp. 11-22, SI File No. WSI-11Q-203-6.

19. Frank, R. B. and DeBold, T. A., "Properties of an Age-Hardenable Corrosion-Resistant Ni-Based Alloy", Materials Performance, NACE, September, 1988, pp. 59-66, SI File No. WSI-11Q-203-7.

20. ABB Atom AB, "Stress Corrosion Cracking of Alloys 600 and 182 in BWR Environments - Interim Report", TR-100658, EPRI, May 1992.

APPENDIX A

Detailed Description of Weld Residual Stress
and Stress Intensity Factor Analyses for the
Sequoyah Lower CRDM Canopy Seal Weld Overlay Repair

INTRODUCTION

SI reported on the overlay designed for the Zion spare CRDM canopy seal [1][1]. The Zion canopy seal and overlay design are identical to the Sequoyah CRDM lower canopy seal and overlay design. A weld mock-up was prepared for the Zion design and verified against the welding residual stress model. This appendix provides the details of the residual stress analyses performed to support the weld overlay design at Zion and its application to the current overlay design for Sequoyah.

WELD MODELING BACKGROUND

The **WELD3** software for welding analysis consists of several computer programs which are used for predicting temperature transients, predicting residual stress changes due to these temperature transients, and then graphically presenting the results of the temperature and stress analyses. The stress predictions are made through the use of a thermal-elastic-plastic finite element program. The programs which are responsible for temperature predictions rely on a variety of analytical solutions to basic heat conduction problems associated with moving and stationary heat sources, on semi-empirical formulas and approximations to other heating methods of interest such as induction heating, and on nonlinear heat transfer finite element methods.

The methodology for modeling welds was initially developed at Battelle's Columbus Laboratories under funding first from the U.S. Nuclear Regulatory Commission and then from the Electric Power Research Institute [2-7]. Since this initial work, extensions and refinements have been made to the methodology through continued EPRI support [8] as well as through applications of the methodology to a variety of electric power industry related problems [9-17].

The WELDS II software evolved with the methodology [2-8], and as a result of the code evolution, and a low emphasis on computational efficiency, the WELDS II software became inefficient, highly patched, and generally difficult to maintain. The solution to these problems has been the development

---

[1]Reference numbers refer to those at the end of this appendix.

of a completely rewritten set of software tools known as **WELD3** [18,19]. Since the people who originally developed the methodology and the WELDS II software have developed **WELD3**, all that was learned from the evolution of the WELDS II software has been applied to the design, development, and verification of the new software. The **WELD3** software is used for the weld modeling of this study.

OVERLAY WELDING TEMPERATURE CALCULATIONS

The geometry of the lower CRDM canopy seal is defined in Figures A-1 and A-2. Figure A-3 shows the axisymmetric finite element grid which was used for the **WELD3** simulations of the weld overlay. The model did not include pre-existing cracks. The assumed mechanical boundary conditions and the analysis coordinate system are also illustrated in Figure A-3. The boundary conditions did not allow rotation at either end of the modeled region, but did allow unconstrained radial or axial shrinkage and expansion. For the thermal analyses, all model boundaries were assumed to be insulated.

Heat Input Rates.

The overlay welding technique was assumed to result in an electrical input energy of 13.9 kJ/in for the passes of the first weld layer and 16.6 kJ/in for the passes of the remaining layers. The welding speed for all layers was assumed to be 3.5 ipm. These energy rates resulted from actual amperage, voltage and weld speed used during construction of the Zion mock-up overlay repairs at Welding Services, Inc. [20]. The finite element thermal solutions assumed a weld heat input efficiency of 40%. This means that the thermal input was 40% of the electrical input energy. This efficiency was based on the work of Christensen, et al [21] on TIG welding of steel as reported by Masubuchi [22]. It was found in the thermal modeling that this efficiency resulted in reasonable temperatures for the simulation of the first weld layer. A higher efficiency would have resulted in the model predicting burn-through.

Definition of Model Weld Segments

One major simplification of the weld overlay modeling methodology is the grouping of several weld passes into a weld segment [4,9,10]. This reduces the input preparation and computational expense in proportion to the number of passes which are grouped into a modeled segment. Figure A-4 shows how the finite elements used to represent the overlay weld material were grouped into weld segments. Sections A, B, C, and D of Figure A-4 are the sections for which through thickness residual stresses and crack growth rates were considered.

Figure A-4 shows the model which reflects the overlay design. As can be seen, this model assumed up to three weld layers with each layer being 0.120 inches thick. The welding sequence was that passes were generally put down starting from the top of the canopy seal. This sequence and the "end-in" sequence of the first layer was adopted in an attempt to minimize the possibility of burn-through.

In grouping passes into model segments for the present analysis, it was assumed that as thinner sections are modeled, the number of passes that can be reasonably included in a segment becomes smaller. Therefore, while some heavy section weld overlays have been modeled by grouping as many as 10 passes into a segment (more typically 4 or 5), the models of this study grouped approximately two passes into a weld segment.

In butt weld and overlay simulations of heavier sections, it has generally been found necessary to modify the thermal analysis to account for modeling more than one pass per model segment [5,10]. When using analytical solutions, this is usually accomplished by artificially widening the computed isotherms to match the width of the weld segment. Due to the tendency for weld passes to overlap, due to the grouping of only two passes into a weld segment, and due to the difficulty of adopting the isotherm widening technique when using a numerical thermal analysis approach, no such modifications were applied to the thermal analyses of this study. The credibility of the isotherms from the resulting finite element thermal analyses and the fact that sufficient heat input existed to raise the

Structural Integrity Associates, Inc.

weld segments and neighboring material to temperatures at which stresses are largely relieved, support the reasonableness of the adopted analysis procedures.

Weld Deposition Modeling Approach

The **WELD3** finite element thermal analysis simulated the sequential deposition of weld metal by sequentially activating appropriate elements and nodes as each weld segment was "deposited". The output from the thermal analysis which was used as input for the stress analysis consisted of a file of element temperatures. Inactive elements were given a temperature which was above the stress-free temperature defined in the stress analysis input. Elements above the stress-free temperature have an insignificant stiffness and are assumed (i.e., forced) to have zero stress and strain and thus do not significantly affect the stresses or displacements in the material which does exist. The stress free temperature was selected so as to be consistent with the input mechanical property data. In the present analyses, the stress-free temperature was assumed to be 2000°F. It can be seen from the assumed temperature dependent properties of Table A-1 that this temperature resulted in the stiffness of the stress-free or "inactive" elements being small compared to the stiffness of "active" elements.

Transient Thermal Modeling Approach

The combination of thin sections and curved boundaries of the canopy seal made the usual temperature calculation procedures for welded overlays inappropriate. Typically, weld overlays have been applied to sections which could be accurately represented as being an insulated half space, or as being a uniform thickness plate or pipe wall. The wall is generally assumed to be insulated at the outer surface and the inner surface is either assumed to be insulated or to have a water heat sink. Transient thermal solutions for a steadily moving point heat source and such idealized boundary conditions are easily obtained using analytical solutions. Temperatures for the canopy seal weld overlay simulations were computed using the finite element method. This numerical method was better able to model the curved boundaries of the canopy seal geometry than simple analytical models and also made it possible to include the effects of temperature dependent thermal properties. While it would have been possible to include other factors such as convective or radiant heat losses at the

surfaces, the present analyses assumed all surfaces were insulated (i.e., heat loss at the surfaces was included in the welding efficiency factor). While the finite element model has apparent advantages over the analytical models, the movement of the welding arc in the circumferential direction cannot be exactly represented using a 2D axisymmetric finite element model.

Since the numerical thermal model simulated a 3D moving heat source problem using a 2D axisymmetric assumption, some approximations were inherent [18]. The heat input to the 2D numerical model was computed from the welding heat input rate (Btu/in) by multiplying this input rate by the circumferential length of the pass or segment being modeled. This amount of heat was input to the model at nodes which were interior to the weld segment being deposited using a ramp function (with respect to time) which started from zero at -1 second, rose linearly to a peak value at t=0, and then decreased linearly to zero at +1 second. Using this approach, t=0 approximately represented the time when the welding arc passed the plane for which the thermal transient was being modeled. This approach has been found to produce results which are relatively insensitive to the length of time used for the ramp function heat input [18].

Using the 2D axisymmetric finite element approach for modeling the thermal transient due to a moving point heat source has been found to predict peak temperatures which tend to be on the order of 10% higher then those from a comparable 3D analytical solution [18]. This tendency is apparently the result of heat flow parallel to the heat source path in the 3D solution that is not reflected in the 2D solution. That is, the cool material ahead of the heat source acts as a heat sink for times shortly after the passing of the heat source. For times when the heat source is several thicknesses beyond the modeled section, the 2D and 3D solutions are in near perfect agreement (assuming material and geometric representations are consistent for both solutions).

Another factor which enters the thermal analysis when using the numerical solution approach rather than an analytical approach is the effect of time step size and the number of time-steps used to obtain the transient thermal solution. For the present analyses, 10 time-steps of 0.2 seconds were used for the two-second heat input phase of the solution. Then time-step sizes were increased to values ranging from 0.25 to 1.0 seconds depending on the cooling rate (i.e., thickness of the segment being

SIR-95-105, Rev. 0   A-6   Structural Integrity Associates, Inc.

modeled and the time). A sensitivity study on time step size showed that changing time-step size by a factor of two did not significantly affect the results.

It was found that the combination of using temperature dependent properties and finite time-step sizes tended to result in some integration-related error. The method for quantifying this error was to compute the heat content of the entire model and then to compare this to the specified heat input. It was found that the heat content could become 5 to 10% greater than the specified heat input. The origin of this discrepancy was determined to be the temperature-dependent properties and the solution procedure which uses temperatures at the beginning of the increment to interpolate material properties. Since temperatures generally increase during the time period that was modeled and heat capacity increases with temperature, the solution tended to underestimate heat capacity and thus over-predicted temperatures.

The combined effect of the time-step integration error and the 2D modeling effect discussed previously, could have produced temperatures on the order of 15% above those that would be predicted using a 3D model and very small time-step sizes. While this may sound like a rather large error, it should be kept in mind that the welding heat efficiency has an uncertainty of at least 10% (more likely 20%). It is possible to adjust the heat input to the model so that calculated heat contents are more in line with the desired welding heat input, thus correcting to some extent the integration related error. The overlay analysis used this correction approach by reducing nodal heat inputs by 5%. Therefore, heat content errors were reduced to 0 to 5% above the desired heat input. To the extent that higher heat input rates are believed to create less favorable residual stresses for the canopy seal overlay geometry, any tendency of the model and modeling assumptions to over-predict temperatures is believed to introduce conservatism into the analysis. Therefore, with the uncertainty regarding actual welding efficiency, the approach was to err on the side of higher temperatures. The analysis did not predict unreasonably high temperatures during the welding of the first overlay layer (when errors in heat input would be most apparent); therefore, it seems that the analysis did not produce overly conservative results.

TEMPERATURE RESULTS

Since no thermocouple measurements were taken during the Zion mock-up welding, the primary basis for judging the reasonableness of the thermal analysis results was in terms of peak inner surface temperatures during the welding of the first overlay layer, and in terms of temperatures in the newly deposited material for times just after "passing" of the arc. Figures A-5 through A-8 contain isotherm plots for four of the 16 modeled weld segments of the analysis which assumed three weld layers at a thickness of 0.120 inches per layer. The isotherms are for the times at which temperatures were used for input to the residual stress analysis. The first plot for each segment is for the time when the new material has cooled to about 2000°F. The second plot is for the time when the new material has cooled to about 1100°F.

Figure A-5 shows isotherms for the weld segment of the first layer which produced the highest maximum inner surface temperature (about 2200°F). The plot is for a time shortly after this peak temperature was reached and thus has an inner surface temperature of about 2000°F. The isotherms clearly illustrate the effects of the thinner section below the weld.

Figure A-6 shows the isotherms for Segment 8 (which is in the second weld layer). Though the heat input for this layer is greater than for the first layer, the additional thickness results in lower peak inner surface temperatures than computed for the first layer. The peak computed inner surface temperature for the second weld layer was about 1125°F and occurred for Segment 9.

Figure A-7 shows the isotherms for Segment 14 which is the third from last segment of the third and last layer. The peak computed inner surface temperature for this layer of about 650°F occurred for this segment. The isotherm plot at 7.0 seconds corresponds approximately to the time of this peak temperature.

Figure A-8 shows the isotherms for the last segment of the last layer. This segment has the fastest cooling rate of all modeled segments due to the large volume of material surrounding the weld. The

peak inner surface temperature for this segment was about 375°F and did not occur until a time of about 8 seconds. By this time the weld region had cooled to about 550°F.

OVERLAY WELDING STRESS CALCULATIONS

The welding thermal transient for each weld segment was represented in the residual stress simulation by three temperature distributions. The first distribution corresponded to the point in time when the newly deposited material had cooled to about 2000°F. The second distribution corresponded to the point in time when the newly deposited material had cooled to about 1100°F. The third distribution was a uniform interpass temperature of 100°F (which was also assumed as the initial and final temperature).

The above described temperature analyses produced 48 temperature distributions for the 3-layer simulation. To determine the residual stresses, these temperature distributions were input to a 2D, incremental, thermal-elastic-plastic finite element stress analysis using the WELD3 software. The stress analysis assumed axisymmetric behavior as is usually done when modeling circumferential welds of axisymmetric geometries.

Essentially, all verification of the weld modeling methodology has involved showing that 2D models can provide reasonable estimates of residual stresses due to welding. The ability to use 2D models is fortuitous since the cost of doing 3D analyses would limit weld simulations to welds of little practical interest. For example, a recent study did a 3D analysis of a one-inch single pass weld on a 4 x 4 x 0.5 inch plate [23]. Extrapolating the cost of this analysis, a 3D analysis of a typical butt weld on a 24 inch pipe would take about one hour of Cray 2 CPU time for each 2 inches of weld. A 36 pass weld would, therefore, require about 1300 hours of Cray 2 CPU time (typically costing in excess of $1000.00 per hour).

Each temperature change associated with going from one temperature distribution to the next was simulated by subdividing the change into ten increments. This number of increments has been found to provide a good balance between solution stability/equilibrium/ convergence and cost.

Comparisons of predicted overlay induced stresses with measured overlay stresses have only been made for relatively heavy section overlays (typically with initial wall thicknesses of about an inch). The primary basis for expecting the methodology to provide reasonable predictions for the canopy seal is that the overlay welding methodology is a modification of an earlier developed butt weld modeling methodology which has been shown to reasonably predict stresses in sections as thin as 0.180-inches [2,3,18].

RESIDUAL STRESS RESULTS

Unlike overlays on heavier sections, the residual stress state of the canopy seal changed significantly as additional layers were added to the overlay. Residual stresses also sometimes changed significantly from the welding of one pass to the next. To determine the sensitivity of the final predicted residual stresses to overlay design parameters such as number of layers, layer thickness, welding direction, and weld bead position, stresses have been plotted and examined at various stages of overlay completion for the overlay design.

Stress Results for the Overlay Design

Figures A-9 and A-10 show the stresses at Sections A, B, C, and D after completion of each layer of the 3-layer design. It is seen that there is a significant improvement in the inner surface stresses with each additional layer. Examination of stress contour plots covering the entire seal region showed that the peak inner surface meridional stress occurred at Section D. Preliminary crack growth calculations further suggested that the through-thickness meridional stress distribution at Section D results in the most rapid crack growth rates of the Sections A through D.

Effect of Operating Temperature on Residual Stresses

All of the residual stress plots presented above were for the overlay welding reference temperature of 100°F. Since the overlay design calls for Inconel 625 weld metal to be used on a 304/308L

stainless steel component, and since the Inconel has a different coefficient of thermal expansion from the stainless steel, it is necessary to consider the effect of going to an operating temperature of 550°F.

Figure A-11 shows the residual stresses at the Sections A, B, C, and D at 550°F. Section D remains the critical section in terms of the least favorable meridional stresses as a result of the more tensile inner surface stresses.

Figure A-12 compares the Section D stresses for the 100°F and the 550°F conditions. The change in stress that is seen is due to the stainless steel having a larger coefficient of thermal expansion than the Inconel. For the meridional stresses, there are two effects occurring. First, the whole seal region is being stretched axially due to the larger expansion of the head/cap assembly. This stretching tends to make the inner seal surface more tensile and the outer surface less tensile. However, the stainless steel at the inner surface of the seal has its expansion constrained by the Inconel overlay so that stresses in the stainless steel portion of the seal actually become less tensile in spite of the overall tendency of the seal to have increased tensile stress at the inner surface. Stress intensity factor calculations showed that the crack growth rates for cracks with initial depths of up to 0.075 inches are smaller for the 550°F stress distribution than for the 100°F distribution.

STRESS INTENSITY FACTOR EVALUATIONS

All crack growth calculations have been done using the stress corrosion crack growth option of the pc-CRACK LEFM module [24]. However, the crack growth calculations for the overlay configuration were verified using stress intensity factor versus crack depth data developed with a finite element approach that accurately reflected the seal/overlay geometry. All crack growth calculations, were made using stress intensity factors calculated from an approximate geometric representation provided within pc-CRACK known as "Model A". This model is for a long surface crack in a half space.

Structural Integrity Associates, Inc.

The following discussion compares stress intensity factors based on the finite element method with those based on the approximate pc-CRACK geometric model and shows that use of the pc-CRACK Model A provided realistic crack growth predictions.

The Finite Element Mesh and Boundary Conditions

The geometry used for the finite element based stress intensity factor calculations was the 3-layer, 120 mil per layer, overlay design. Since the finite element mesh that was used for the overlay welding simulation did not provide for the introduction of a crack at the critical Section D, a special mesh was constructed for the stress intensity factor calculation. This mesh is shown in Figure A-13. The mesh differed from that of Figure A-3 in two respects. First, less of the head adapter was modeled. Second, the CRDM tube and the head adapter were not connected. Stress intensity factor results were found to be insensitive (approximately 1%) to the type of boundary conditions used at boundaries B1 and B2, thus justifying the first modeling change. No connection between the CRDM tube and the head adapter was assumed since the resulting reduction in radial restraint of the plug was believed to be more realistic and also produced slightly larger (approximately 5%), and thus more conservative, stress intensity factors.

The Stress Intensity Factor Calculation Method

The method used for stress intensity factor calculations was based on the concept of elastic energy release rate, and made use of the relationship between energy release rate and the stress intensity factor. Because the method was an energy method, accurate results could be obtained without resorting to highly refined finite element grids or special crack tip elements. While the method can be used to calculate mode II as well as mode I stress intensity factors, the mode II component was not significant for the residual stresses of the present study, and therefore only mode I behavior was considered.

The method consisted of generating an influence matrix relating nodal displacements and forces along the Section D crack plane. This matrix was constructed from a series of finite element analyses in

which different crack lengths were simulated by uncoupling node pairs along the crack plane. For the mesh of Figure A-13, which has 16 elements through the thickness at the crack plane, 15 crack lengths were modeled. Each crack length required a single elastic solution. The matrix was generated using unit nodal forces and, therefore, the resulting matrix could be used to calculate stress intensity factors for any stress distribution.

This method has been previously used to study elastic crack growth behavior in planar and axisymmetric bodies [25]. Figure A-14 compares a stress intensity versus crack depth solution obtained using this method to the exact solution given in [26]. Experience suggests that the stress intensity factor solutions resulting from the use of this method should be accurate to within 10% for the mesh refinement used in this study.

Stress Intensity Factor Results

The elastic modulus used for the stress intensity factor calculations was 28.0×10^6 psi (Inconel 625 at 550°F) and the Poisson ratio was 0.3. In converting from energy release rate to stress intensity factor, the crack tip was assumed to be in a state of plane strain.

Stress intensity factors for three stress distributions were considered. The first was the residual meridional stress at Section D after completion of the 3-layer overlay (120 mils/layer) and after heating to a uniform temperature of 550°F. The second stress distribution was the residual meridional stress existing at Section C for the same conditions. The third stress distribution was an assumed uniform applied stress of 2 ksi. For the finite element based method, the residual stress distribution was represented in a piece-wise linear manner. Therefore, there was little if any approximation involved in representing the stress distribution.

For the pc-CRACK-based method, it was necessary to fit the stress distributions with a third order polynomial. Therefore, in addition to the geometric approximation, there was also a stress distribution approximation. Only for the uniform applied stress was there no approximation of the stress distribution for the pc-CRACK calculations. Figure A-15 shows the quality of fit that could

A-13

Structural Integrity Associates, Inc.

be achieved for the two residual stress distributions using the third order polynomial assumed by pc-CRACK. Since crack growth is not predicted to result in crack depths greater than 0.2 inches over the lifetime of the overlay repair, the quality of the stress fit was improved by limiting the range of the fit to the first 0.2 inches of the wall thickness. Fitting stresses over the entire wall thickness significantly reduced the quality of fit with the reduction in quality being most significant for the Section D stress distribution. Figure A-16a compares the WELD3 and pc-CRACK stress intensity factor behavior for the uniform applied stress of 2 ksi. Since there was no stress distribution approximation in the calculations for this case, the difference in solutions is due to the difference in the assumed geometries and errors in the solution methods. The pc-CRACK results are about 10% above the WELD3 results at a depth of 0.1 inches. As might be expected, the pc-CRACK model becomes nonconservative for crack depths greater than half the wall thickness. Figure A-16b shows the pc-CRACK computed stress intensity factor distributions resulting from the polynomial fits of Figure A-15. Since the fits were for stresses within the first 0.2 inches of wall thickness, the stress intensity factors are only valid for crack depths up to 0.2 inches. The WELD3 based stress intensity factors and the pc-CRACK results are seen to be in good agreement over the range of crack depths up to 0.2 inches.

APPENDIX A

REFERENCES

1. Structural Integrity Associates Report SIR-88-040, Revision 0, "Design and Analysis of a Weld Overlay Repair for the Zion Station CRDM Canopy Seal Welds", December, 1988.

2. Rybicki, E. F., et al, "Residual Stresses at Girth-Butt Welds in Pipes and Pressure Vessels", Final Report to U.S. Nuclear Regulatory Commission, Division of Reactor Safety, Research under Contract No. AT (49-24)-0293, NUREG-0376, published November, 1977.

3. Rybicki, E. F., et al, "A Finite Element Model for Residual Stresses and Deflections in Girth Butt Welded Pipes", Journal of Pressure Vessel Technology, Vol. 100, No. 3, August, 1978, pp. 256-262.

4. Rybicki, E. F., et al, "Residual Stresses Due to Weld Repairs, Cladding and Electron Beam Welds and Effect of Residual Stresses on Fracture Behavior", Final Report to U.S. Nuclear Regulatory Commission, Division of Reactor Safety, Research under Contract No. AT (49-24)-0293, NUREG-0559, published December, 1978.

5. Rybicki, E. F. and Stonesifer, R. B., "Computation of Residual Stresses Due to Multipass Welds in Piping Systems", Journal of Pressure Vessel Technology, Vol. 101, No. 2, May 1979, pp. 149-154.

6. Rybicki, E. F. and Stonesifer, R. B., "An Analysis Procedure for Predicting Weld Repair Residual Stresses in Thick-Walled Vessels", Journal of Pressure Vessel Technology, Vol. 102, No. 3, 1980, pp. 323-331.

7. Brust, F. W. and Stonesifer, R. B., "Effect of Weld Parameters on Residual Stresses in BWR Piping Systems", Final Report to Electric Power Research Institute, NP-1743, Research Project 1174-1, March 1981.

8. Rybicki, E. F., et al, "Computational Residual Stress Analysis for Induction Heating of Welded BWR Pipes", Final Report prepared for the Electric Power Research Institute by the University of Tulsa, EPRI NP-2662-LD, Project T113-6, December 1982.

9. Stonesifer, R. B. and McConaghy, J. M., "Residual Stress Analysis of Sleeve to Safe-end Welds", prepared for Nuclear Technology Incorporated by Battelle Columbus Laboratories, Columbus, OH, December, 1978.

10. "Optimization of Weld Overlay Repair for BWR Piping Phase I", prepared for Electric Power Research Institute by NUTECH Engineers, Inc., San Jose, CA, June, 1983.

11. Tang, S. S., Stonesifer, R. B., and Javid, A., "Design Report for Recirculation Piping Sweep-o-lets Repair and Flaw Evaluation Brown's Ferry Nuclear Plant Unit 1", prepared for Tennessee Valley Authority by Structural Integrity Associates, San Jose, California, October 1983.

12. Stonesifer, R. B., Kuo, A. Y., and Gerber, T. L., "Analysis of Browns Ferry Unit 3 Jet Pump Instrumentation Nozzle Safe-end Repair", prepared for Tennessee Valley Authority by Structural Integrity Associates, San Jose, California, July, 1984.

13. Stonesifer, R. B., Tang, S. S., "An Evaluation of IHSI Temperature and Heating Cycle Limitations", prepared for NUTECH Testing Corporation by Structural Integrity Associates, San Jose, California, August 1984.

14. Stonesifer, R. B., "Browns Ferry Unit 2 Recirculation Inlet Safe-ends Determination of Residual Stress Distribution for 'Modified Full Structural' Weld Overlay", prepared for Tennessee Valley Authority by Structural Integrity Associates, San Jose, California, September, 1986.

15. "Development of Inconel Weld Overlay Repair for Low Alloy Steel Nozzle to Safe-end Joint", prepared for Georgia Power Co. and Electric Power Research Institute by Georgia Power Co. and Structural Integrity Associates, October, 1986.

16. "Contingency Plan for Inconel Weld Overlay Repair to Carbon Steel to Cast Valve in RHR System at Fitzpatrick", prepared for New York Power Authority by Structural Integrity Associates, San Jose, California, December, 1986.

17. Stonesifer, R. B., "WELDS II Residual Stress Analysis of Resistance Heating Stress Improvement of Welded Pipes", prepared for New York Power Authority by Structural Integrity Associates, San Jose, California, August, 1987.

18. Stonesifer, R. B., "WELD3 Verification Manual", prepared by Computational Mechanics, Inc., Julian, PA, November 1988.

19. Stonesifer, R. B., "Input Description and User Guide for WELD3", prepared by Computational Mechanics, Inc., Julian, PA, November 1988.

20. Naughton, T., Telecopy of Welding Technique Sheets from Welding Services Inc. to Structural Integrity Associates on October 26, 1988.

21. Christensen, N., Davis, V. de L., and Gjermundsen, K., "Distribution of Temperatures in Arc Welding", British Welding Journal, 12(2), 1965.

22. Masubuchi, K., Analysis of Welded Structures, Pergamon Press, New York, 1980.

23. Goldak, J., et al, "Progress in Computing Residual Stress and Strain in Welds", Advances in Welding Science and Technology, Ed. S. A. David, May, 1986.

24. **pc-CRACK** User's Manual, Version 2.0 Structural Integrity Associates, August, 1989.

25. Rybicki, E. F., Stonesifer, R. B., and Olson R. J., "Stress Intensity Factors due to Residual Stresses in Thin-Walled Girth Welded Pipes", Journal of Pressure Vessel Technology, Vol. 103, 1981, pp. 66-75.

26. Tada, H., Paris, P. C., and Irwin, G. R., The Stress Analysis of Cracks Handbook, Del Research Corporation, Hellertown, PA, 1973.

27. ASME Boiler & Pressure Vessel Code, 1968 Edition with Winter, 1968 Addendum.

Table A-1

Summary of Thermal and Mechanical Properties
Used in the **WELD3** Weld Overlay Simulations

Material 1 (304 stainless steel)

Temp (F)	E (ksi)	Poisson Ratio	CTE (1/F)	H' (ksi)	Yield (ksi)	k (Btu/in-sec-F)	c (Btu/in^3-F)
50	28,700	0.26	8.16E-6	539.7	36.0	1.82E-4	3.12E-2
300	27,100	0.28	8.94E-6	452.3	31.1	2.12E-4	3.46E-2
550	25,800	0.31	9.60E-6	364.8	25.9	2.42E-4	3.71E-2
750	24,200	0.32	10.03E-6	296.3	22.3	2.66E-4	3.81E-2
1000	22,500	0.30	10.56E-6	217.9	18.5	2.96E-4	3.89E-2
1300	20,200	0.28	11.41E-6	139.0	14.9	3.32E-4	3.99E-2
1600	16,000	0.24	12.63E-6	79.6	10.2	3.68E-4	4.19E-2
2100	10	0.22	14.88E-6	1.0	1.0	4.28E-4	4.58E-2

Material 2 (Inconel 625 weld)

Temp (F)	E (ksi)	Poisson Ratio	CTE (1/F)	H' (ksi)	Yield (ksi)	k (Btu/in-sec-F)	c (Btu/in^3-F)
50	30,000	0.30	7.20E-6	539.7	53.0	1.32E-4	3.00E-2
300	28,800	0.30	7.20E-6	452.3	42.4	1.57E-4	3.22E-2
550	28,000	0.30	7.50E-6	364.8	37.8	1.83E-4	3.41E-2
750	27,000	0.30	7.90E-6	296.3	36.7	2.06E-4	3.63E-2
1000	25,100	0.30	9.40E-6	217.9	37.0	2.34E-4	3.82E-2
1300	23,400	0.30	11.20E-6	139.0	39.0	2.66E-4	4.09E-2
1600	18,500	0.30	13.00E-6	79.6	24.8	3.06E-4	4.35E-2
2100	10	0.30	16.00E-6	1.0	1.0	3.70E-4	4.80E-2

Material Properties taken from ASME Section III [27]
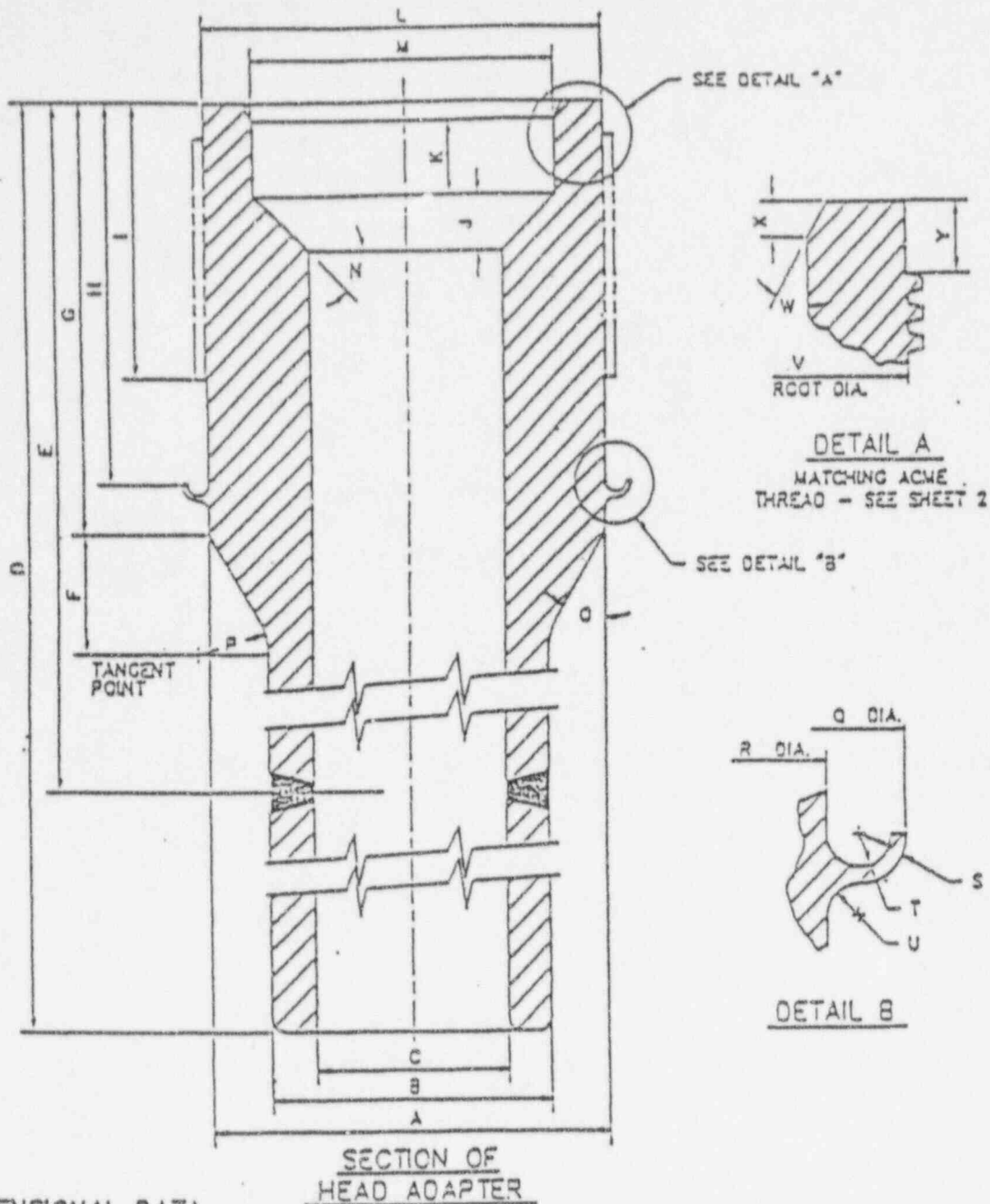
SECTION OF HEAD ADAPTER

SEE DETAIL "A"

DETAIL A
MATCHING ACME
THREAD — SEE SHEET 2

ROOT DIA.

SEE DETAIL "B"

Q DIA.
R DIA.

DETAIL B

TANGENT POINT

DIMENSIONAL DATA

A = 5.66"	F = 2.604"	K = 1.370"	P = 1.0"	U = 0.160"
B = 4.0"	G = 6.0"	L = 5.701"	Q = 6.45"	V = 5.738 / 5.7:
C = 2.75"	H = 5.177"	M = 4.300"	R = 5.66"	W = 30°
D = 27.75 to 59.28	I = 3.875"	N = 45°	S = 0.075"	X = 0.25"
E = 11.0"	J = 0.78"	O = 30°	T = 0.160"	Y = 0.50"

Figure A-1. Geometry of Spare CRDM Head Adapter Used for Canopy Seal Weld Overlay Model Development
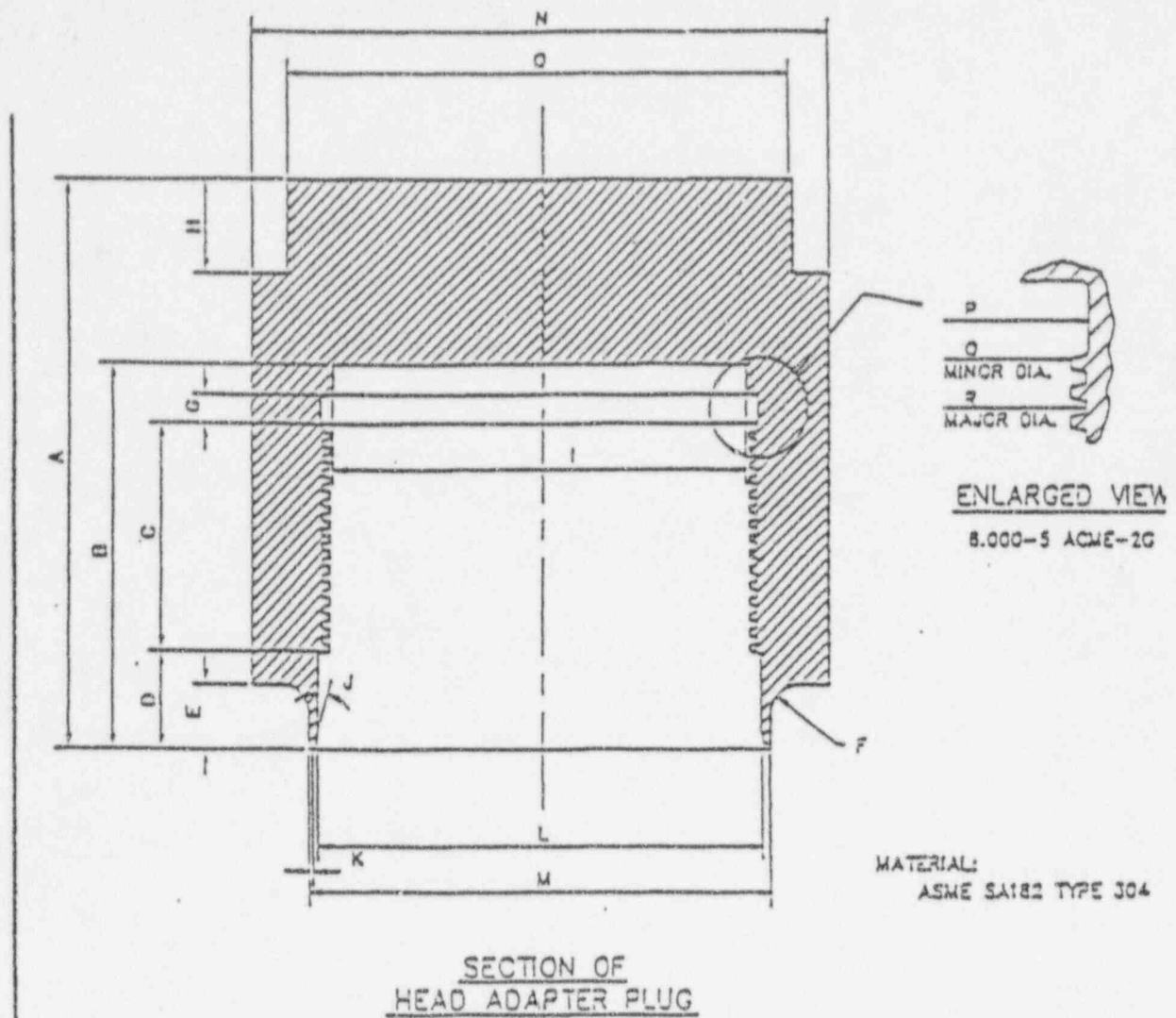
Structural Integrity Associates, Inc.

ENLARGED VIEW
8.000-5 ACME-2G

MATERIAL:
ASME SA182 TYPE 304

SECTION OF
HEAD ADAPTER PLUG

DIMENSIONAL DATA

A = 7.59"	H = 1.25"	O = 6.995"
B = 5.125"	I = 5.71"	P = 6.06"
C = 3.00"	J = 15°	Q = 5.80"
D = 1.30"	K = 0.075"	R = 6.02"
E = 0.485"	L = 6.122"	
F = 0.40"	M = 6.440"	
G = 0.40"	N = 8.00"	

Figure A-2. Geometry of Spare CRDM Head Adapter Plug Used for Canopy Seal Weld Overlay
Model Development
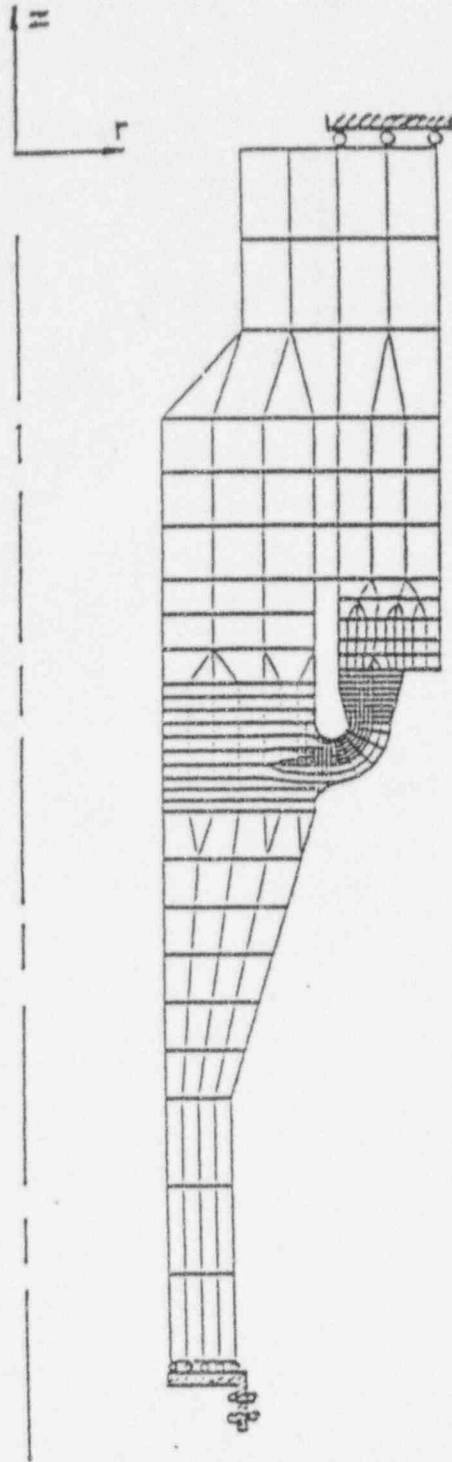
Figure A-3. **WELD3** Axisymmetric Finite Element Grid Used for Overlay Weld Modeling with Illustration of Boundary Conditions

Structural Integrity Associates, Inc.
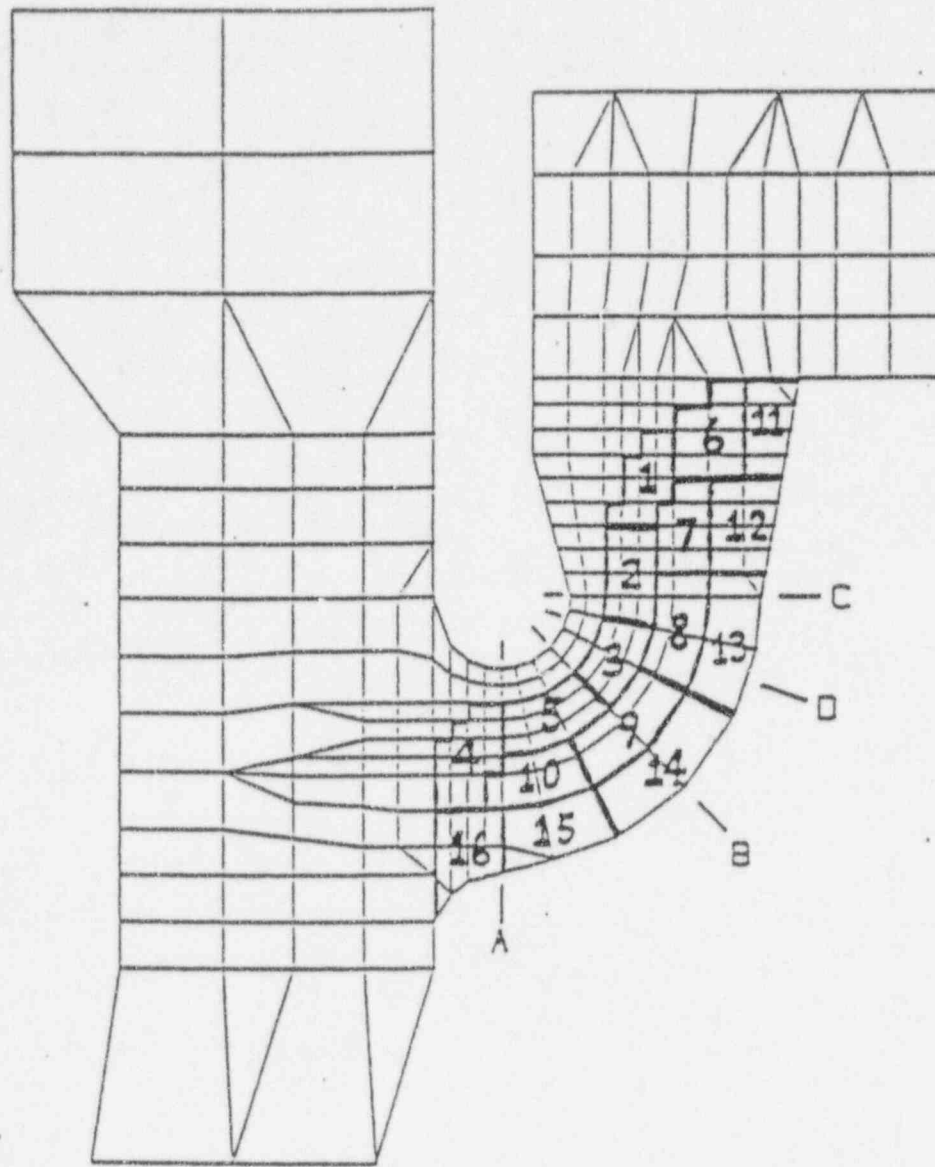
Figure A-4. Definition of Overlay Weld Model Segments for the Overlay Design Analysis

Structural Integrity Associates, Inc.

SIR-95-105, Rev. 0

A-23

Structural Integrity Associates, Inc.

Temperature (F)	
A	200
B	400
C	600
D	800
E	1000
F	1200
G	1400
H	1600
I	1800
J	2000

TEM3A

Temperature (F)	
A	200
B	400
C	600
D	800
E	1000
F	1200
G	1400
H	1600
I	1800
J	2000

TEM3B
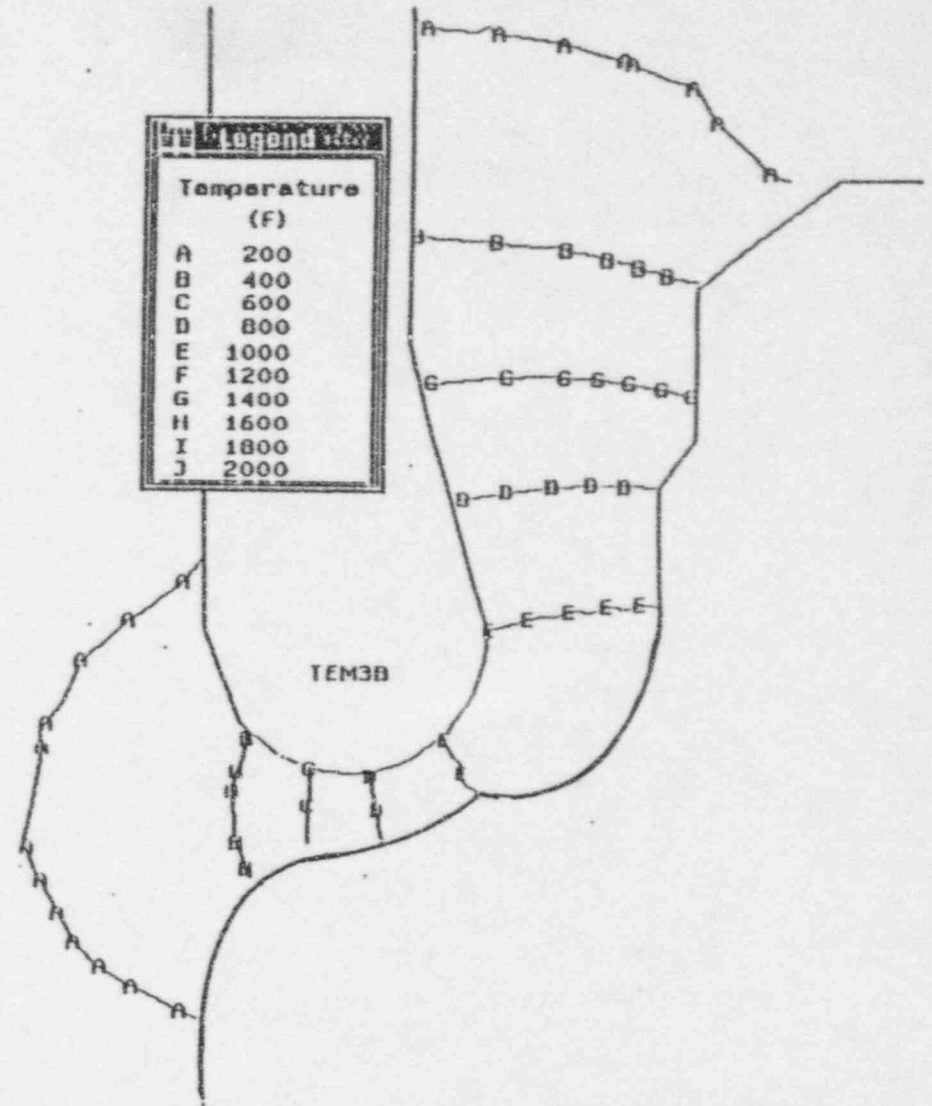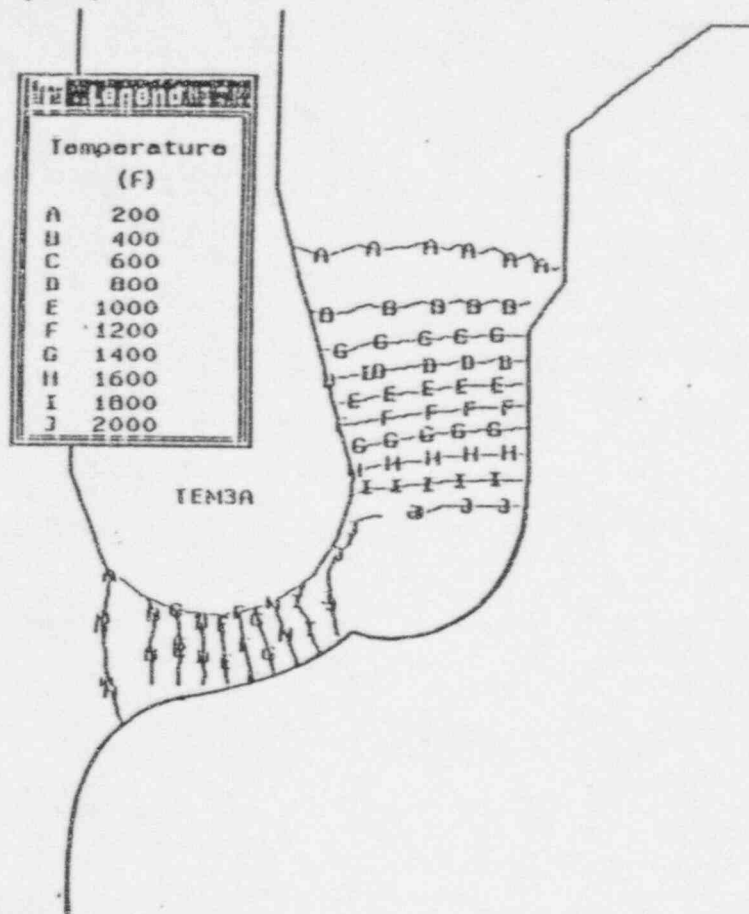
Figure A-5. Isotherms for Simulation of a Weld Pass Near the Center of the Seal and in the First Weld Layer

Layer 2, Segment 8, t = 2.0 sec

Layer 2, Segment 8, t = 8.0 sec
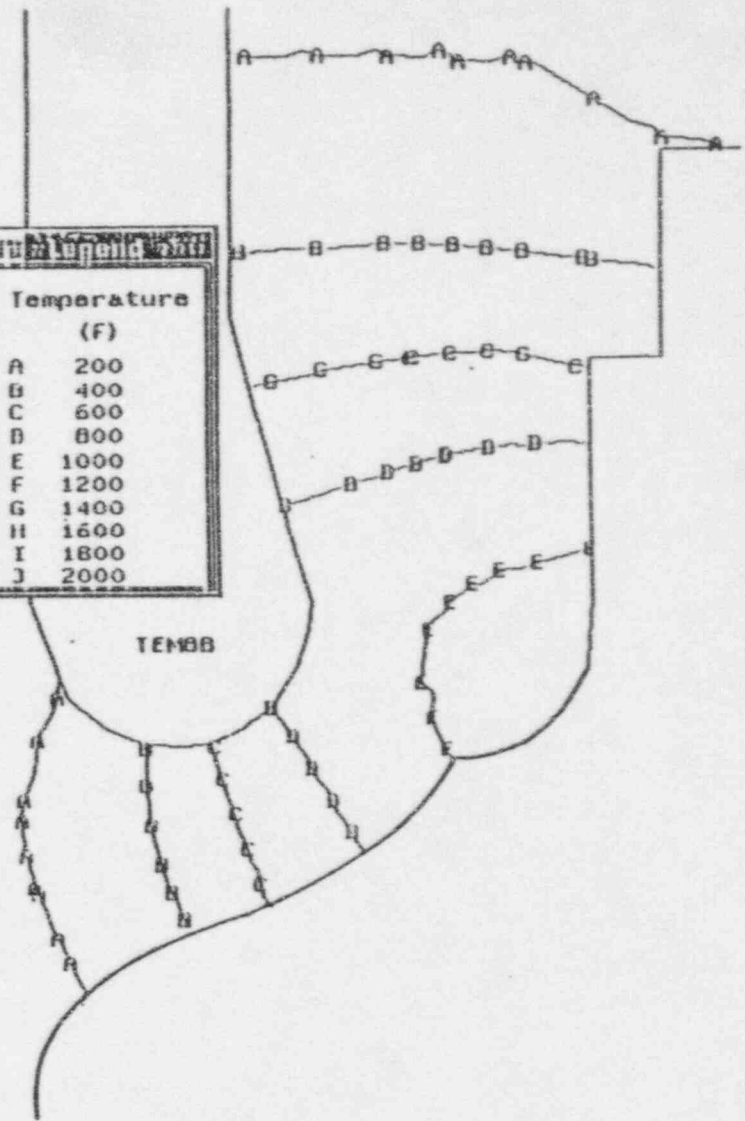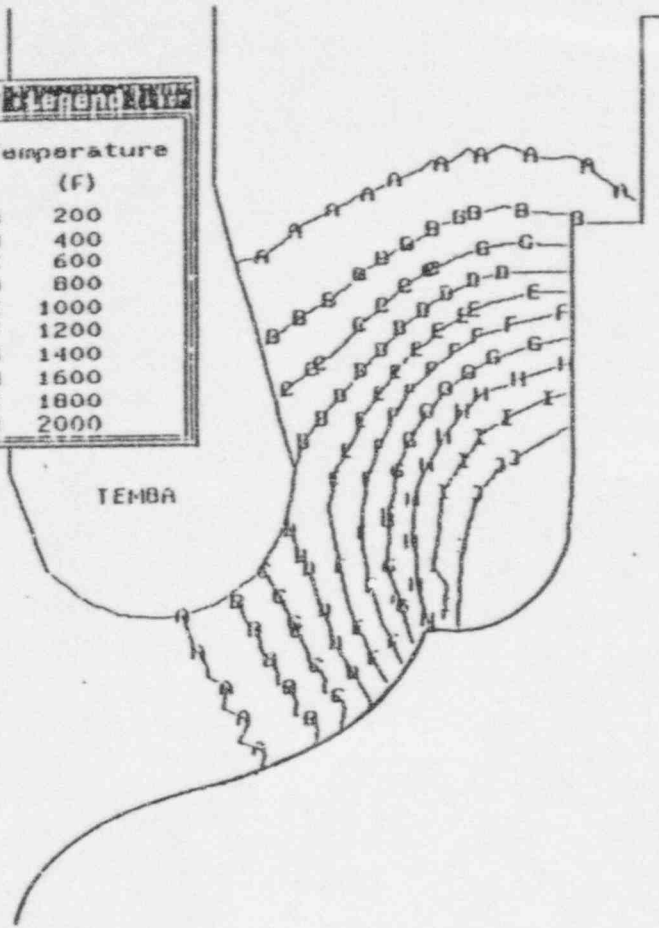
Figure A-6. Isotherms for Simulation of a Weld Pass Near the Center of the Seal and in the Second Weld Layer

Structural Integrity Associates, Inc.

Legend

Temperature
(F)

A	200
B	400
C	600
D	800
E	1000
F	1200
G	1400
H	1600
I	1800
J	2000

TEM14A (120 mil)

Legend

Temperature
(F)

A	200
B	400
C	600
D	800
E	1000
F	1200
G	1400
H	1600
I	1800
J	2000

TEM14B (120 mil)

Layer 3, Segment 14, t = 2.0 sec

Layer 3, Segment 14, t = 7.0 sec
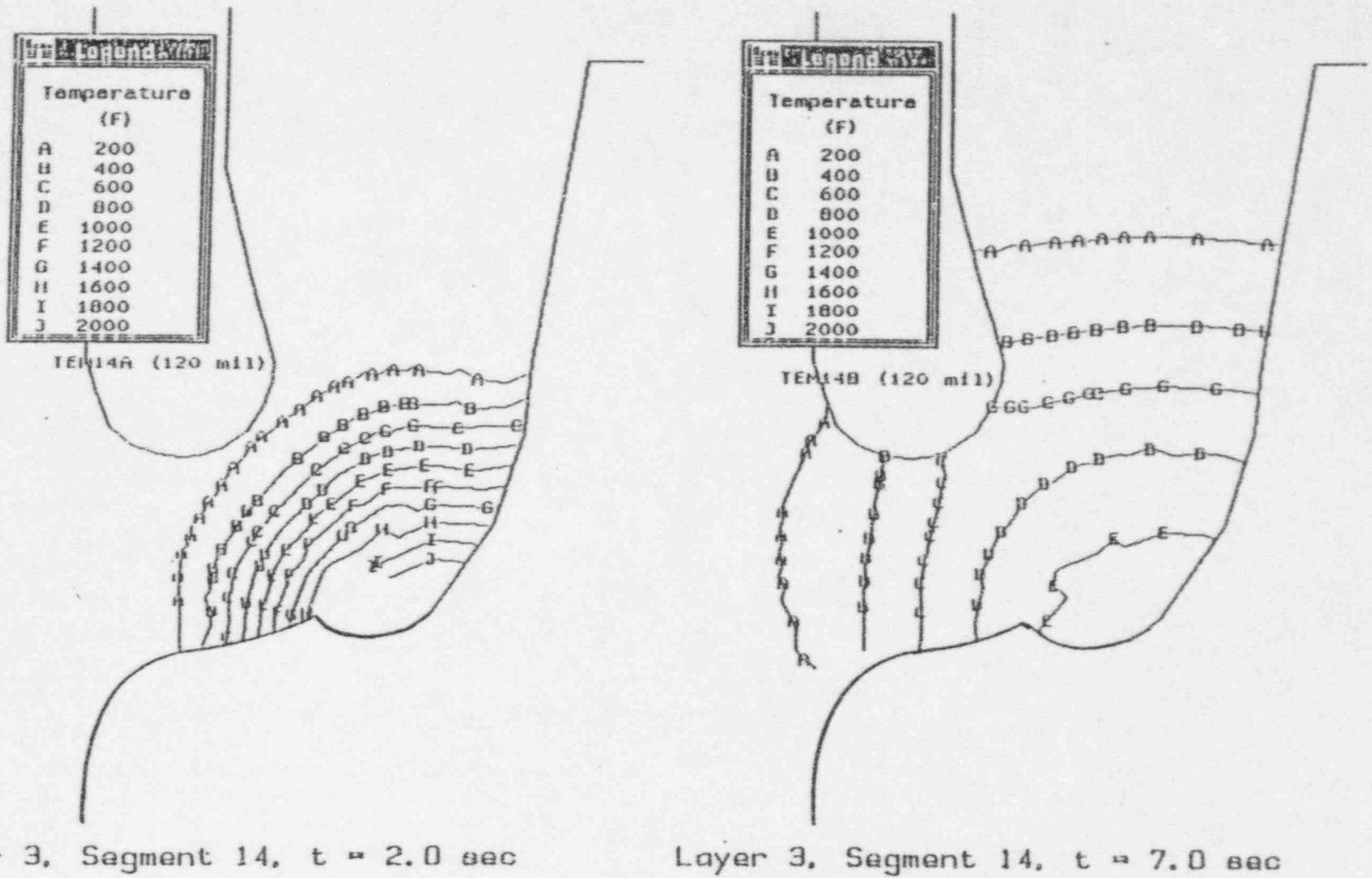
Figure A-7. Isotherms for Simulation of a Weld Pass Near the Center of the Seal and in the Third Weld Layer

Layer 3, Segment 16, t = 1.25 sec

Layer 3, Segment 16, t = 3.5 sec

Legend

Temperature
(F)

A	200
B	400
C	600
D	800
E	1000
F	1200
G	1400
H	1600
I	1800
J	2000

TEM16A (120 mil)

Legend

Temperature
(F)

A	200
B	400
C	600
D	800
E	1000
F	1200
G	1400
H	1600
I	1800
J	2000

TEM16B (120 mil)
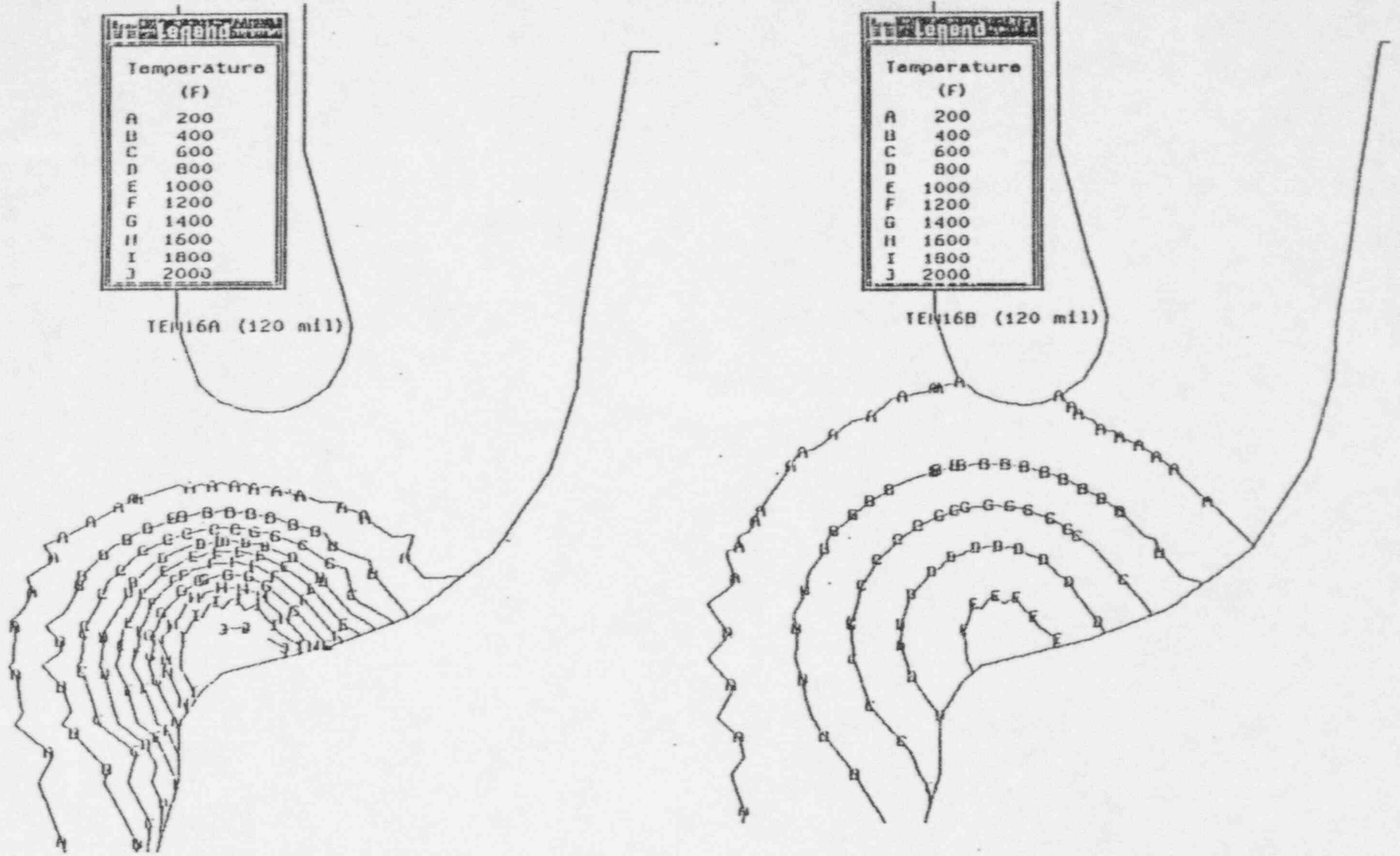
Figure A-8. Isotherms for Simulation of the Weld Pass of the Last Weld Layer
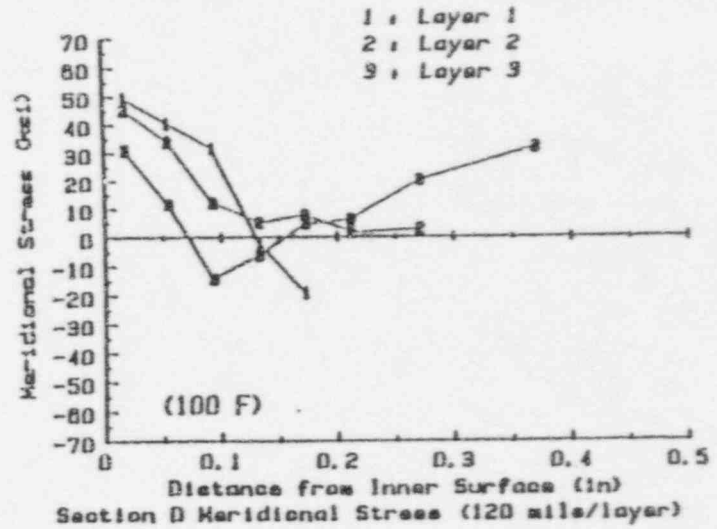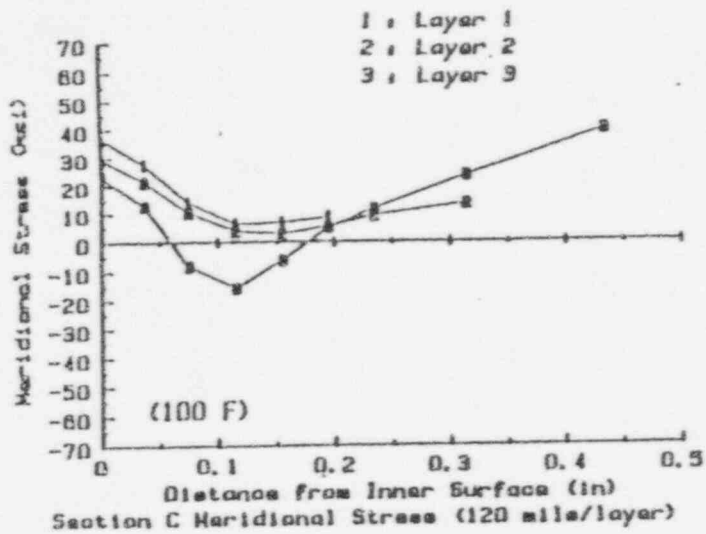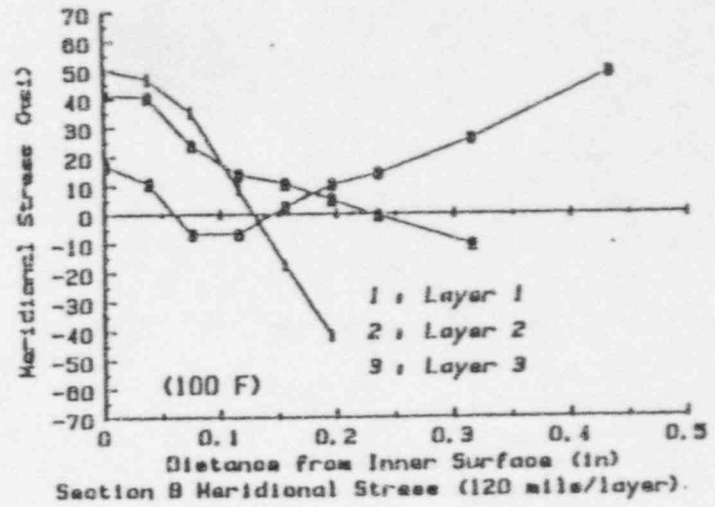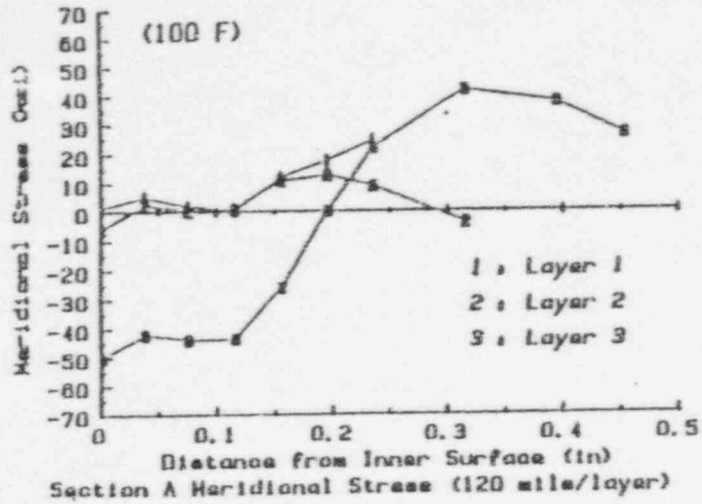
Figure A-9. Meridional Stresses at Sections A, B, C, and D After Each Layer of the 3-layer Overlay Design
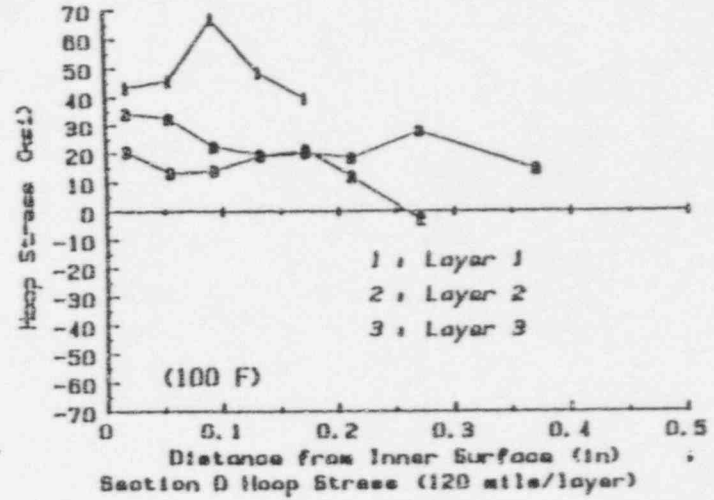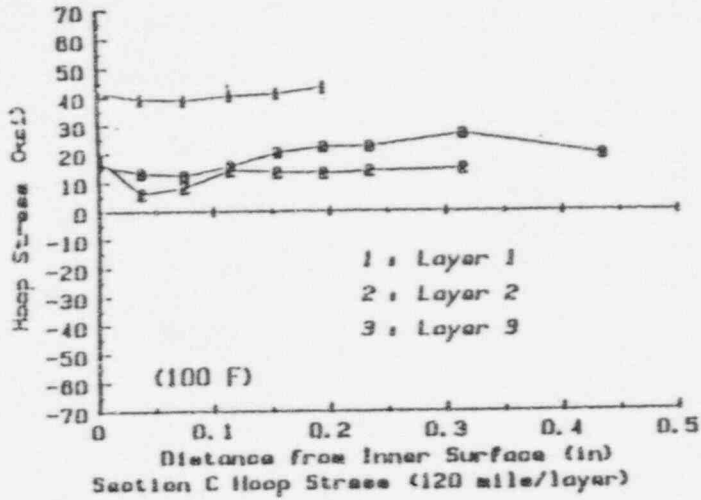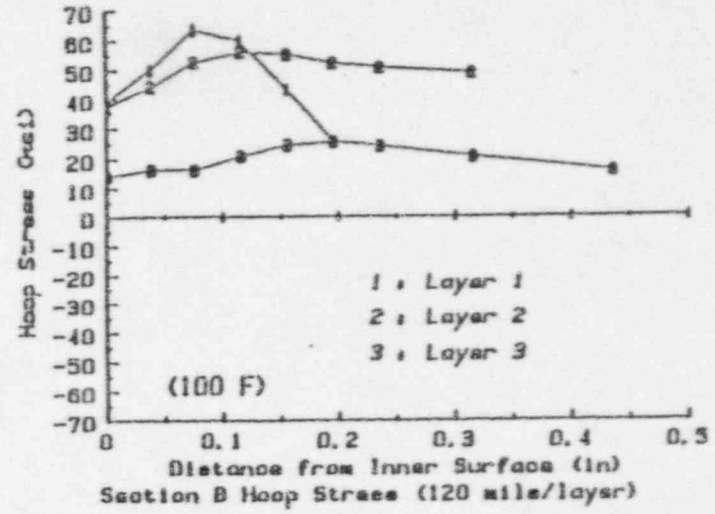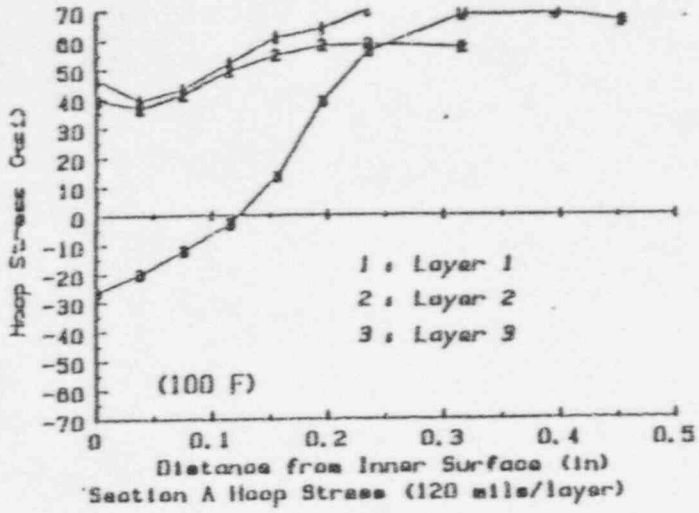
Figure A-10.   Hoop Stresses at Sections A, B, C, and D After Each Layer of the 3-Layer Overlay Design
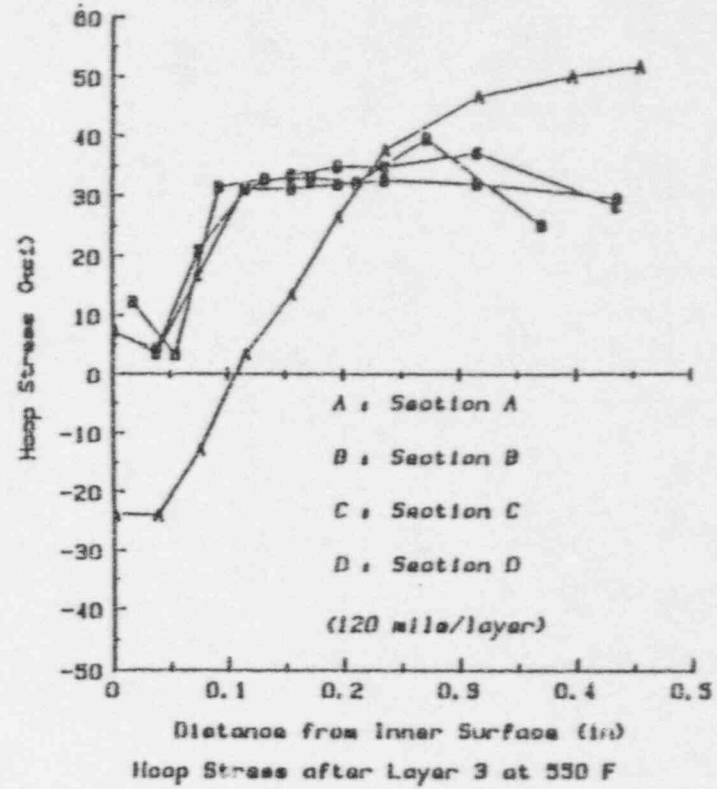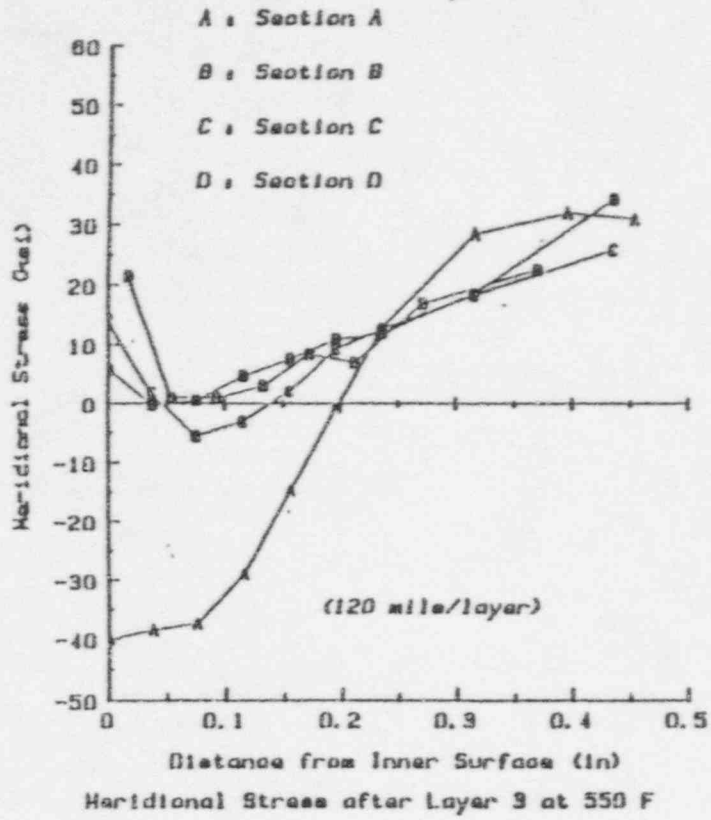
Figure A-11. Stresses at Sections A, B, C, and D After the Last Layer of the 3-Layer Overlay Design and After Being Heated to 550°F
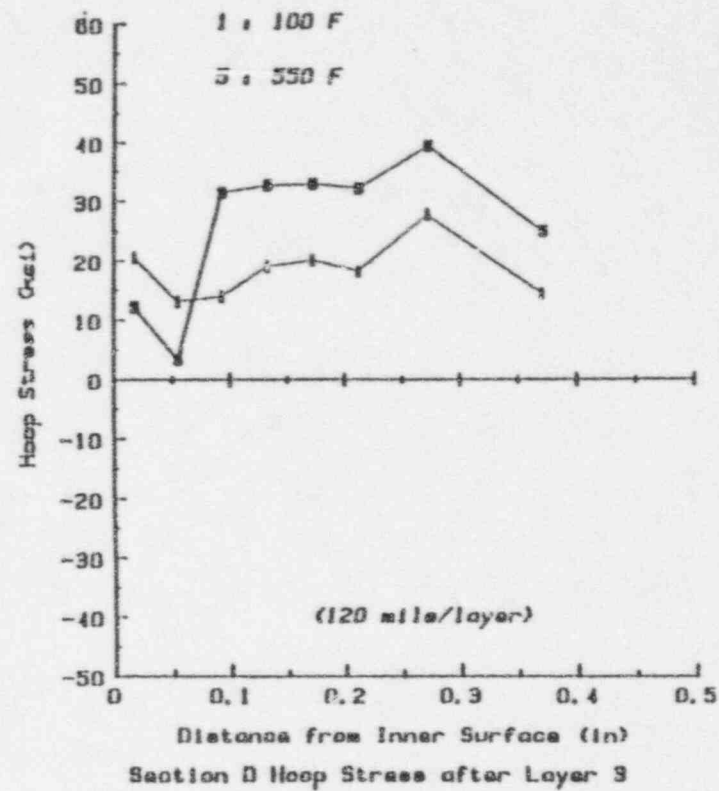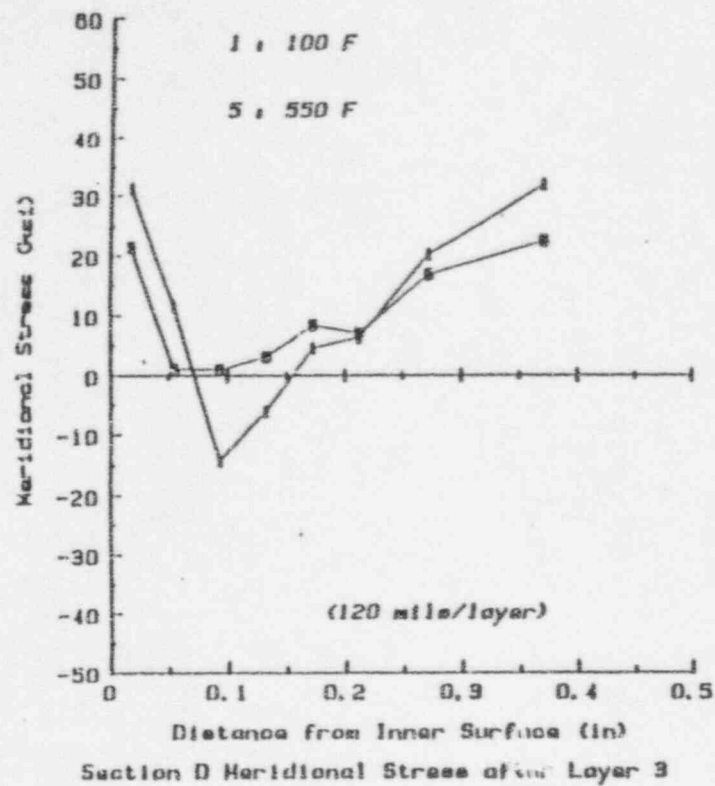
Figure A-12.   Comparison of Stresses at Section D for the As-welded Condition at 100°F and After Heating to 550°F
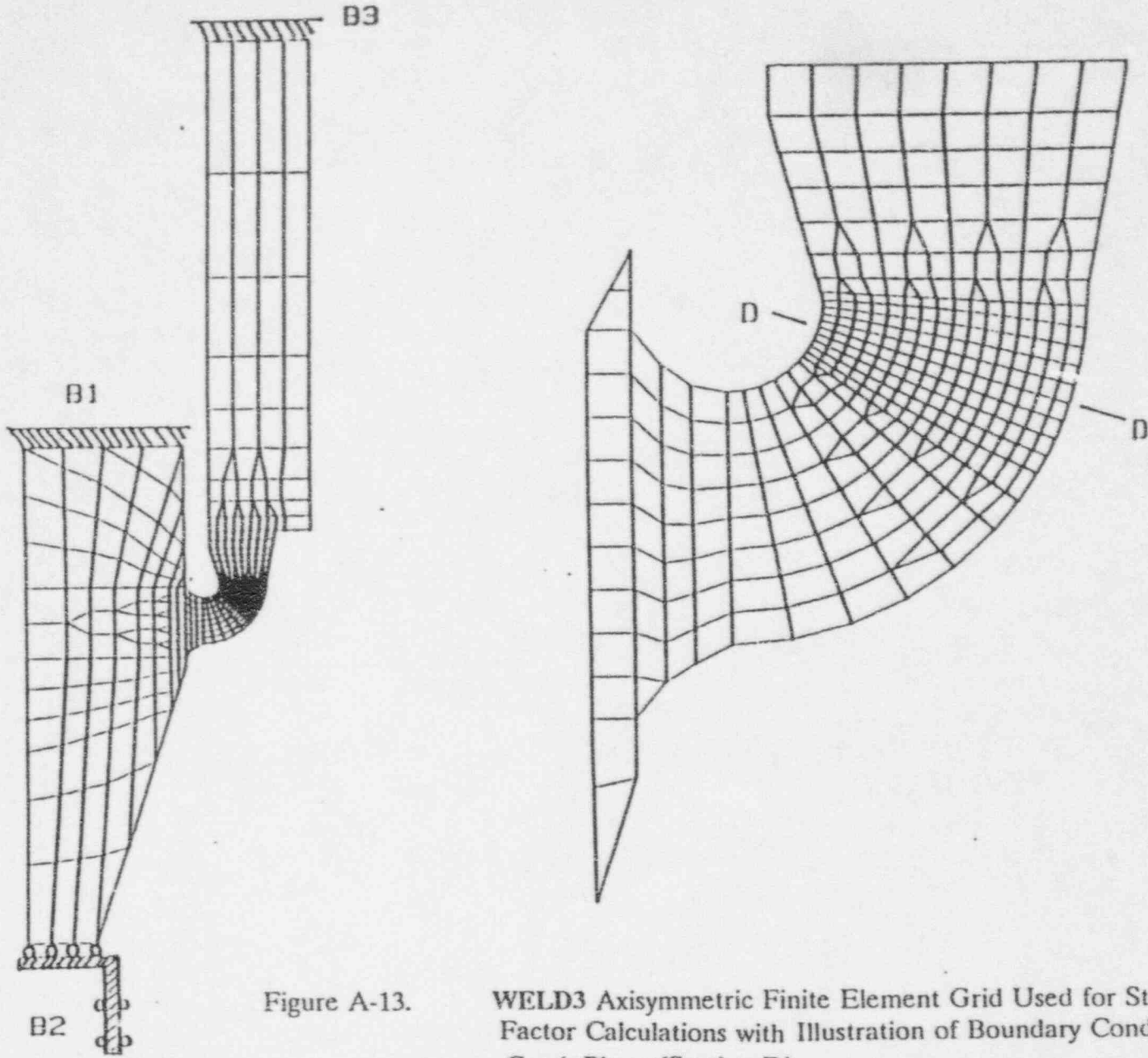
Figure A-13.   WELD3 Axisymmetric Finite Element Grid Used for Stress Intensity Factor Calculations with Illustration of Boundary Conditions and the Crack Plane (Section D)
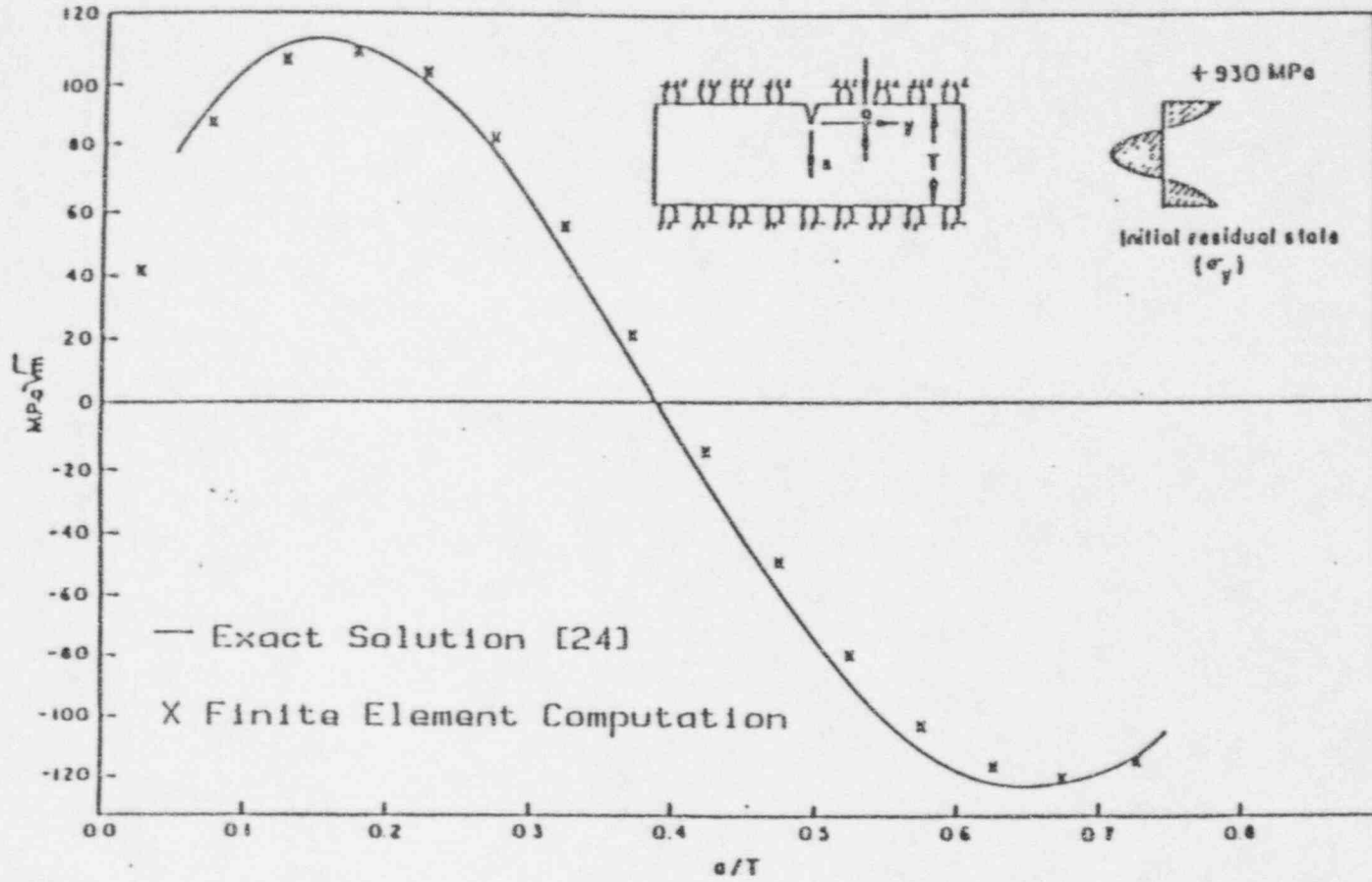
Figure A-14.   An Illustration of the Accuracy of the Finite Element (WELD3), Energy-Based Method for Stress Intensity Factor Determinations
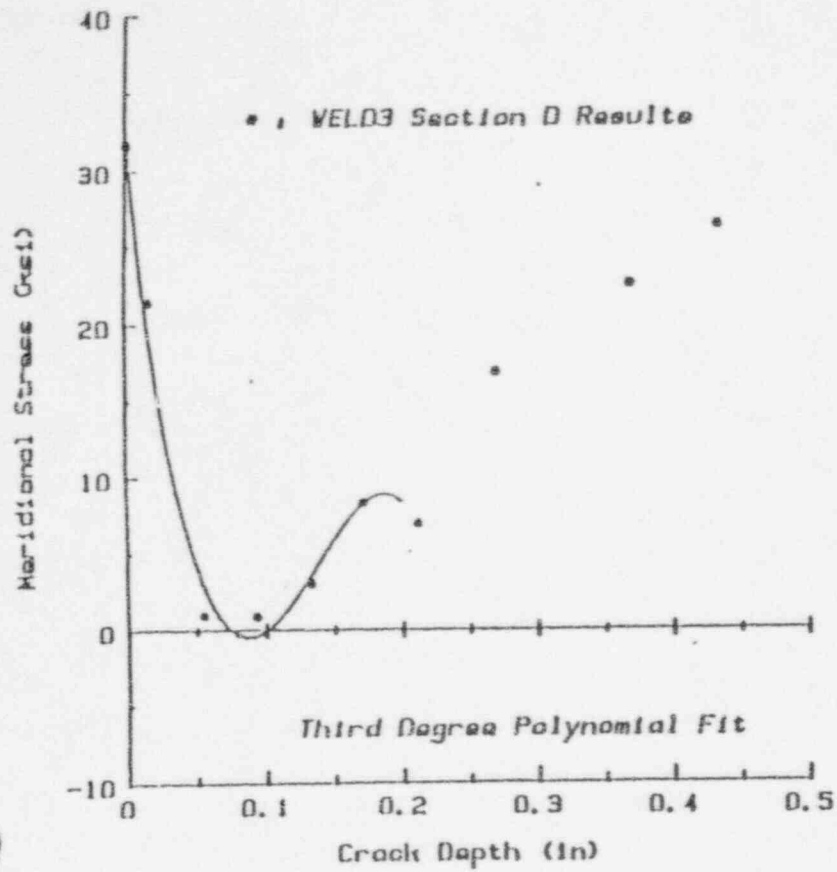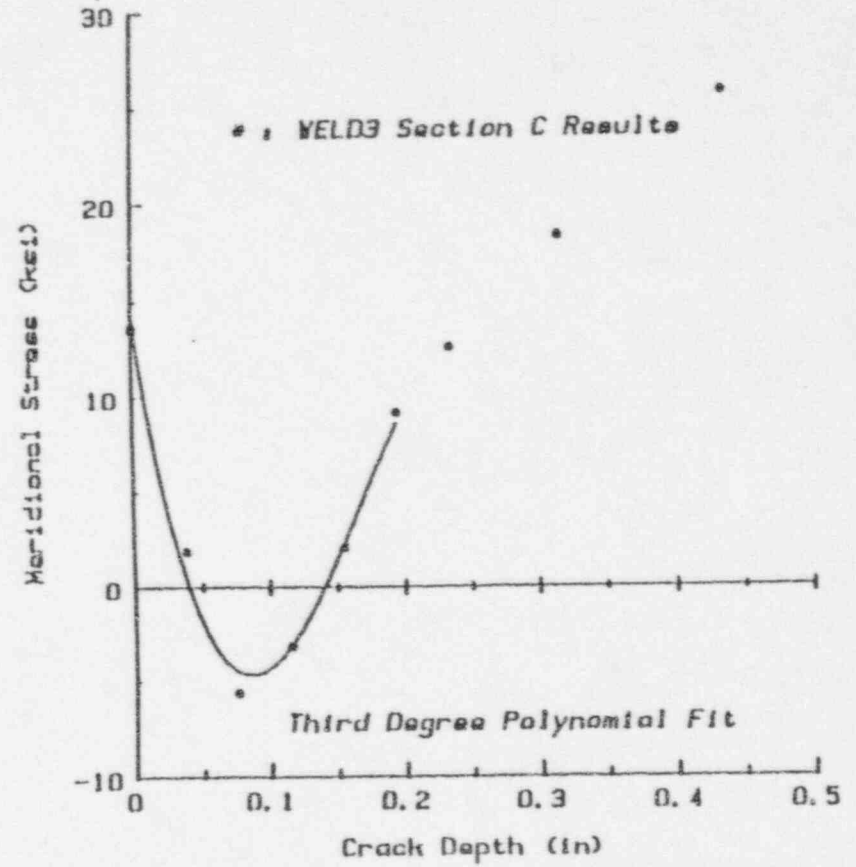
Figure A-15.   Illustration of pc-CRACK Third Degree Polynomial Curve Fits for Meridional Stresses at Sections C and D of the Overlay Design

a. Uniform 2 ksi applied stress   b. Section D and C residual stresses

Figure A-16.   Comparison of WELD3 Stress Intensity Factor Calculations with Those of pc-CRACK

APPENDIX B

pcCRACK SCC Crack Growth Results

Date: 25-Sept-1995
Time: 12:55: 8.65

STRESS CORROSION CRACK GROWTH ANALYSIS

WSI-20Q: SEQUOYAH CRDM LOWER CSW OVERLAY, SECTION C

INITIAL CRACK SIZE= 0.0750
MAX CRACK SIZE FOR SCCG= 0.8000

STRESS CORROSION CRACK GROWTH LAW

LAW ID	C	N	Kthres	K1C
NRC/10	3.590E-09	2.1610	0.0000	200.0000

STRESS COEFFICIENTS

CASE ID	C0	C1	C2	C3
BEND	1.7128	-5.8723	0.0000	0.0000
MEMBRANE	0.7100	0.0000	0.0000	0.0000
SECC	24.9810	-618.1000	3314.0000	-4183.0000
SECD	40.9851	-788.8973	3968.8642	-5013.4105
APPLIED	10.0000	0.0000	0.0000	0.0000

Kmax

CASE ID	SCALE FACTOR
SECC	1.0000
APPLIED	0.2000

TIME	TIME INCREMENT	PRINT INCREMENT
500000.0	1000.0	1000.0

crack model: CONTINUOUS SURFACE CRACK IN HALF SPACE

CRACK SIZE	STRESS INTENSITY FACTOR				
	CASE BEND	CASE MEMBRANE	CASE SECC	CASE SECD	CASE APPLIED
0.0160	0.416	0.178	4.861	8.481	2.511
0.0320	0.568	0.252	5.145	9.756	3.551
0.0480	0.670	0.309	4.494	9.578	4.349
0.0640	0.745	0.357	3.441	8.728	5.022
0.0800	0.801	0.399	2.249	7.578	5.615
0.0960	0.843	0.437	1.076	6.348	6.151
0.1120	0.872	0.472	0.031	5.187	6.644
0.1280	0.892	0.504	-0.812	4.195	7.102
0.1440	0.903	0.535	-1.403	3.443	7.533
0.1600	0.906	0.564	-1.709	2.977	7.941
0.1760	0.903	0.591	-1.708	2.828	8.328
0.1920	0.893	0.618	-1.391	3.010	8.698
0.2080	0.878	0.643	-0.760	3.526	9.054
0.2240	0.858	0.667	0.179	4.368	9.395
0.2400	0.832	0.690	1.407	5.522	9.725
0.2560	0.802	0.713	2.905	6.961	10.044

0.2720	0.767	0.735	4.642	8.653	10.353
0.2880	0.729	0.756	6.587	10.561	10.653
0.3040	0.686	0.777	8.699	12.639	10.945
0.3200	0.640	0.797	10.935	14.835	11.230
0.3360	0.590	0.817	13.248	17.094	11.507
0.3520	0.537	0.836	15.586	19.354	11.778
0.3680	0.480	0.855	17.891	21.550	12.043
0.3840	0.420	0.873	20.106	23.610	12.302
0.4000	0.357	0.891	22.166	25.459	12.555
0.4160	0.291	0.909	24.005	27.018	12.804
0.4320	0.222	0.926	25.552	28.202	13.048
0.4480	0.150	0.943	26.734	28.926	13.287
0.4640	0.075	0.960	27.474	29.097	13.522
0.4800	-0.002	0.976	27.693	28.621	13.754
0.4960	-0.082	0.993	27.309	27.400	13.981
0.5120	-0.165	1.009	26.237	25.333	14.205
0.5280	-0.250	1.024	24.388	22.313	14.425
0.5440	-0.337	1.040	21.672	18.233	14.642
0.5600	-0.427	1.055	17.996	12.982	14.855
0.5760	-0.519	1.070	13.265	6.445	15.066
0.5920	-0.613	1.084	7.379	-1.495	15.274
0.6080	-0.710	1.099	0.239	-10.958	15.479
0.6240	-0.809	1.113	-8.259	-22.068	15.681
0.6400	-0.910	1.128	-18.219	-34.949	15.881
0.6560	-1.013	1.142	-29.750	-49.732	16.078
0.6720	-1.118	1.155	-42.961	-66.547	16.273
0.6880	-1.226	1.169	-57.964	-85.528	16.466
0.7040	-1.335	1.183	-74.874	-106.812	16.656
0.7200	-1.447	1.196	-93.805	-130.538	16.845
0.7360	-1.560	1.209	-114.878	-156.847	17.031
0.7520	-1.675	1.222	-138.211	-185.884	17.215
0.7680	-1.792	1.235	-163.928	-217.794	17.397
0.7840	-1.911	1.248	-192.152	-252.727	17.577
0.8000	-2.032	1.261	-223.011	-290.834	17.756

TIME	KMAX	DA/DT	DA	A	A/THK
1000.0	3.71	6.093E-08	0.0001	0.0751	0.000
2000.0	3.70	6.078E-08	0.0001	0.0751	0.000
3000.0	3.70	6.064E-08	0.0001	0.0752	0.000
4000.0	3.69	6.049E-08	0.0001	0.0752	0.000
5000.0	3.69	6.035E-08	0.0001	0.0753	0.000
6000.0	3.69	6.021E-08	0.0001	0.0754	0.000
7000.0	3.68	6.006E-08	0.0001	0.0754	0.000
8000.0	3.68	5.992E-08	0.0001	0.0755	0.000
9000.0	3.67	5.978E-08	0.0001	0.0755	0.000
10000.0	3.67	5.964E-08	0.0001	0.0756	0.000
11000.0	3.67	5.950E-08	0.0001	0.0757	0.000
12000.0	3.66	5.936E-08	0.0001	0.0757	0.000
13000.0	3.66	5.922E-08	0.0001	0.0758	0.000
14000.0	3.65	5.908E-08	0.0001	0.0758	0.000
15000.0	3.65	5.894E-08	0.0001	0.0759	0.000
16000.0	3.65	5.880E-08	0.0001	0.0760	0.000
17000.0	3.64	5.867E-08	0.0001	0.0760	0.000
18000.0	3.64	5.853E-08	0.0001	0.0761	0.000
19000.0	3.64	5.839E-08	0.0001	0.0761	0.000
20000.0	3.63	5.826E-08	0.0001	0.0762	0.000
21000.0	3.63	5.812E-08	0.0001	0.0762	0.000
22000.0	3.62	5.799E-08	0.0001	0.0763	0.000

23000.0	3.62	5.785E-08	0.0001	0.0764	0.000
24000.0	3.62	5.772E-08	0.0001	0.0764	0.000
25000.0	3.61	5.758E-08	0.0001	0.0765	0.000
26000.0	3.61	5.745E-08	0.0001	0.0765	0.000
27000.0	3.60	5.732E-08	0.0001	0.0766	0.000
28000.0	3.60	5.719E-08	0.0001	0.0767	0.000
29000.0	3.60	5.705E-08	0.0001	0.0767	0.000
30000.0	3.59	5.692E-08	0.0001	0.0768	0.000
31000.0	3.59	5.679E-08	0.0001	0.0768	0.000
32000.0	3.58	5.666E-08	0.0001	0.0769	0.000
33000.0	3.58	5.653E-08	0.0001	0.0770	0.000
34000.0	3.58	5.640E-08	0.0001	0.0770	0.000
35000.0	3.57	5.627E-08	0.0001	0.0771	0.000
36000.0	3.57	5.615E-08	0.0001	0.0772	0.000
37000.0	3.57	5.602E-08	0.0001	0.0772	0.000
38000.0	3.56	5.589E-08	0.0001	0.0773	0.000
39000.0	3.56	5.576E-08	0.0001	0.0773	0.000
40000.0	3.55	5.564E-08	0.0001	0.0774	0.000
41000.0	3.55	5.551E-08	0.0001	0.0774	0.000
42000.0	3.55	5.538E-08	0.0001	0.0775	0.000
43000.0	3.54	5.526E-08	0.0001	0.0776	0.000
44000.0	3.54	5.513E-08	0.0001	0.0776	0.000
45000.0	3.54	5.501E-08	0.0001	0.0777	0.000
46000.0	3.53	5.489E-08	0.0001	0.0777	0.000
47000.0	3.53	5.476E-08	0.0001	0.0778	0.000
48000.0	3.52	5.464E-08	0.0001	0.0778	0.000
49000.0	3.52	5.452E-08	0.0001	0.0779	0.000
50000.0	3.52	5.439E-08	0.0001	0.0779	0.000
51000.0	3.51	5.427E-08	0.0001	0.0780	0.000
52000.0	3.51	5.415E-08	0.0001	0.0780	0.000
53000.0	3.51	5.403E-08	0.0001	0.0781	0.000
54000.0	3.50	5.391E-08	0.0001	0.0781	0.000
55000.0	3.50	5.379E-08	0.0001	0.0782	0.000
56000.0	3.50	5.367E-08	0.0001	0.0782	0.000
57000.0	3.49	5.355E-08	0.0001	0.0783	0.000
58000.0	3.49	5.343E-08	0.0001	0.0783	0.000
59000.0	3.49	5.331E-08	0.0001	0.0784	0.000
60000.0	3.48	5.319E-08	0.0001	0.0784	0.000
61000.0	3.48	5.307E-08	0.0001	0.0785	0.000
62000.0	3.47	5.296E-08	0.0001	0.0785	0.000
63000.0	3.47	5.284E-08	0.0001	0.0786	0.000
64000.0	3.47	5.272E-08	0.0001	0.0786	0.000
65000.0	3.46	5.261E-08	0.0001	0.0787	0.000
66000.0	3.46	5.249E-08	0.0001	0.0787	0.000
67000.0	3.46	5.238E-08	0.0001	0.0788	0.000
68000.0	3.45	5.226E-08	0.0001	0.0788	0.000
69000.0	3.45	5.215E-08	0.0001	0.0789	0.000
70000.0	3.45	5.203E-08	0.0001	0.0789	0.000
71000.0	3.44	5.192E-08	0.0001	0.0790	0.000
72000.0	3.44	5.180E-08	0.0001	0.0790	0.000
73000.0	3.44	5.169E-08	0.0001	0.0791	0.000
74000.0	3.43	5.158E-08	0.0001	0.0791	0.000
75000.0	3.43	5.147E-08	0.0001	0.0792	0.000
76000.0	3.43	5.135E-08	0.0001	0.0793	0.000
77000.0	3.42	5.124E-08	0.0001	0.0793	0.000
78000.0	3.42	5.113E-08	0.0001	0.0794	0.000
79000.0	3.41	5.102E-08	0.0001	0.0794	0.000
80000.0	3.41	5.091E-08	0.0001	0.0795	0.000
81000.0	3.41	5.080E-08	0.0001	0.0795	0.000
82000.0	3.40	5.069E-08	0.0001	0.0796	0.000
83000.0	3.40	5.058E-08	0.0001	0.0796	0.000
84000.0	3.40	5.047E-08	0.0001	0.0797	0.000
85000.0	3.39	5.036E-08	0.0001	0.0797	0.000

Structural Integrity Associates, Inc.

86000.0	3.39	5.025E-08	0.0001	0.0798	0.000
87000.0	3.39	5.015E-08	0.0001	0.0798	0.000
88000.0	3.38	5.004E-08	0.0001	0.0799	0.000
89000.0	3.38	4.993E-08	0.0000	0.0799	0.000
90000.0	3.38	4.982E-08	0.0000	0.0800	0.000
91000.0	3.37	4.972E-08	0.0000	0.0800	0.000
92000.0	3.37	4.961E-08	0.0000	0.0801	0.000
93000.0	3.37	4.951E-08	0.0000	0.0801	0.000
94000.0	3.36	4.940E-08	0.0000	0.0802	0.000
95000.0	3.36	4.930E-08	0.0000	0.0802	0.000
96000.0	3.36	4.919E-08	0.0000	0.0803	0.000
97000.0	3.35	4.909E-08	0.0000	0.0803	0.000
98000.0	3.35	4.899E-08	0.0000	0.0804	0.000
99000.0	3.35	4.888E-08	0.0000	0.0804	0.000
100000.0	3.34	4.878E-08	0.0000	0.0805	0.000
101000.0	3.34	4.868E-08	0.0000	0.0805	0.000
102000.0	3.34	4.858E-08	0.0000	0.0805	0.000
103000.0	3.34	4.848E-08	0.0000	0.0806	0.000
104000.0	3.33	4.837E-08	0.0000	0.0806	0.000
105000.0	3.33	4.827E-08	0.0000	0.0807	0.000
106000.0	3.33	4.817E-08	0.0000	0.0807	0.000
107000.0	3.32	4.807E-08	0.0000	0.0808	0.000
108000.0	3.32	4.797E-08	0.0000	0.0808	0.000
109000.0	3.32	4.787E-08	0.0000	0.0809	0.000
110000.0	3.31	4.777E-08	0.0000	0.0809	0.000
111000.0	3.31	4.767E-08	0.0000	0.0810	0.000
112000.0	3.31	4.758E-08	0.0000	0.0810	0.000
113000.0	3.30	4.748E-08	0.0000	0.0811	0.000
114000.0	3.30	4.738E-08	0.0000	0.0811	0.000
115000.0	3.30	4.728E-08	0.0000	0.0812	0.000
116000.0	3.29	4.718E-08	0.0000	0.0812	0.000
117000.0	3.29	4.709E-08	0.0000	0.0813	0.000
118000.0	3.29	4.699E-08	0.0000	0.0813	0.000
119000.0	3.28	4.689E-08	0.0000	0.0814	0.000
120000.0	3.28	4.680E-08	0.0000	0.0814	0.000
121000.0	3.28	4.670E-08	0.0000	0.0815	0.000
122000.0	3.27	4.661E-08	0.0000	0.0815	0.000
123000.0	3.27	4.651E-08	0.0000	0.0815	0.000
124000.0	3.27	4.641E-08	0.0000	0.0816	0.000
125000.0	3.27	4.632E-08	0.0000	0.0816	0.000
126000.0	3.26	4.623E-08	0.0000	0.0817	0.000
127000.0	3.26	4.613E-08	0.0000	0.0817	0.000
128000.0	3.26	4.604E-08	0.0000	0.0818	0.000
129000.0	3.25	4.594E-08	0.0000	0.0818	0.000
130000.0	3.25	4.585E-08	0.0000	0.0819	0.000
131000.0	3.25	4.576E-08	0.0000	0.0819	0.000
132000.0	3.24	4.567E-08	0.0000	0.0820	0.000
133000.0	3.24	4.557E-08	0.0000	0.0820	0.000
134000.0	3.24	4.548E-08	0.0000	0.0821	0.000
135000.0	3.24	4.539E-08	0.0000	0.0821	0.000
136000.0	3.23	4.530E-08	0.0000	0.0821	0.000
137000.0	3.23	4.521E-08	0.0000	0.0822	0.000
138000.0	3.23	4.511E-08	0.0000	0.0822	0.000
139000.0	3.22	4.502E-08	0.0000	0.0823	0.000
140000.0	3.22	4.493E-08	0.0000	0.0823	0.000
141000.0	3.22	4.484E-08	0.0000	0.0824	0.000
142000.0	3.21	4.475E-08	0.0000	0.0824	0.000
143000.0	3.21	4.466E-08	0.0000	0.0825	0.000
144000.0	3.21	4.457E-08	0.0000	0.0825	0.000
145000.0	3.21	4.449E-08	0.0000	0.0825	0.000
146000.0	3.20	4.440E-08	0.0000	0.0826	0.000
147000.0	3.20	4.431E-08	0.0000	0.0826	0.000
148000.0	3.20	4.422E-08	0.0000	0.0827	0.000

149000.0	3.19	4.413E-08	0.0000	0.0827	0.000
150000.0	3.19	4.404E-08	0.0000	0.0828	0.000
151000.0	3.19	4.396E-08	0.0000	0.0828	0.000
152000.0	3.18	4.387E-08	0.0000	0.0829	0.000
153000.0	3.18	4.378E-08	0.0000	0.0829	0.000
154000.0	3.18	4.370E-08	0.0000	0.0829	0.000
155000.0	3.18	4.361E-08	0.0000	0.0830	0.000
156000.0	3.17	4.352E-08	0.0000	0.0830	0.000
157000.0	3.17	4.344E-08	0.0000	0.0831	0.000
158000.0	3.17	4.335E-08	0.0000	0.0831	0.000
159000.0	3.16	4.327E-08	0.0000	0.0832	0.000
160000.0	3.16	4.318E-08	0.0000	0.0832	0.000
161000.0	3.16	4.310E-08	0.0000	0.0832	0.000
162000.0	3.16	4.301E-08	0.0000	0.0833	0.000
163000.0	3.15	4.293E-08	0.0000	0.0833	0.000
164000.0	3.15	4.284E-08	0.0000	0.0834	0.000
165000.0	3.15	4.276E-08	0.0000	0.0834	0.000
166000.0	3.14	4.268E-08	0.0000	0.0835	0.000
167000.0	3.14	4.259E-08	0.0000	0.0835	0.000
168000.0	3.14	4.251E-08	0.0000	0.0835	0.000
169000.0	3.14	4.243E-08	0.0000	0.0836	0.000
170000.0	3.13	4.235E-08	0.0000	0.0836	0.000
171000.0	3.13	4.226E-08	0.0000	0.0837	0.000
172000.0	3.13	4.218E-08	0.0000	0.0837	0.000
173000.0	3.12	4.210E-08	0.0000	0.0838	0.000
174000.0	3.12	4.202E-08	0.0000	0.0838	0.000
175000.0	3.12	4.194E-08	0.0000	0.0838	0.000
176000.0	3.12	4.186E-08	0.0000	0.0839	0.000
177000.0	3.11	4.177E-08	0.0000	0.0839	0.000
178000.0	3.11	4.169E-08	0.0000	0.0840	0.000
179000.0	3.11	4.161E-08	0.0000	0.0840	0.000
180000.0	3.10	4.153E-08	0.0000	0.0840	0.000
181000.0	3.10	4.145E-08	0.0000	0.0841	0.000
182000.0	3.10	4.137E-08	0.0000	0.0841	0.000
183000.0	3.10	4.129E-08	0.0000	0.0842	0.000
184000.0	3.09	4.122E-08	0.0000	0.0842	0.000
185000.0	3.09	4.114E-08	0.0000	0.0843	0.000
186000.0	3.09	4.106E-08	0.0000	0.0843	0.000
187000.0	3.09	4.098E-08	0.0000	0.0843	0.000
188000.0	3.08	4.090E-08	0.0000	0.0844	0.000
189000.0	3.08	4.082E-08	0.0000	0.0844	0.000
190000.0	3.08	4.075E-08	0.0000	0.0845	0.000
191000.0	3.07	4.067E-08	0.0000	0.0845	0.000
192000.0	3.07	4.059E-08	0.0000	0.0845	0.000
193000.0	3.07	4.051E-08	0.0000	0.0846	0.000
194000.0	3.07	4.044E-08	0.0000	0.0846	0.000
195000.0	3.06	4.036E-08	0.0000	0.0847	0.000
196000.0	3.06	4.028E-08	0.0000	0.0847	0.000
197000.0	3.06	4.021E-08	0.0000	0.0847	0.000
198000.0	3.06	4.013E-08	0.0000	0.0848	0.000
199000.0	3.05	4.006E-08	0.0000	0.0848	0.000
200000.0	3.05	3.998E-08	0.0000	0.0849	0.000
201000.0	3.05	3.990E-08	0.0000	0.0849	0.000
202000.0	3.05	3.983E-08	0.0000	0.0849	0.000
203000.0	3.04	3.975E-08	0.0000	0.0850	0.000
204000.0	3.04	3.968E-08	0.0000	0.0850	0.000
205000.0	3.04	3.961E-08	0.0000	0.0851	0.000
206000.0	3.03	3.953E-08	0.0000	0.0851	0.000
207000.0	3.03	3.946E-08	0.0000	0.0851	0.000
208000.0	3.03	3.938E-08	0.0000	0.0852	0.000
209000.0	3.03	3.931E-08	0.0000	0.0852	0.000
210000.0	3.02	3.924E-08	0.0000	0.0853	0.000
211000.0	3.02	3.916E-08	0.0000	0.0853	0.000

212000.0	3.02	3.909E-08	0.0000	0.0853	0.000
213000.0	3.02	3.902E-08	0.0000	0.0854	0.000
214000.0	3.01	3.894E-08	0.0000	0.0854	0.000
215000.0	3.01	3.887E-08	0.0000	0.0855	0.000
216000.0	3.01	3.880E-08	0.0000	0.0855	0.000
217000.0	3.01	3.873E-08	0.0000	0.0855	0.000
218000.0	3.00	3.866E-08	0.0000	0.0856	0.000
219000.0	3.00	3.858E-08	0.0000	0.0856	0.000
220000.0	3.00	3.851E-08	0.0000	0.0856	0.000
221000.0	3.00	3.844E-08	0.0000	0.0857	0.000
222000.0	2.99	3.837E-08	0.0000	0.0857	0.000
223000.0	2.99	3.830E-08	0.0000	0.0858	0.000
224000.0	2.99	3.823E-08	0.0000	0.0858	0.000
225000.0	2.99	3.816E-08	0.0000	0.0858	0.000
226000.0	2.98	3.809E-08	0.0000	0.0859	0.000
227000.0	2.98	3.802E-08	0.0000	0.0859	0.000
228000.0	2.98	3.795E-08	0.0000	0.0860	0.000
229000.0	2.98	3.788E-08	0.0000	0.0860	0.000
230000.0	2.97	3.781E-08	0.0000	0.0860	0.000
231000.0	2.97	3.774E-08	0.0000	0.0861	0.000
232000.0	2.97	3.767E-08	0.0000	0.0861	0.000
233000.0	2.97	3.760E-08	0.0000	0.0861	0.000
234000.0	2.96	3.754E-08	0.0000	0.0862	0.000
235000.0	2.96	3.747E-08	0.0000	0.0862	0.000
236000.0	2.96	3.740E-08	0.0000	0.0863	0.000
237000.0	2.96	3.733E-08	0.0000	0.0863	0.000
238000.0	2.95	3.726E-08	0.0000	0.0863	0.000
239000.0	2.95	3.720E-08	0.0000	0.0864	0.000
240000.0	2.95	3.713E-08	0.0000	0.0864	0.000
241000.0	2.95	3.706E-08	0.0000	0.0864	0.000
242000.0	2.94	3.699E-08	0.0000	0.0865	0.000
243000.0	2.94	3.693E-08	0.0000	0.0865	0.000
244000.0	2.94	3.686E-08	0.0000	0.0865	0.000
245000.0	2.94	3.679E-08	0.0000	0.0866	0.000
246000.0	2.93	3.673E-08	0.0000	0.0866	0.000
247000.0	2.93	3.666E-08	0.0000	0.0867	0.000
248000.0	2.93	3.660E-08	0.0000	0.0867	0.000
249000.0	2.93	3.653E-08	0.0000	0.0867	0.000
250000.0	2.92	3.646E-08	0.0000	0.0868	0.000
251000.0	2.92	3.640E-08	0.0000	0.0868	0.000
252000.0	2.92	3.633E-08	0.0000	0.0868	0.000
253000.0	2.92	3.627E-08	0.0000	0.0869	0.000
254000.0	2.91	3.620E-08	0.0000	0.0869	0.000
255000.0	2.91	3.614E-08	0.0000	0.0870	0.000
256000.0	2.91	3.607E-08	0.0000	0.0870	0.000
257000.0	2.91	3.601E-08	0.0000	0.0870	0.000
258000.0	2.90	3.595E-08	0.0000	0.0871	0.000
259000.0	2.90	3.588E-08	0.0000	0.0871	0.000
260000.0	2.90	3.582E-08	0.0000	0.0871	0.000
261000.0	2.90	3.575E-08	0.0000	0.0872	0.000
262000.0	2.89	3.569E-08	0.0000	0.0872	0.000
263000.0	2.89	3.563E-08	0.0000	0.0872	0.000
264000.0	2.89	3.556E-08	0.0000	0.0873	0.000
265000.0	2.89	3.550E-08	0.0000	0.0873	0.000
266000.0	2.89	3.544E-08	0.0000	0.0873	0.000
267000.0	2.88	3.538E-08	0.0000	0.0874	0.000
268000.0	2.88	3.531E-08	0.0000	0.0874	0.000
269000.0	2.88	3.525E-08	0.0000	0.0874	0.000
270000.0	2.88	3.519E-08	0.0000	0.0875	0.000
271000.0	2.87	3.513E-08	0.0000	0.0875	0.000
272000.0	2.87	3.507E-08	0.0000	0.0876	0.000
273000.0	2.87	3.500E-08	0.0000	0.0876	0.000
274000.0	2.87	3.494E-08	0.0000	0.0876	0.000

275000.0	2.86	3.488E-08	0.0000	0.0877	0.000
276000.0	2.86	3.482E-08	0.0000	0.0877	0.000
277000.0	2.86	3.476E-08	0.0000	0.0877	0.000
278000.0	2.86	3.470E-08	0.0000	0.0878	0.000
279000.0	2.85	3.464E-08	0.0000	0.0878	0.000
280000.0	2.85	3.458E-08	0.0000	0.0878	0.000
281000.0	2.85	3.452E-08	0.0000	0.0879	0.000
282000.0	2.85	3.446E-08	0.0000	0.0879	0.000
283000.0	2.85	3.440E-08	0.0000	0.0879	0.000
284000.0	2.84	3.434E-08	0.0000	0.0880	0.000
285000.0	2.84	3.428E-08	0.0000	0.0880	0.000
286000.0	2.84	3.422E-08	0.0000	0.0880	0.000
287000.0	2.84	3.416E-08	0.0000	0.0881	0.000
288000.0	2.83	3.410E-08	0.0000	0.0881	0.000
289000.0	2.83	3.404E-08	0.0000	0.0881	0.000
290000.0	2.83	3.398E-08	0.0000	0.0882	0.000
291000.0	2.83	3.392E-08	0.0000	0.0882	0.000
292000.0	2.83	3.387E-08	0.0000	0.0882	0.000
293000.0	2.82	3.381E-08	0.0000	0.0883	0.000
294000.0	2.82	3.375E-08	0.0000	0.0883	0.000
295000.0	2.82	3.369E-08	0.0000	0.0883	0.000
296000.0	2.82	3.363E-08	0.0000	0.0884	0.000
297000.0	2.81	3.358E-08	0.0000	0.0884	0.000
298000.0	2.81	3.352E-08	0.0000	0.0884	0.000
299000.0	2.81	3.346E-08	0.0000	0.0885	0.000
300000.0	2.81	3.340E-08	0.0000	0.0885	0.000
301000.0	2.80	3.335E-08	0.0000	0.0885	0.000
302000.0	2.80	3.329E-08	0.0000	0.0886	0.000
303000.0	2.80	3.323E-08	0.0000	0.0886	0.000
304000.0	2.80	3.317E-08	0.0000	0.0886	0.000
305000.0	2.80	3.312E-08	0.0000	0.0887	0.000
306000.0	2.79	3.306E-08	0.0000	0.0887	0.000
307000.0	2.79	3.301E-08	0.0000	0.0887	0.000
308000.0	2.79	3.295E-08	0.0000	0.0888	0.000
309000.0	2.79	3.289E-08	0.0000	0.0888	0.000
310000.0	2.79	3.284E-08	0.0000	0.0888	0.000
311000.0	2.78	3.278E-08	0.0000	0.0889	0.000
312000.0	2.78	3.273E-08	0.0000	0.0889	0.000
313000.0	2.78	3.267E-08	0.0000	0.0889	0.000
314000.0	2.78	3.262E-08	0.0000	0.0890	0.000
315000.0	2.77	3.256E-08	0.0000	0.0890	0.000
316000.0	2.77	3.251E-08	0.0000	0.0890	0.000
317000.0	2.77	3.245E-08	0.0000	0.0891	0.000
318000.0	2.77	3.240E-08	0.0000	0.0891	0.000
319000.0	2.77	3.234E-08	0.0000	0.0891	0.000
320000.0	2.76	3.229E-08	0.0000	0.0892	0.000
321000.0	2.76	3.223E-08	0.0000	0.0892	0.000
322000.0	2.76	3.218E-08	0.0000	0.0892	0.000
323000.0	2.76	3.213E-08	0.0000	0.0893	0.000
324000.0	2.75	3.207E-08	0.0000	0.0893	0.000
325000.0	2.75	3.202E-08	0.0000	0.0893	0.000
326000.0	2.75	3.196E-08	0.0000	0.0894	0.000
327000.0	2.75	3.191E-08	0.0000	0.0894	0.000
328000.0	2.75	3.186E-08	0.0000	0.0894	0.000
329000.0	2.74	3.180E-08	0.0000	0.0895	0.000
330000.0	2.74	3.175E-08	0.0000	0.0895	0.000
331000.0	2.74	3.170E-08	0.0000	0.0896	0.000
332000.0	2.74	3.165E-08	0.0000	0.0896	0.000
333000.0	2.74	3.159E-08	0.0000	0.0896	0.000
334000.0	2.73	3.154E-08	0.0000	0.0896	0.000
335000.0	2.73	3.149E-08	0.0000	0.0896	0.000
336000.0	2.73	3.144E-08	0.0000	0.0897	0.000
337000.0	2.73	3.138E-08	0.0000	0.0897	0.000

338000.0	2.73	3.133E-08	0.0000	0.0897	0.000
339000.0	2.72	3.128E-08	0.0000	0.0898	0.000
340000.0	2.72	3.123E-08	0.0000	0.0898	0.000
341000.0	2.72	3.118E-08	0.0000	0.0898	0.000
342000.0	2.72	3.113E-08	0.0000	0.0899	0.000
343000.0	2.71	3.107E-08	0.0000	0.0899	0.000
344000.0	2.71	3.102E-08	0.0000	0.0899	0.000
345000.0	2.71	3.097E-08	0.0000	0.0900	0.000
346000.0	2.71	3.092E-08	0.0000	0.0900	0.000
347000.0	2.71	3.087E-08	0.0000	0.0901	0.000
348000.0	2.70	3.082E-08	0.0000	0.0901	0.000
349000.0	2.70	3.077E-08	0.0000	0.0901	0.000
350000.0	2.70	3.072E-08	0.0000	0.0901	0.000
351000.0	2.70	3.067E-08	0.0000	0.0902	0.000
352000.0	2.70	3.062E-08	0.0000	0.0902	0.000
353000.0	2.69	3.057E-08	0.0000	0.0902	0.000
354000.0	2.69	3.052E-08	0.0000	0.0903	0.000
355000.0	2.69	3.047E-08	0.0000	0.0903	0.000
356000.0	2.69	3.042E-08	0.0000	0.0903	0.000
357000.0	2.69	3.037E-08	0.0000	0.0904	0.000
358000.0	2.68	3.032E-08	0.0000	0.0904	0.000
359000.0	2.68	3.027E-08	0.0000	0.0904	0.000
360000.0	2.68	3.022E-08	0.0000	0.0904	0.000
361000.0	2.68	3.017E-08	0.0000	0.0905	0.000
362000.0	2.68	3.012E-08	0.0000	0.0905	0.000
363000.0	2.67	3.008E-08	0.0000	0.0905	0.000
364000.0	2.67	3.003E-08	0.0000	0.0906	0.000
365000.0	2.67	2.998E-08	0.0000	0.0906	0.000
366000.0	2.67	2.993E-08	0.0000	0.0906	0.000
367000.0	2.67	2.988E-08	0.0000	0.0907	0.000
368000.0	2.66	2.983E-08	0.0000	0.0907	0.000
369000.0	2.66	2.979E-08	0.0000	0.0907	0.000
370000.0	2.66	2.974E-08	0.0000	0.0907	0.000
371000.0	2.66	2.969E-08	0.0000	0.0907	0.000
372000.0	2.66	2.964E-08	0.0000	0.0908	0.000
373000.0	2.65	2.959E-08	0.0000	0.0908	0.000
374000.0	2.65	2.955E-08	0.0000	0.0908	0.000
375000.0	2.65	2.950E-08	0.0000	0.0909	0.000
376000.0	2.65	2.945E-08	0.0000	0.0909	0.000
377000.0	2.65	2.941E-08	0.0000	0.0909	0.000
378000.0	2.64	2.936E-08	0.0000	0.0910	0.000
379000.0	2.64	2.931E-08	0.0000	0.0910	0.000
380000.0	2.64	2.927E-08	0.0000	0.0910	0.000
381000.0	2.64	2.922E-08	0.0000	0.0910	0.000
382000.0	2.64	2.917E-08	0.0000	0.0911	0.000
383000.0	2.63	2.913E-08	0.0000	0.0911	0.000
384000.0	2.63	2.908E-08	0.0000	0.0911	0.000
385000.0	2.63	2.903E-08	0.0000	0.0912	0.000
386000.0	2.63	2.899E-08	0.0000	0.0912	0.000
387000.0	2.63	2.894E-08	0.0000	0.0912	0.000
388000.0	2.62	2.890E-08	0.0000	0.0912	0.000
389000.0	2.62	2.885E-08	0.0000	0.0913	0.000
390000.0	2.62	2.880E-08	0.0000	0.0913	0.000
391000.0	2.62	2.876E-08	0.0000	0.0913	0.000
392000.0	2.62	2.871E-08	0.0000	0.0914	0.000
393000.0	2.62	2.867E-08	0.0000	0.0914	0.000
394000.0	2.61	2.862E-08	0.0000	0.0914	0.000
395000.0	2.61	2.858E-08	0.0000	0.0914	0.000
396000.0	2.61	2.853E-08	0.0000	0.0915	0.000
397000.0	2.61	2.849E-08	0.0000	0.0915	0.000
398000.0	2.61	2.844E-08	0.0000	0.0915	0.000
399000.0	2.60	2.840E-08	0.0000	0.0916	0.000
400000.0	2.60	2.835E-08	0.0000	0.0916	0.000

401000.0	2.60	2.831E-08	0.0000	0.0916	0.000
402000.0	2.60	2.826E-08	0.0000	0.0916	0.000
403000.0	2.60	2.822E-08	0.0000	0.0917	0.000
404000.0	2.59	2.818E-08	0.0000	0.0917	0.000
405000.0	2.59	2.813E-08	0.0000	0.0917	0.000
406000.0	2.59	2.809E-08	0.0000	0.0918	0.000
407000.0	2.59	2.804E-08	0.0000	0.0918	0.000
408000.0	2.59	2.800E-08	0.0000	0.0918	0.000
409000.0	2.59	2.796E-08	0.0000	0.0919	0.000
410000.0	2.58	2.791E-08	0.0000	0.0919	0.000
411000.0	2.58	2.787E-08	0.0000	0.0919	0.000
412000.0	2.58	2.783E-08	0.0000	0.0920	0.000
413000.0	2.58	2.778E-08	0.0000	0.0920	0.000
414000.0	2.58	2.774E-08	0.0000	0.0920	0.000
415000.0	2.57	2.770E-08	0.0000	0.0920	0.000
416000.0	2.57	2.766E-08	0.0000	0.0921	0.000
417000.0	2.57	2.761E-08	0.0000	0.0921	0.000
418000.0	2.57	2.757E-08	0.0000	0.0921	0.000
419000.0	2.57	2.753E-08	0.0000	0.0921	0.000
420000.0	2.56	2.748E-08	0.0000	0.0922	0.000
421000.0	2.56	2.744E-08	0.0000	0.0922	0.000
422000.0	2.56	2.740E-08	0.0000	0.0922	0.000
423000.0	2.56	2.736E-08	0.0000	0.0923	0.000
424000.0	2.56	2.732E-08	0.0000	0.0923	0.000
425000.0	2.56	2.727E-08	0.0000	0.0923	0.000
426000.0	2.55	2.723E-08	0.0000	0.0923	0.000
427000.0	2.55	2.719E-08	0.0000	0.0924	0.000
428000.0	2.55	2.715E-08	0.0000	0.0924	0.000
429000.0	2.55	2.711E-08	0.0000	0.0924	0.000
430000.0	2.55	2.707E-08	0.0000	0.0924	0.000
431000.0	2.54	2.702E-08	0.0000	0.0925	0.000
432000.0	2.54	2.698E-08	0.0000	0.0925	0.000
433000.0	2.54	2.694E-08	0.0000	0.0925	0.000
434000.0	2.54	2.690E-08	0.0000	0.0925	0.000
435000.0	2.54	2.686E-08	0.0000	0.0926	0.000
436000.0	2.54	2.682E-08	0.0000	0.0926	0.000
437000.0	2.53	2.678E-08	0.0000	0.0926	0.000
438000.0	2.53	2.674E-08	0.0000	0.0926	0.000
439000.0	2.53	2.670E-08	0.0000	0.0927	0.000
440000.0	2.53	2.666E-08	0.0000	0.0927	0.000
441000.0	2.53	2.662E-08	0.0000	0.0927	0.000
442000.0	2.53	2.658E-08	0.0000	0.0927	0.000
443000.0	2.52	2.654E-08	0.0000	0.0928	0.000
444000.0	2.52	2.650E-08	0.0000	0.0928	0.000
445000.0	2.52	2.646E-08	0.0000	0.0928	0.000
446000.0	2.52	2.642E-08	0.0000	0.0928	0.000
447000.0	2.52	2.638E-08	0.0000	0.0929	0.000
448000.0	2.51	2.634E-08	0.0000	0.0929	0.000
449000.0	2.51	2.630E-08	0.0000	0.0929	0.000
450000.0	2.51	2.626E-08	0.0000	0.0930	0.000
451000.0	2.51	2.622E-08	0.0000	0.0930	0.000
452000.0	2.51	2.618E-08	0.0000	0.0930	0.000
453000.0	2.51	2.614E-08	0.0000	0.0930	0.000
454000.0	2.50	2.610E-08	0.0000	0.0931	0.000
455000.0	2.50	2.606E-08	0.0000	0.0931	0.000
456000.0	2.50	2.602E-08	0.0000	0.0931	0.000
457000.0	2.50	2.598E-08	0.0000	0.0931	0.000
458000.0	2.50	2.594E-08	0.0000	0.0932	0.000
459000.0	2.50	2.590E-08	0.0000	0.0932	0.000
460000.0	2.49	2.587E-08	0.0000	0.0932	0.000
461000.0	2.49	2.583E-08	0.0000	0.0932	0.000
462000.0	2.49	2.579E-08	0.0000	0.0933	0.000
463000.0	2.49	2.575E-08	0.0000	0.0933	0.000

464000.0	2.49	2.571E-08	0.0000	0.0933	0.000
465000.0	2.49	2.567E-08	0.0000	0.0933	0.000
466000.0	2.48	2.564E-08	0.0000	0.0934	0.000
467000.0	2.48	2.560E-08	0.0000	0.0934	0.000
468000.0	2.48	2.556E-08	0.0000	0.0934	0.000
469000.0	2.48	2.552E-08	0.0000	0.0934	0.000
470000.0	2.48	2.548E-08	0.0000	0.0935	0.000
471000.0	2.48	2.545E-08	0.0000	0.0935	0.000
472000.0	2.47	2.541E-08	0.0000	0.0935	0.000
473000.0	2.47	2.537E-08	0.0000	0.0935	0.000
474000.0	2.47	2.533E-08	0.0000	0.0936	0.000
475000.0	2.47	2.530E-08	0.0000	0.0936	0.000
476000.0	2.47	2.526E-08	0.0000	0.0936	0.000
477000.0	2.46	2.522E-08	0.0000	0.0936	0.000
478000.0	2.46	2.518E-08	0.0000	0.0937	0.000
479000.0	2.46	2.515E-08	0.0000	0.0937	0.000
480000.0	2.46	2.511E-08	0.0000	0.0937	0.000
481000.0	2.46	2.507E-08	0.0000	0.0937	0.000
482000.0	2.46	2.504E-08	0.0000	0.0938	0.000
483000.0	2.45	2.500E-08	0.0000	0.0938	0.000
484000.0	2.45	2.496E-08	0.0000	0.0938	0.000
485000.0	2.45	2.493E-08	0.0000	0.0938	0.000
486000.0	2.45	2.489E-08	0.0000	0.0939	0.000
487000.0	2.45	2.485E-08	0.0000	0.0939	0.000
488000.0	2.45	2.482E-08	0.0000	0.0939	0.000
489000.0	2.44	2.478E-08	0.0000	0.0939	0.000
490000.0	2.44	2.475E-08	0.0000	0.0940	0.000
491000.0	2.44	2.471E-08	0.0000	0.0940	0.000
492000.0	2.44	2.467E-08	0.0000	0.0940	0.000
493000.0	2.44	2.464E-08	0.0000	0.0940	0.000
494000.0	2.44	2.460E-08	0.0000	0.0941	0.000
495000.0	2.44	2.457E-08	0.0000	0.0941	0.000
496000.0	2.43	2.453E-08	0.0000	0.0941	0.000
497000.0	2.43	2.450E-08	0.0000	0.0941	0.000
498000.0	2.43	2.446E-08	0.0000	0.0942	0.000
499000.0	2.43	2.442E-08	0.0000	0.0942	0.000
500000.0	2.43	2.439E-08	0.0000	0.0942	0.000

Date: 25-Sept-1995
Time: 12:57:47.66

STRESS CORROSION CRACK GROWTH ANALYSIS

WSI-20Q: SEQUOYAH CRDM LOWER CSW OVERLAY, SECTION D

INITIAL CRACK SIZE= 0.0750
MAX CRACK SIZE FOR SCCG= 0.8000

STRESS CORROSION CRACK GROWTH LAW

LAW ID	C	N	Kthres	K1C
NRC/10	3.590E-09	2.1610	0.0000	200.0000

STRESS COEFFICIENTS

CASE ID	C0	C1	C2	C3
BEND	1.7128	-5.8723	0.0000	0.0000
MEMBRANE	0.7100	0.0000	0.0000	0.0000
SECC	24.9810	-618.1000	3314.0000	-4183.0000
SECD	40.9851	-788.8973	3968.8642	-5013.4105
APPLIED	10.0000	0.0000	0.0000	0.0000

CASE ID	Kmax SCALE FACTOR
SECD	1.0000
APPLIED	0.2000

TIME	TIME INCREMENT	PRINT INCREMENT
500000.0	1000.0	1000.0

crack model:CONTINUOUS SURFACE CRACK IN HALF SPACE

CRACK SIZE	STRESS INTENSITY FACTOR				
	CASE BEND	CASE MEMBRANE	CASE SECC	CASE SECD	CASE APPLIED
0.0160	0.416	0.178	4.861	8.481	2.511
0.0320	0.568	0.252	5.145	9.756	3.551
0.0480	0.670	0.309	4.494	9.578	4.349
0.0640	0.745	0.357	3.441	8.728	5.022
0.0800	0.801	0.399	2.249	7.578	5.615
0.0960	0.843	0.437	1.076	6.348	6.151
0.1120	0.872	0.472	0.031	5.187	6.644
0.1280	0.892	0.504	-0.812	4.195	7.102
0.1440	0.903	0.535	-1.403	3.443	7.533
0.1600	0.906	0.564	-1.709	2.977	7.941
0.1760	0.903	0.591	-1.708	2.828	8.328
0.1920	0.893	0.618	-1.391	3.010	8.698
0.2080	0.878	0.643	-0.760	3.526	9.054
0.2240	0.858	0.667	0.179	4.368	9.395
0.2400	0.832	0.690	1.407	5.522	9.725

0.2560	0.802	0.713	2.905	6.961	10.044
0.2720	0.767	0.735	4.642	8.653	10.353
0.2880	0.729	0.756	6.587	10.561	10.653
0.3040	0.686	0.777	8.699	12.638	10.945
0.3200	0.640	0.797	10.935	14.835	11.230
0.3360	0.590	0.817	13.248	17.094	11.507
0.3520	0.537	0.836	15.586	19.354	11.778
0.3680	0.480	0.855	17.891	21.550	12.043
0.3840	0.420	0.873	20.106	23.610	12.302
0.4000	0.357	0.891	22.166	25.459	12.555
0.4160	0.291	0.909	24.005	27.018	12.804
0.4320	0.222	0.926	25.552	28.202	13.048
0.4480	0.150	0.943	26.734	28.926	13.287
0.4640	0.075	0.960	27.474	29.097	13.522
0.4800	-0.002	0.976	27.693	28.621	13.754
0.4960	-0.082	0.993	27.309	27.400	13.981
0.5120	-0.165	1.009	26.237	25.333	14.205
0.5280	-0.250	1.024	24.388	22.313	14.425
0.5440	-0.337	1.040	21.672	18.233	14.642
0.5600	-0.427	1.055	17.996	12.982	14.855
0.5760	-0.519	1.070	13.265	6.445	15.066
0.5920	-0.613	1.084	7.379	-1.495	15.274
0.6080	-0.710	1.099	0.239	-10.958	15.479
0.6240	-0.809	1.113	-8.259	-22.068	15.681
0.6400	-0.910	1.128	-18.219	-34.949	15.881
0.6560	-1.013	1.142	-29.750	-49.732	16.078
0.6720	-1.118	1.155	-42.961	-66.547	16.273
0.6880	-1.226	1.169	-57.964	-85.528	16.466
0.7040	-1.335	1.183	-74.874	-106.812	16.656
0.7200	-1.447	1.196	-93.805	-130.538	16.845
0.7360	-1.560	1.209	-114.878	-156.847	17.031
0.7520	-1.675	1.222	-138.211	-185.884	17.215
0.7680	-1.792	1.235	-163.928	-217.794	17.397
0.7840	-1.911	1.248	-192.152	-252.727	17.577
0.8000	-2.032	1.261	-223.011	-290.834	17.756

TIME	KMAX	DA/DT	DA	A	A/THK
1000.0	9.02	4.165E-07	0.0004	0.0754	0.000
2000.0	9.00	4.138E-07	0.0004	0.0758	0.000
3000.0	8.97	4.112E-07	0.0004	0.0762	0.000
4000.0	8.94	4.086E-07	0.0004	0.0767	0.000
5000.0	8.92	4.060E-07	0.0004	0.0771	0.000
6000.0	8.89	4.034E-07	0.0004	0.0775	0.000
7000.0	8.86	4.008E-07	0.0004	0.0779	0.000
8000.0	8.84	3.983E-07	0.0004	0.0783	0.000
9000.0	8.81	3.958E-07	0.0004	0.0787	0.000
10000.0	8.79	3.933E-07	0.0004	0.0790	0.000
11000.0	8.76	3.909E-07	0.0004	0.0794	0.000
12000.0	8.74	3.885E-07	0.0004	0.0798	0.000
13000.0	8.71	3.861E-07	0.0004	0.0802	0.000
14000.0	8.69	3.836E-07	0.0004	0.0806	0.000
15000.0	8.66	3.810E-07	0.0004	0.0810	0.000
16000.0	8.63	3.785E-07	0.0004	0.0814	0.000
17000.0	8.61	3.760E-07	0.0004	0.0817	0.000
18000.0	8.58	3.735E-07	0.0004	0.0821	0.000
19000.0	8.55	3.710E-07	0.0004	0.0825	0.000
20000.0	8.53	3.686E-07	0.0004	0.0828	0.000
21000.0	8.50	3.662E-07	0.0004	0.0832	0.000

Structural Integrity Associates, Inc.

22000.0	8.48	3.638E-07	0.0004	0.0836	0.000
23000.0	8.45	3.614E-07	0.0004	0.0839	0.000
24000.0	8.42	3.591E-07	0.0004	0.0843	0.000
25000.0	8.40	3.568E-07	0.0004	0.0847	0.000
26000.0	8.37	3.545E-07	0.0004	0.0850	0.000
27000.0	8.35	3.522E-07	0.0004	0.0854	0.000
28000.0	8.32	3.500E-07	0.0003	0.0857	0.000
29000.0	8.30	3.477E-07	0.0003	0.0861	0.000
30000.0	8.28	3.455E-07	0.0003	0.0864	0.000
31000.0	8.25	3.433E-07	0.0003	0.0867	0.000
32000.0	8.23	3.412E-07	0.0003	0.0871	0.000
33000.0	8.20	3.390E-07	0.0003	0.0874	0.000
34000.0	8.18	3.369E-07	0.0003	0.0878	0.000
35000.0	8.16	3.348E-07	0.0003	0.0881	0.000
36000.0	8.13	3.327E-07	0.0003	0.0884	0.000
37000.0	8.11	3.307E-07	0.0003	0.0888	0.000
38000.0	8.09	3.286E-07	0.0003	0.0891	0.000
39000.0	8.06	3.266E-07	0.0003	0.0894	0.000
40000.0	8.04	3.246E-07	0.0003	0.0897	0.000
41000.0	8.02	3.226E-07	0.0003	0.0901	0.000
42000.0	7.99	3.207E-07	0.0003	0.0904	0.000
43000.0	7.97	3.187E-07	0.0003	0.0907	0.000
44000.0	7.95	3.168E-07	0.0003	0.0910	0.000
45000.0	7.93	3.149E-07	0.0003	0.0913	0.000
46000.0	7.91	3.130E-07	0.0003	0.0916	0.000
47000.0	7.88	3.111E-07	0.0003	0.0920	0.000
48000.0	7.86	3.093E-07	0.0003	0.0923	0.000
49000.0	7.84	3.074E-07	0.0003	0.0926	0.000
50000.0	7.82	3.056E-07	0.0003	0.0929	0.000
51000.0	7.80	3.038E-07	0.0003	0.0932	0.000
52000.0	7.78	3.020E-07	0.0003	0.0935	0.000
53000.0	7.75	3.002E-07	0.0003	0.0938	0.000
54000.0	7.73	2.985E-07	0.0003	0.0941	0.000
55000.0	7.71	2.967E-07	0.0003	0.0944	0.000
56000.0	7.69	2.950E-07	0.0003	0.0947	0.000
57000.0	7.67	2.933E-07	0.0003	0.0950	0.000
58000.0	7.65	2.916E-07	0.0003	0.0953	0.000
59000.0	7.63	2.899E-07	0.0003	0.0956	0.000
60000.0	7.61	2.882E-07	0.0003	0.0958	0.000
61000.0	7.59	2.866E-07	0.0003	0.0961	0.000
62000.0	7.57	2.850E-07	0.0003	0.0964	0.000
63000.0	7.55	2.834E-07	0.0003	0.0967	0.000
64000.0	7.53	2.819E-07	0.0003	0.0970	0.000
65000.0	7.51	2.804E-07	0.0003	0.0973	0.000
66000.0	7.49	2.789E-07	0.0003	0.0975	0.000
67000.0	7.48	2.774E-07	0.0003	0.0978	0.000
68000.0	7.46	2.759E-07	0.0003	0.0981	0.000
69000.0	7.44	2.745E-07	0.0003	0.0984	0.000
70000.0	7.42	2.730E-07	0.0003	0.0986	0.000
71000.0	7.40	2.716E-07	0.0003	0.0989	0.000
72000.0	7.39	2.702E-07	0.0003	0.0992	0.000
73000.0	7.37	2.688E-07	0.0003	0.0994	0.000
74000.0	7.35	2.673E-07	0.0003	0.0997	0.000
75000.0	7.33	2.660E-07	0.0003	0.1000	0.000
76000.0	7.31	2.646E-07	0.0003	0.1002	0.000
77000.0	7.30	2.632E-07	0.0003	0.1005	0.000
78000.0	7.28	2.618E-07	0.0003	0.1008	0.000
79000.0	7.26	2.605E-07	0.0003	0.1010	0.000
80000.0	7.24	2.591E-07	0.0003	0.1013	0.000
81000.0	7.23	2.578E-07	0.0003	0.1015	0.000
82000.0	7.21	2.565E-07	0.0003	0.1018	0.000
83000.0	7.19	2.552E-07	0.0003	0.1021	0.000
84000.0	7.18	2.539E-07	0.0003	0.1023	0.000

85000.0	7.16	2.526E-07	0.0003	0.1026	0.000
86000.0	7.14	2.513E-07	0.0003	0.1028	0.000
87000.0	7.13	2.501E-07	0.0003	0.1031	0.000
88000.0	7.11	2.488E-07	0.0002	0.1033	0.000
89000.0	7.09	2.476E-07	0.0002	0.1036	0.000
90000.0	7.08	2.463E-07	0.0002	0.1038	0.000
91000.0	7.06	2.451E-07	0.0002	0.1041	0.000
92000.0	7.04	2.439E-07	0.0002	0.1043	0.000
93000.0	7.03	2.427E-07	0.0002	0.1045	0.000
94000.0	7.01	2.415E-07	0.0002	0.1048	0.000
95000.0	7.00	2.403E-07	0.0002	0.1050	0.000
96000.0	6.98	2.391E-07	0.0002	0.1053	0.000
97000.0	6.96	2.379E-07	0.0002	0.1055	0.000
98000.0	6.95	2.367E-07	0.0002	0.1057	0.000
99000.0	6.93	2.356E-07	0.0002	0.1060	0.000
100000.0	6.92	2.344E-07	0.0002	0.1062	0.000
101000.0	6.90	2.333E-07	0.0002	0.1064	0.000
102000.0	6.89	2.322E-07	0.0002	0.1067	0.000
103000.0	6.87	2.311E-07	0.0002	0.1069	0.000
104000.0	6.85	2.299E-07	0.0002	0.1071	0.000
105000.0	6.84	2.288E-07	0.0002	0.1074	0.000
106000.0	6.82	2.277E-07	0.0002	0.1076	0.000
107000.0	6.81	2.266E-07	0.0002	0.1078	0.000
108000.0	6.79	2.256E-07	0.0002	0.1080	0.000
109000.0	6.78	2.245E-07	0.0002	0.1083	0.000
110000.0	6.76	2.234E-07	0.0002	0.1085	0.000
111000.0	6.75	2.224E-07	0.0002	0.1087	0.000
112000.0	6.73	2.213E-07	0.0002	0.1089	0.000
113000.0	6.72	2.203E-07	0.0002	0.1092	0.000
114000.0	6.70	2.192E-07	0.0002	0.1094	0.000
115000.0	6.69	2.182E-07	0.0002	0.1096	0.000
116000.0	6.68	2.172E-07	0.0002	0.1098	0.000
117000.0	6.66	2.162E-07	0.0002	0.1100	0.000
118000.0	6.65	2.152E-07	0.0002	0.1102	0.000
119000.0	6.63	2.142E-07	0.0002	0.1105	0.000
120000.0	6.62	2.132E-07	0.0002	0.1107	0.000
121000.0	6.60	2.122E-07	0.0002	0.1109	0.000
122000.0	6.59	2.112E-07	0.0002	0.1111	0.000
123000.0	6.58	2.103E-07	0.0002	0.1113	0.000
124000.0	6.56	2.093E-07	0.0002	0.1115	0.000
125000.0	6.55	2.083E-07	0.0002	0.1117	0.000
126000.0	6.53	2.074E-07	0.0002	0.1119	0.000
127000.0	6.52	2.064E-07	0.0002	0.1121	0.000
128000.0	6.51	2.056E-07	0.0002	0.1123	0.000
129000.0	6.50	2.048E-07	0.0002	0.1125	0.000
130000.0	6.49	2.040E-07	0.0002	0.1127	0.000
131000.0	6.47	2.032E-07	0.0002	0.1130	0.000
132000.0	6.46	2.025E-07	0.0002	0.1132	0.000
133000.0	6.45	2.017E-07	0.0002	0.1134	0.000
134000.0	6.44	2.009E-07	0.0002	0.1136	0.000
135000.0	6.43	2.002E-07	0.0002	0.1138	0.000
136000.0	6.42	1.994E-07	0.0002	0.1140	0.000
137000.0	6.41	1.987E-07	0.0002	0.1142	0.000
138000.0	6.39	1.979E-07	0.0002	0.1144	0.000
139000.0	6.38	1.972E-07	0.0002	0.1145	0.000
140000.0	6.37	1.964E-07	0.0002	0.1147	0.000
141000.0	6.36	1.957E-07	0.0002	0.1149	0.000
142000.0	6.35	1.950E-07	0.0002	0.1151	0.000
143000.0	6.34	1.942E-07	0.0002	0.1153	0.000
144000.0	6.33	1.935E-07	0.0002	0.1155	0.000
145000.0	6.32	1.928E-07	0.0002	0.1157	0.000
146000.0	6.31	1.921E-07	0.0002	0.1159	0.000
147000.0	6.30	1.914E-07	0.0002	0.1161	0.000

148000.0	6.29	1.907E-07	0.0002	0.1163	0.000
149000.0	6.27	1.900E-07	0.0002	0.1165	0.000
150000.0	6.26	1.893E-07	0.0002	0.1167	0.000
151000.0	6.25	1.886E-07	0.0002	0.1169	0.000
152000.0	6.24	1.879E-07	0.0002	0.1170	0.000
153000.0	6.23	1.872E-07	0.0002	0.1172	0.000
154000.0	6.22	1.865E-07	0.0002	0.1174	0.000
155000.0	6.21	1.858E-07	0.0002	0.1176	0.000
156000.0	6.20	1.852E-07	0.0002	0.1178	0.000
157000.0	6.19	1.845E-07	0.0002	0.1180	0.000
158000.0	6.18	1.838E-07	0.0002	0.1182	0.000
159000.0	6.17	1.832E-07	0.0002	0.1183	0.000
160000.0	6.16	1.825E-07	0.0002	0.1185	0.000
161000.0	6.15	1.818E-07	0.0002	0.1187	0.000
162000.0	6.14	1.812E-07	0.0002	0.1189	0.000
163000.0	6.13	1.805E-07	0.0002	0.1191	0.000
164000.0	6.12	1.799E-07	0.0002	0.1192	0.000
165000.0	6.11	1.792E-07	0.0002	0.1194	0.000
166000.0	6.10	1.786E-07	0.0002	0.1196	0.000
167000.0	6.09	1.780E-07	0.0002	0.1198	0.000
168000.0	6.08	1.773E-07	0.0002	0.1200	0.000
169000.0	6.07	1.767E-07	0.0002	0.1201	0.000
170000.0	6.06	1.761E-07	0.0002	0.1203	0.000
171000.0	6.05	1.755E-07	0.0002	0.1205	0.000
172000.0	6.04	1.748E-07	0.0002	0.1207	0.000
173000.0	6.03	1.742E-07	0.0002	0.1208	0.000
174000.0	6.02	1.736E-07	0.0002	0.1210	0.000
175000.0	6.01	1.730E-07	0.0002	0.1212	0.000
176000.0	6.00	1.724E-07	0.0002	0.1214	0.000
177000.0	5.99	1.718E-07	0.0002	0.1215	0.000
178000.0	5.98	1.712E-07	0.0002	0.1217	0.000
179000.0	5.97	1.706E-07	0.0002	0.1219	0.000
180000.0	5.96	1.700E-07	0.0002	0.1220	0.000
181000.0	5.95	1.694E-07	0.0002	0.1222	0.000
182000.0	5.94	1.688E-07	0.0002	0.1224	0.000
183000.0	5.93	1.683E-07	0.0002	0.1225	0.000
184000.0	5.92	1.677E-07	0.0002	0.1227	0.000
185000.0	5.91	1.671E-07	0.0002	0.1229	0.000
186000.0	5.90	1.665E-07	0.0002	0.1230	0.000
187000.0	5.89	1.660E-07	0.0002	0.1232	0.000
188000.0	5.89	1.654E-07	0.0002	0.1234	0.000
189000.0	5.88	1.648E-07	0.0002	0.1235	0.000
190000.0	5.87	1.643E-07	0.0002	0.1237	0.000
191000.0	5.86	1.637E-07	0.0002	0.1239	0.000
192000.0	5.85	1.632E-07	0.0002	0.1240	0.000
193000.0	5.84	1.626E-07	0.0002	0.1242	0.000
194000.0	5.83	1.621E-07	0.0002	0.1244	0.000
195000.0	5.82	1.615E-07	0.0002	0.1245	0.000
196000.0	5.81	1.610E-07	0.0002	0.1247	0.000
197000.0	5.80	1.604E-07	0.0002	0.1248	0.000
198000.0	5.79	1.599E-07	0.0002	0.1250	0.000
199000.0	5.78	1.593E-07	0.0002	0.1252	0.000
200000.0	5.78	1.588E-07	0.0002	0.1253	0.000
201000.0	5.77	1.583E-07	0.0002	0.1255	0.000
202000.0	5.76	1.578E-07	0.0002	0.1256	0.000
203000.0	5.75	1.572E-07	0.0002	0.1258	0.000
204000.0	5.74	1.567E-07	0.0002	0.1260	0.000
205000.0	5.73	1.562E-07	0.0002	0.1261	0.000
206000.0	5.72	1.557E-07	0.0002	0.1263	0.000
207000.0	5.71	1.552E-07	0.0002	0.1264	0.000
208000.0	5.70	1.546E-07	0.0002	0.1266	0.000
209000.0	5.70	1.541E-07	0.0002	0.1267	0.000
210000.0	5.69	1.536E-07	0.0002	0.1269	0.000

211000.0	5.68	1.531E-07	0.0002	0.1270	0.000
212000.0	5.67	1.526E-07	0.0002	0.1272	0.000
213000.0	5.66	1.521E-07	0.0002	0.1273	0.000
214000.0	5.65	1.516E-07	0.0002	0.1275	0.000
215000.0	5.64	1.511E-07	0.0002	0.1276	0.000
216000.0	5.64	1.506E-07	0.0002	0.1278	0.000
217000.0	5.63	1.502E-07	0.0002	0.1279	0.000
218000.0	5.62	1.497E-07	0.0001	0.1281	0.000
219000.0	5.61	1.493E-07	0.0001	0.1282	0.000
220000.0	5.61	1.489E-07	0.0001	0.1284	0.000
221000.0	5.60	1.485E-07	0.0001	0.1285	0.000
222000.0	5.59	1.482E-07	0.0001	0.1287	0.000
223000.0	5.59	1.478E-07	0.0001	0.1288	0.000
224000.0	5.58	1.475E-07	0.0001	0.1290	0.000
225000.0	5.57	1.471E-07	0.0001	0.1291	0.000
226000.0	5.57	1.468E-07	0.0001	0.1293	0.000
227000.0	5.56	1.464E-07	0.0001	0.1294	0.000
228000.0	5.56	1.461E-07	0.0001	0.1296	0.000
229000.0	5.55	1.457E-07	0.0001	0.1297	0.000
230000.0	5.54	1.454E-07	0.0001	0.1299	0.000
231000.0	5.54	1.451E-07	0.0001	0.1300	0.000
232000.0	5.53	1.447E-07	0.0001	0.1302	0.000
233000.0	5.53	1.444E-07	0.0001	0.1304	0.000
234000.0	5.52	1.440E-07	0.0001	0.1306	0.000
235000.0	5.51	1.437E-07	0.0001	0.1307	0.000
236000.0	5.51	1.434E-07	0.0001	0.1309	0.000
237000.0	5.50	1.430E-07	0.0001	0.1310	0.000
238000.0	5.50	1.427E-07	0.0001	0.1312	0.000
239000.0	5.49	1.424E-07	0.0001	0.1313	0.000
240000.0	5.48	1.420E-07	0.0001	0.1314	0.000
241000.0	5.48	1.417E-07	0.0001	0.1316	0.000
242000.0	5.47	1.414E-07	0.0001	0.1317	0.000
243000.0	5.47	1.410E-07	0.0001	0.1319	0.000
244000.0	5.46	1.407E-07	0.0001	0.1320	0.000
245000.0	5.46	1.404E-07	0.0001	0.1321	0.000
246000.0	5.45	1.401E-07	0.0001	0.1323	0.000
247000.0	5.44	1.397E-07	0.0001	0.1324	0.000
248000.0	5.44	1.394E-07	0.0001	0.1326	0.000
249000.0	5.43	1.391E-07	0.0001	0.1327	0.000
250000.0	5.43	1.388E-07	0.0001	0.1328	0.000
251000.0	5.42	1.385E-07	0.0001	0.1330	0.000
252000.0	5.41	1.381E-07	0.0001	0.1331	0.000
253000.0	5.41	1.378E-07	0.0001	0.1333	0.000
254000.0	5.40	1.375E-07	0.0001	0.1334	0.000
255000.0	5.40	1.372E-07	0.0001	0.1335	0.000
256000.0	5.39	1.369E-07	0.0001	0.1337	0.000
257000.0	5.39	1.366E-07	0.0001	0.1338	0.000
258000.0	5.38	1.363E-07	0.0001	0.1339	0.000
259000.0	5.37	1.359E-07	0.0001	0.1341	0.000
260000.0	5.37	1.356E-07	0.0001	0.1342	0.000
261000.0	5.36	1.353E-07	0.0001	0.1343	0.000
262000.0	5.36	1.350E-07	0.0001	0.1345	0.000
263000.0	5.35	1.347E-07	0.0001	0.1346	0.000
264000.0	5.35	1.344E-07	0.0001	0.1347	0.000
265000.0	5.34	1.341E-07	0.0001	0.1349	0.000
266000.0	5.34	1.338E-07	0.0001	0.1350	0.000
267000.0	5.33	1.335E-07	0.0001	0.1351	0.000
268000.0	5.32	1.332E-07	0.0001	0.1353	0.000
269000.0	5.32	1.329E-07	0.0001	0.1354	0.000
270000.0	5.31	1.326E-07	0.0001	0.1355	0.000
271000.0	5.31	1.323E-07	0.0001	0.1357	0.000
272000.0	5.30	1.320E-07	0.0001	0.1357	0.000
273000.0	5.30	1.317E-07	0.0001	0.1358	0.000

274000.0	5.29	1.314E-07	0.0001	0.1359	0.000
275000.0	5.29	1.311E-07	0.0001	0.1361	0.000
276000.0	5.28	1.308E-07	0.0001	0.1362	0.000
277000.0	5.27	1.305E-07	0.0001	0.1363	0.000
278000.0	5.27	1.302E-07	0.0001	0.1365	0.000
279000.0	5.26	1.300E-07	0.0001	0.1366	0.000
280000.0	5.26	1.297E-07	0.0001	0.1367	0.000
281000.0	5.25	1.294E-07	0.0001	0.1368	0.000
282000.0	5.25	1.291E-07	0.0001	0.1370	0.000
283000.0	5.24	1.288E-07	0.0001	0.1371	0.000
284000.0	5.24	1.285E-07	0.0001	0.1372	0.000
285000.0	5.23	1.282E-07	0.0001	0.1374	0.000
286000.0	5.23	1.280E-07	0.0001	0.1375	0.000
287000.0	5.22	1.277E-07	0.0001	0.1376	0.000
288000.0	5.22	1.274E-07	0.0001	0.1377	0.000
289000.0	5.21	1.271E-07	0.0001	0.1379	0.000
290000.0	5.20	1.268E-07	0.0001	0.1380	0.000
291000.0	5.20	1.266E-07	0.0001	0.1381	0.000
292000.0	5.19	1.263E-07	0.0001	0.1383	0.000
293000.0	5.19	1.260E-07	0.0001	0.1384	0.000
294000.0	5.18	1.257E-07	0.0001	0.1385	0.000
295000.0	5.18	1.255E-07	0.0001	0.1386	0.000
296000.0	5.17	1.252E-07	0.0001	0.1388	0.000
297000.0	5.17	1.249E-07	0.0001	0.1389	0.000
298000.0	5.16	1.246E-07	0.0001	0.1390	0.000
299000.0	5.16	1.244E-07	0.0001	0.1391	0.000
300000.0	5.15	1.241E-07	0.0001	0.1393	0.000
301000.0	5.15	1.238E-07	0.0001	0.1394	0.000
302000.0	5.14	1.236E-07	0.0001	0.1395	0.000
303000.0	5.14	1.233E-07	0.0001	0.1396	0.000
304000.0	5.13	1.230E-07	0.0001	0.1397	0.000
305000.0	5.13	1.228E-07	0.0001	0.1399	0.000
306000.0	5.12	1.225E-07	0.0001	0.1400	0.000
307000.0	5.12	1.222E-07	0.0001	0.1401	0.000
308000.0	5.11	1.220E-07	0.0001	0.1402	0.000
309000.0	5.11	1.217E-07	0.0001	0.1404	0.000
310000.0	5.10	1.215E-07	0.0001	0.1405	0.000
311000.0	5.10	1.212E-07	0.0001	0.1406	0.000
312000.0	5.09	1.209E-07	0.0001	0.1407	0.000
313000.0	5.09	1.207E-07	0.0001	0.1408	0.000
314000.0	5.08	1.204E-07	0.0001	0.1410	0.000
315000.0	5.08	1.202E-07	0.0001	0.1411	0.000
316000.0	5.07	1.199E-07	0.0001	0.1412	0.000
317000.0	5.07	1.197E-07	0.0001	0.1413	0.000
318000.0	5.06	1.194E-07	0.0001	0.1414	0.000
319000.0	5.06	1.191E-07	0.0001	0.1416	0.000
320000.0	5.05	1.189E-07	0.0001	0.1417	0.000
321000.0	5.05	1.186E-07	0.0001	0.1418	0.000
322000.0	5.04	1.184E-07	0.0001	0.1419	0.000
323000.0	5.04	1.181E-07	0.0001	0.1420	0.000
324000.0	5.03	1.179E-07	0.0001	0.1422	0.000
325000.0	5.03	1.176E-07	0.0001	0.1423	0.000
326000.0	5.02	1.174E-07	0.0001	0.1424	0.000
327000.0	5.02	1.171E-07	0.0001	0.1425	0.000
328000.0	5.01	1.169E-07	0.0001	0.1426	0.000
329000.0	5.01	1.167E-07	0.0001	0.1427	0.000
330000.0	5.00	1.164E-07	0.0001	0.1429	0.000
331000.0	5.00	1.162E-07	0.0001	0.1430	0.000
332000.0	4.99	1.159E-07	0.0001	0.1431	0.000
333000.0	4.99	1.157E-07	0.0001	0.1432	0.000
334000.0	4.98	1.154E-07	0.0001	0.1433	0.000
335000.0	4.98	1.152E-07	0.0001	0.1434	0.000
336000.0	4.97	1.150E-07	0.0001	0.1435	0.000

337000.0	4.97	1.147E-07	0.0001	0.1437	0.000
338000.0	4.96	1.145E-07	0.0001	0.1438	0.000
339000.0	4.96	1.142E-07	0.0001	0.1439	0.000
340000.0	4.95	1.140E-07	0.0001	0.1440	0.000
341000.0	4.95	1.138E-07	0.0001	0.1441	0.000
342000.0	4.95	1.136E-07	0.0001	0.1442	0.000
343000.0	4.94	1.135E-07	0.0001	0.1443	0.000
344000.0	4.94	1.134E-07	0.0001	0.1445	0.000
345000.0	4.94	1.132E-07	0.0001	0.1446	0.000
346000.0	4.94	1.131E-07	0.0001	0.1447	0.000
347000.0	4.93	1.130E-07	0.0001	0.1448	0.000
348000.0	4.93	1.128E-07	0.0001	0.1449	0.000
349000.0	4.93	1.127E-07	0.0001	0.1450	0.000
350000.0	4.93	1.126E-07	0.0001	0.1451	0.000
351000.0	4.92	1.124E-07	0.0001	0.1452	0.000
352000.0	4.92	1.123E-07	0.0001	0.1454	0.000
353000.0	4.92	1.122E-07	0.0001	0.1455	0.000
354000.0	4.91	1.120E-07	0.0001	0.1456	0.000
355000.0	4.91	1.119E-07	0.0001	0.1457	0.000
356000.0	4.91	1.118E-07	0.0001	0.1458	0.000
357000.0	4.91	1.116E-07	0.0001	0.1459	0.000
358000.0	4.90	1.115E-07	0.0001	0.1460	0.000
359000.0	4.90	1.114E-07	0.0001	0.1461	0.000
360000.0	4.90	1.112E-07	0.0001	0.1463	0.000
361000.0	4.90	1.111E-07	0.0001	0.1464	0.000
362000.0	4.89	1.110E-07	0.0001	0.1465	0.000
363000.0	4.89	1.109E-07	0.0001	0.1466	0.000
364000.0	4.89	1.107E-07	0.0001	0.1467	0.000
365000.0	4.88	1.106E-07	0.0001	0.1468	0.000
366000.0	4.88	1.105E-07	0.0001	0.1469	0.000
367000.0	4.88	1.103E-07	0.0001	0.1470	0.000
368000.0	4.88	1.102E-07	0.0001	0.1471	0.000
369000.0	4.87	1.101E-07	0.0001	0.1473	0.000
370000.0	4.87	1.099E-07	0.0001	0.1474	0.000
371000.0	4.87	1.098E-07	0.0001	0.1475	0.000
372000.0	4.87	1.097E-07	0.0001	0.1476	0.000
373000.0	4.86	1.096E-07	0.0001	0.1477	0.000
374000.0	4.86	1.094E-07	0.0001	0.1478	0.000
375000.0	4.86	1.093E-07	0.0001	0.1479	0.000
376000.0	4.86	1.092E-07	0.0001	0.1480	0.000
377000.0	4.85	1.090E-07	0.0001	0.1481	0.000
378000.0	4.85	1.089E-07	0.0001	0.1482	0.000
379000.0	4.85	1.088E-07	0.0001	0.1483	0.000
380000.0	4.85	1.087E-07	0.0001	0.1485	0.000
381000.0	4.84	1.085E-07	0.0001	0.1486	0.000
382000.0	4.84	1.084E-07	0.0001	0.1487	0.000
383000.0	4.84	1.083E-07	0.0001	0.1488	0.000
384000.0	4.83	1.082E-07	0.0001	0.1489	0.000
385000.0	4.83	1.080E-07	0.0001	0.1490	0.000
386000.0	4.83	1.079E-07	0.0001	0.1491	0.000
387000.0	4.83	1.078E-07	0.0001	0.1492	0.000
388000.0	4.82	1.077E-07	0.0001	0.1493	0.000
389000.0	4.82	1.075E-07	0.0001	0.1494	0.000
390000.0	4.82	1.074E-07	0.0001	0.1495	0.000
391000.0	4.82	1.073E-07	0.0001	0.1496	0.000
392000.0	4.81	1.072E-07	0.0001	0.1497	0.000
393000.0	4.81	1.070E-07	0.0001	0.1499	0.000
394000.0	4.81	1.069E-07	0.0001	0.1500	0.000
395000.0	4.81	1.068E-07	0.0001	0.1501	0.000
396000.0	4.80	1.067E-07	0.0001	0.1502	0.000
397000.0	4.80	1.065E-07	0.0001	0.1503	0.000
398000.0	4.80	1.064E-07	0.0001	0.1504	0.000
399000.0	4.80	1.063E-07	0.0001	0.1505	0.000

400000.0	4.79	1.062E-07	0.0001	0.1506	0.000
401000.0	4.79	1.061E-07	0.0001	0.1507	0.000
402000.0	4.79	1.059E-07	0.0001	0.1508	0.000
403000.0	4.79	1.058E-07	0.0001	0.1509	0.000
404000.0	4.78	1.057E-07	0.0001	0.1510	0.000
405000.0	4.78	1.056E-07	0.0001	0.1511	0.000
406000.0	4.78	1.055E-07	0.0001	0.1512	0.000
407000.0	4.78	1.053E-07	0.0001	0.1513	0.000
408000.0	4.77	1.052E-07	0.0001	0.1514	0.000
409000.0	4.77	1.051E-07	0.0001	0.1516	0.000
410000.0	4.77	1.050E-07	0.0001	0.1517	0.000
411000.0	4.77	1.048E-07	0.0001	0.1518	0.000
412000.0	4.76	1.047E-07	0.0001	0.1519	0.000
413000.0	4.76	1.046E-07	0.0001	0.1520	0.000
414000.0	4.76	1.045E-07	0.0001	0.1521	0.000
415000.0	4.76	1.044E-07	0.0001	0.1522	0.000
416000.0	4.75	1.043E-07	0.0001	0.1523	0.000
417000.0	4.75	1.041E-07	0.0001	0.1524	0.000
418000.0	4.75	1.040E-07	0.0001	0.1525	0.000
419000.0	4.75	1.039E-07	0.0001	0.1526	0.000
420000.0	4.74	1.038E-07	0.0001	0.1527	0.000
421000.0	4.74	1.037E-07	0.0001	0.1528	0.000
422000.0	4.74	1.035E-07	0.0001	0.1529	0.000
423000.0	4.74	1.034E-07	0.0001	0.1530	0.000
424000.0	4.73	1.033E-07	0.0001	0.1531	0.000
425000.0	4.73	1.032E-07	0.0001	0.1532	0.000
426000.0	4.73	1.031E-07	0.0001	0.1533	0.000
427000.0	4.73	1.030E-07	0.0001	0.1534	0.000
428000.0	4.72	1.028E-07	0.0001	0.1535	0.000
429000.0	4.72	1.027E-07	0.0001	0.1536	0.000
430000.0	4.72	1.026E-07	0.0001	0.1537	0.000
431000.0	4.72	1.025E-07	0.0001	0.1538	0.000
432000.0	4.71	1.024E-07	0.0001	0.1539	0.000
433000.0	4.71	1.023E-07	0.0001	0.1540	0.000
434000.0	4.71	1.021E-07	0.0001	0.1541	0.000
435000.0	4.71	1.020E-07	0.0001	0.1542	0.000
436000.0	4.70	1.019E-07	0.0001	0.1543	0.000
437000.0	4.70	1.018E-07	0.0001	0.1544	0.000
438000.0	4.70	1.017E-07	0.0001	0.1545	0.000
439000.0	4.70	1.016E-07	0.0001	0.1546	0.000
440000.0	4.69	1.015E-07	0.0001	0.1547	0.000
441000.0	4.69	1.013E-07	0.0001	0.1549	0.000
442000.0	4.69	1.012E-07	0.0001	0.1550	0.000
443000.0	4.69	1.011E-07	0.0001	0.1551	0.000
444000.0	4.68	1.010E-07	0.0001	0.1552	0.000
445000.0	4.68	1.009E-07	0.0001	0.1553	0.000
446000.0	4.68	1.008E-07	0.0001	0.1554	0.000
447000.0	4.68	1.007E-07	0.0001	0.1555	0.000
448000.0	4.67	1.006E-07	0.0001	0.1556	0.000
449000.0	4.67	1.004E-07	0.0001	0.1557	0.000
450000.0	4.67	1.003E-07	0.0001	0.1558	0.000
451000.0	4.67	1.002E-07	0.0001	0.1559	0.000
452000.0	4.66	1.001E-07	0.0001	0.1560	0.000
453000.0	4.66	1.000E-07	0.0001	0.1561	0.000
454000.0	4.66	9.989E-08	0.0001	0.1562	0.000
455000.0	4.66	9.978E-08	0.0001	0.1563	0.000
456000.0	4.66	9.967E-08	0.0001	0.1564	0.000
457000.0	4.65	9.956E-08	0.0001	0.1565	0.000
458000.0	4.65	9.944E-08	0.0001	0.1566	0.000
459000.0	4.65	9.933E-08	0.0001	0.1567	0.000
460000.0	4.65	9.922E-08	0.0001	0.1568	0.000
461000.0	4.64	9.911E-08	0.0001	0.1569	0.000
462000.0	4.64	9.900E-08	0.0001	0.1570	0.000

463000.0	4.64	9.890E-08	0.0001	0.1571	0.000
464000.0	4.64	9.879E-08	0.0001	0.1572	0.000
465000.0	4.63	9.868E-08	0.0001	0.1573	0.000
466000.0	4.63	9.857E-08	0.0001	0.1573	0.000
467000.0	4.63	9.846E-08	0.0001	0.1574	0.000
468000.0	4.63	9.835E-08	0.0001	0.1575	0.000
469000.0	4.62	9.824E-08	0.0001	0.1576	0.000
470000.0	4.62	9.813E-08	0.0001	0.1577	0.000
471000.0	4.62	9.803E-08	0.0001	0.1578	0.000
472000.0	4.62	9.792E-08	0.0001	0.1579	0.000
473000.0	4.62	9.781E-08	0.0001	0.1580	0.000
474000.0	4.61	9.770E-08	0.0001	0.1581	0.000
475000.0	4.61	9.759E-08	0.0001	0.1582	0.000
476000.0	4.61	9.749E-08	0.0001	0.1583	0.000
477000.0	4.61	9.738E-08	0.0001	0.1584	0.000
478000.0	4.60	9.727E-08	0.0001	0.1585	0.000
479000.0	4.60	9.717E-08	0.0001	0.1586	0.000
480000.0	4.60	9.706E-08	0.0001	0.1587	0.000
481000.0	4.60	9.695E-08	0.0001	0.1588	0.000
482000.0	4.59	9.685E-08	0.0001	0.1589	0.000
483000.0	4.59	9.674E-08	0.0001	0.1590	0.000
484000.0	4.59	9.664E-08	0.0001	0.1591	0.000
485000.0	4.59	9.653E-08	0.0001	0.1592	0.000
486000.0	4.58	9.643E-08	0.0001	0.1593	0.000
487000.0	4.58	9.632E-08	0.0001	0.1594	0.000
488000.0	4.58	9.622E-08	0.0001	0.1595	0.000
489000.0	4.58	9.611E-08	0.0001	0.1596	0.000
490000.0	4.58	9.601E-08	0.0001	0.1597	0.000
491000.0	4.57	9.590E-08	0.0001	0.1598	0.000
492000.0	4.57	9.580E-08	0.0001	0.1599	0.000
493000.0	4.57	9.569E-08	0.0001	0.1600	0.000
494000.0	4.57	9.559E-08	0.0001	0.1601	0.000
495000.0	4.57	9.554E-08	0.0001	0.1602	0.000
496000.0	4.56	9.552E-08	0.0001	0.1603	0.000
497000.0	4.56	9.550E-08	0.0001	0.1604	0.000
498000.0	4.56	9.548E-08	0.0001	0.1604	0.000
499000.0	4.56	9.546E-08	0.0001	0.1605	0.000
500000.0	4.56	9.545E-08	0.0001	0.1606	0.000